ABSTRACT

D.W. HENDRIKS

METALLURGICAL ENGINEERING

INTERACTION OF AMINE AND STARCH IN QUARTZ FLOTATION

Simultaneous adsorption of tritiated dodecylamine and carbon-14 starch on quartz was investigated using two channel liquid scintillation counting. The effect of adsorption on floatability was determined using a modified Hallimond tube.

Amine adsorption was found to obey the equation $\Gamma = KC^n$. Starch additions increased the slope in dilute amine solutions and decreased the slope in concentrated amine solutions. Adsorption of amine increased with pH, with a sharp rise in adsorption occurring between pH 8 and pH 10.

Adsorption of starch increased with concentration. Increasing amine additions increased starch adsorption up to 10^2 μmole/l amine. Higher amine additions decreased starch adsorption.

Floatability increased with amine concentration to 10^3 μmole/l amine and decreased at 10^4 μmole/l amine. The flotation peak was observed in slightly alkaline solutions. The depressant effect of starch is related to the relative amount of amine and starch adsorbed.

The mutual adsorption effects of amine and starch are explained in terms of complex formation.

INTERACTION OF AMINE AND STARCH IN QUARTZ FLOTATION

Acknowledgements

The author wishes to express his gratitude to Dr. G.W. Smith for his guidance and encouragement during the course of this work.

He is also indebted to the Mines Branch, Department of Energy, Mines and Resources and to the National Research Council for personal financial support and for financing the practical costs of this study.

The author would also like to thank his wife, Barbara, for her patience, understanding and encouragement given throughout this work.

INDEX

List of Figures	(iii)
List of Tables	(vi)
Introduction	1
Theoretical Review	3
Flotation	3
Electrical Double Layer	4
Adsorption (a) Physical Adsorption	7
(b) Chemisorption	8
Adsorption Isotherms	9
(a) Langmuir Equation	9
(b) Freundlich Equation	11
(c) B.E.T. Equation	11
Dodecylamine	13
Starch	15
Quartz-Amine	16
Quartz-Amine-Starch	19
Statement of Intent	21
Experimental	22
Materials and Chemicals	22
Experimental Procedures	27
Results	32
Discussion	56
Suggestions for Future Work	75

Appendices

I	Quartz Analysis	76
II	Equilibrium Tests	84
III	Surface Area Determination	88
IV	Solution Analysis	107
V	Tables of Experimental Results	114

List of Figures

Figure		Page
1	Electrical Double Layer.	5
2	Flotation Cell.	30
3	Gas Control System for Flotation Cell.	31
4	Adsorption Density of Amine as a Function of Concentration: pH 4.	33
5	Adsorption Density of Amine as a Function of Concentration: pH 7.	34
6	Adsorption Density of Amine as a Function of Concentration: pH 10.	35
7	Adsorption Density of Amine as a Function of Initial Starch Concentration (Amine-10 μmole/l).	36
8	Adsorption Density of Amine as a Function of Initial Starch Concentration (Amine-100 μmole/l).	37
9	Adsorption Density of Amine as a Function of Initial Starch Concentration (Amine-1000 μmole/l).	38
10	Adsorption Density of Amine as a Function of Initial Starch Concentration (Amine-10,000 μmole/l).	39
11	Adsorption Density of Amine as a Function of pH (Starch-zero).	40

12	Adsorption Density of Amine as a Function of pH (Starch-100 mg/l).	41
13	Adsorption Density of Amine as a Function of pH (Starch-400 mg/l).	42
14	Adsorption Density of Amine as a Function of pH (Starch-1000 mg/l).	43
15	Adsorption Density of Starch as a Function of Amine Concentration and pH (Starch-400 mg/l).	45
16	Adsorption Density of Starch as a Function of Amine Concentration and pH (Starch-1000 mg/l).	46
17	Floatability as a Function of Amine Concentration and pH (Starch-zero).	47
18	Floatability as a Function of Amine Concentration and pH (Starch-100 mg/l).	48
19	Floatability as a Function of Amine Concentration and pH (Starch-400 mg/l).	49
20	Floatability as a Function of Amine Concentration and pH (Starch-1000 mg/l).	50
21	Floatability as a Function of Starch Concentration and pH (Amine-10 μmole/l).	51
22	Floatability as a Function of Starch Concentration and pH (Amine-100 μmole/l).	52
23	Floatability as a Function of Starch Concentration and pH (Amine-1000 μmole/l).	53

24	Floatability as a Function of Starch Concentration and pH (Amine-10,000 μmole/l).	54
25	Adsorption Density of Amine as a Function of Amine Concentration.	57
26	Schematic Drawing of Amine Adsorption, Starch Adsorption and Amine-Starch Complex Adsorption.	64
27	Per Cent Floatability Contours as a Function of Amine Concentration and pH (Starch-zero).	67
28	Per Cent Floatability Contours as a Function of Amine Concentration and pH (Starch-1000 mg/l).	68
29	Floatability of Quartz and Hematite as a Function of Amine Concentration, Starch Concentration and pH.	69
30	Available Surface Area as a Function of pH.	73
31	Amine Adsorption as a Function of Time.	86
32	B.E.T. Plot for Nitrogen Adsorption.	90
33	Calibration Curve for 1-Hexadecylpyridinium Bromide.	94
34	Adsorption of H-HPB as a Function of Time.	96
35	Adsorption of 1-HPB as a Function of pH.	98
36	Adsorption Isotherm of 1-HPB on Quartz.	100
37	B.E.T. Plots for 1-HPB Adsorption.	104

List of Tables

Table		Page
1.	Quartz Analysis.	23
2	Differential Flotation Tests 50% Hematite, 50% Quartz.	71
3	Per Cent Surface Coverage.	74
4	Impurities in Quartz.	77
5	X-Ray Identification of Quartz.	79
6	Equilibrium Tests for Amine Adsorption.	87
7	Nitrogen Adsorption Data for Surface Area Determination.	91
8	Calibration Curve for 1-HPB.	95
9	Equilibrium Tests for 1-HPB Adsorption.	97
10	Adsorption of 1-HPB as a Function of pH.	99
11	Adsorption of 1-HPB as a Function of Concentration: pH 8.	101
12	Adsorption of 1-HPB as a Function of Concentration: pH 9.7.	102
13	Adsorption of 1-HPB as a Function of Concentration: pH 12.	103
14	Modified B.E.T. Data for 1-HPB Adsorption: pH 8, 9.7 and 12.	105
15	Efficiency and Quench Ratio for Tritium Standards.	112
16	Efficiency and Quench Ratio of Carbon-14 Standard.	113

17	Results:	Amine 10 μmole/l Starch zero	115
18	Results:	Amine 10 μmole/l Starch 100 mg/l	116
19	Results:	Amine 10 μmole/l Starch 400 mg/l	117
20	Results:	Amine 10 μmole/l Starch 1000 mg/l	118
21	Results:	Amine 100 μmole/l Starch zero	119
22	Results:	Amine 100 μmole/l Starch 100 mg/l	120
23	Results:	Amine 100 μmole/l Starch 400 mg/l	121
24	Results:	Amine 100 μmole/l Starch 1000 mg/l	122
25	Results:	Amine 1000 μmole/l Starch zero	123
26	Results:	Amine 1000 μmole/l Starch 100 mg/l	124
27	Results:	Amine 1000 μmole/l Starch 400 mg/l	125
28	Results:	Amine 1000 μmole/l Starch 1000 mg/l	126
29	Results:	Amine 10,000 μmole/l Starch zero	127

30	Results:	Amine 10,000 μmole/l Starch 100 mg/l	128
31	Results:	Amine 10,000 μmole/l Starch 400 mg/l	129
32	Results:	Amine 10,000 μmole/l Starch 1000 mg/l	130
33	Results:	Amine zero Starch 100, 400, 1000 mg/l	131
34	Natural Floatability of Quartz.		133

I. INTRODUCTION

Fifty years ago, an iron ore deposit was economically viable if the ore could be sent directly to a smelter. The tremendous increase in demand for iron ore, coupled with a decrease in availability of direct smelting ores, made it economically feasible to mine lower grade deposits. These ores must be beneficiated in some manner to produce a concentrate of suitable grade and physical properties to be acceptable to the smelter.

In 1968, iron ore production in Canada was 42.4 million long tons.[1] (Due to strikes, 1969 production was 35.7 million long tons.) Production was expected to reach 45 million long tons in 1970 and 60 million long tons by 1975.[2] The present over supply of iron ore is expected to become one of a balance of supply and demand, if not one of undersupply in the near future.[2]

At present, more than 90% of iron ores are beneficiated in some manner.[3] The most common methods of concentrating iron ores utilize the physical properties of iron minerals. These include the use of Humphrey spirals, tabling, heavy media, magnetic and electrostatic separations.[4] These methods have been found to be ineffective in concentrating fine particles (<50 microns), taconites or specular hematites. At Wabush

mines, using a combination of electrostatic and spiral methods, a grade of 66.3% Fe is obtained but recovery is only 40%.[5]

Froth flotation is an effective process for separating finely divided solids. Considerable work has been done to devise an effective flotation scheme for concentration of iron oxides.[6-10] The process, while only of minor importance at present, will play an increasingly important role in the beneficiation of iron ores in the future. Further improvements, however, will require a better understanding of the mechanisms involved in the flotation or depression of iron oxides and of associated gangue materials.

II. THEORETICAL REVIEW

FLOTATION

Flotation is a physico-chemical process for separating finely divided solids suspended in a liquid according to differences in affinity for a gaseous phase. The solids and liquid are mixed to form a pulp through which the gas is bubbled. Particles with an affinity for the gas phase (hydrophobic) become attached to the gas bubbles. If the specific gravity of the resulting particle-bubble aggregate is less than the pulp, the aggregate will rise to the surface and can be removed as a froth. Particles with an affinity for the liquid phase (hydrophilic) will remain in the pulp. For economic reasons, the liquid used is almost universally water and the gas phase is air. The products of flotation are a tailing, containing the gangue or waste material, and one or more concentrates containing the valuable minerals.

Mineral particles seldom have the required surface properties for flotation. The surface characteristics are altered by the addition of chemicals, known as collectors and modifiers, to the pulp. Collectors are heteropolar compounds which contain a polar group and a non-polar hydrocarbon chain. When adsorbed on the mineral surface via the polar group, the hydrocarbon chain provides the required hydrophobicity for flotation. Modifiers are used as depressants, activators or to control pH. Depressants, by adsorbing on the mineral surface or by

preventing collector adsorption, create or maintain hydrophilic surfaces. Activators are used to enhance adsorption of collectors.

ELECTRICAL DOUBLE LAYER

The surface of any mineral or liquid differs from the interior in that intermolecular forces at the surface are not balanced. When the mineral is placed in water, surface bonding tends to hold the surface ions at the surface and the polar attraction of the liquid tends to pull the ions into solution. When some ions enter the solution, an electrostatic force is created at the surface, due to the charge separation, which opposes the tendency to solvate surface ions. This electrostatic distribution is known as the electrical double layer.

Helmholtz[11], in the first theoretical analysis of this distribution, assumed the ions to be tightly bound to the surface and compared the double layer to a parallel plate condenser. Gouy[12] and Chapman[13] extended the theory to include thermal agitation of the solution ions. Stern[14] modified the theory to include the finite dimensions of the ions. Minor modifications by Grahame[15], to account for covalent bonds and Van der Waal forces, complete the modern view of the electrical double layer.

The electrical double layer can be divided into three regions (Fig. 1). The first layer is essentially a disturbed crystal lattice. The ions may originate in either phase and

FIGURE I

ELECTRICAL DOUBLE LAYER

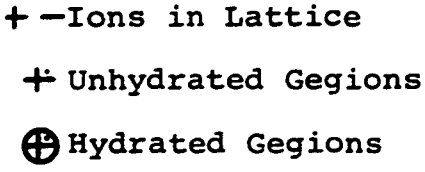

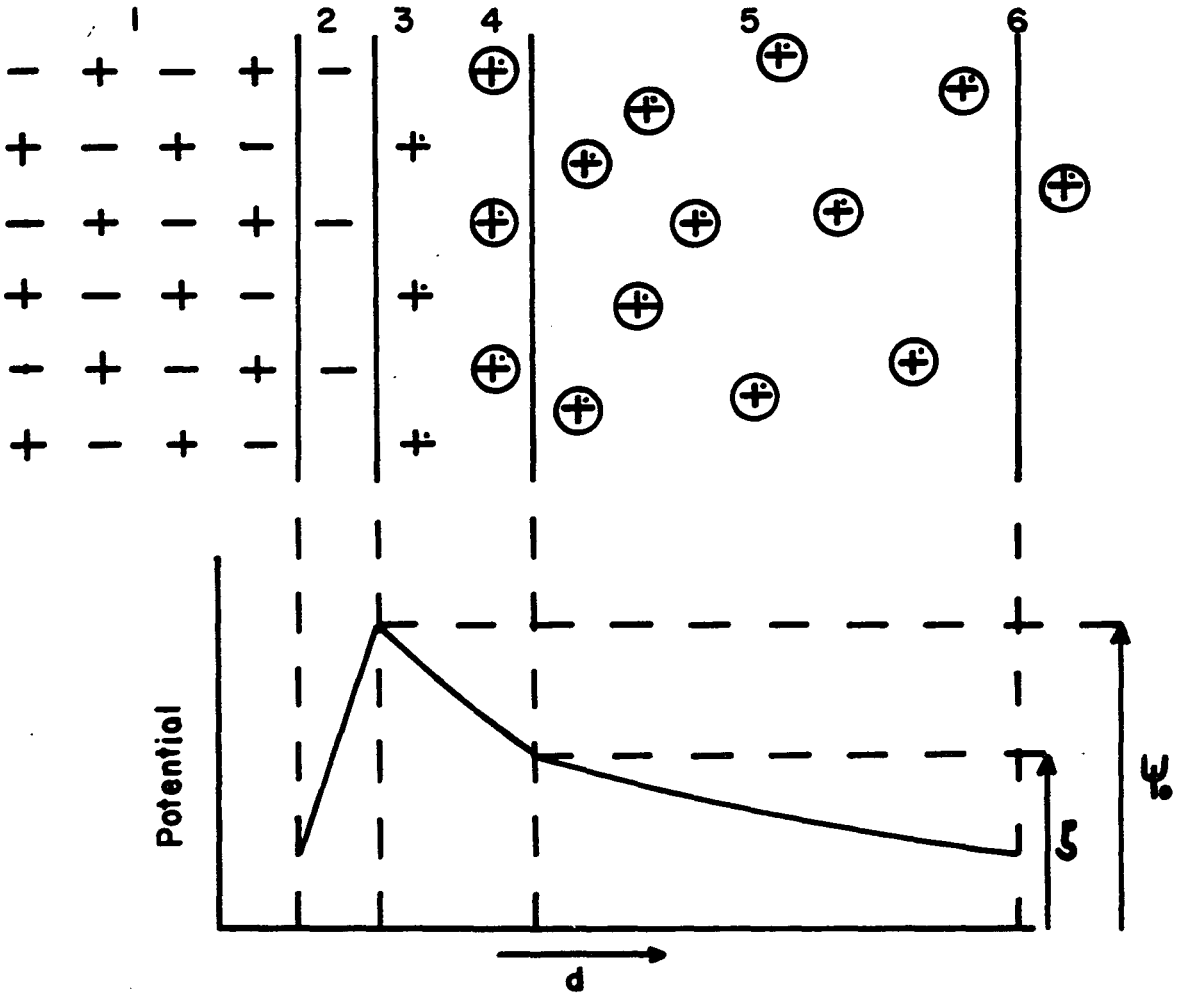

(1) Unaltered Crystal Lattice

(2) Altered Crystal Lattice - Potential Determining Ions

(3) Grahame's "Inner Helmholtz Layer" } Stern Layer

(4) Grahame's "Outer Helmholtz Layer" }

(5) Diffuse (Gouy) Layer

(6) Centre of Charge of Gouy Layer

are known as the potential determining ions (p.d.i.).

In the second region, known as the Stern layer, ions are bound firmly to the surface and occupy regular sites with respect to the crystal lattice. It is thought that some ions in this layer become dehydrated and are specifically adsorbed. Grahame named the dehydrated and hydrated ionic regions the inner and outer Helmholtz planes respectively. Excess ions in this region of opposite charge to the surface charge are known as gegions. The outer region, which can be considered an extension of the Stern layer, is known as the diffuse or Gouy layer. Gegions in this layer are mobile and their concentration decreases exponentially until the concentration is equal to that in the bulk solution.

The potential at the surface due to the p.d.i. is known as the surface potential (ψ_o). The zeta potential (ζ) is the potential at the shear plane between gegions held firmly to the surface and the mobile gegions in the diffuse layer. The shear plane is usually between the Gouy and Stern layers. The zeta potential can be changed by adding any cations or anions to the solution, through changes in ionic strength and layer thickness. The surface potential can only be altered by changing the concentration of the potential determining ions in the bulk solution.

For mineral oxides in aqueous solution, it is generally accepted that hydrogen and hydroxyl ions are the potential

determining ions.[16] Thus, changes in pH alter the surface and zeta potentials of mineral oxides, both becoming more negative as the pH is increased. The point at which the zeta potential is zero is the zero-point-of-charge (z.p.c.). The point at which both the surface and zeta potentials are zero is termed the iso-electric point (i.e.p.).

ADSORPTION

The attachment of molecules or atoms of one material (adsorbate) to the surface of another (adsorbent) is called adsorption. The contiguous area between them is referred to as the interface. Adsorption from solution is complex due to the presence of the solvent. Adsorption is usually classified as physical adsorption or chemical adsorption.

Physical Adsorption

Van der Waal forces are thought to be responsible for physical adsorption. Physical adsorption is characterized[17] by the following:

(i) low heats of adsorption, generally less than 3 kcal/mol.

(ii) occurs rapidly and is readily reversible.

(iii) no true bond exists between adsorbate and adsorbent. The adsorbate may be:

(a) An unionized molecule held in the vicinity of the surface by dispersion forces.

(b) an ion held in the Gouy layer of the electrical double layer by electrostatic forces.

(c) an ion held close to the surface by a combination of electrostatic and dispersion forces.

(d) a molecule or ion retained by relatively weak bonding ie. hydrogen bond. (This may equally be described as weak chemisorption.)

Chemisorption

Chemisorption is characterized by the following:

(i) high heat of adsorption (10-100 kcal/mol.)

(ii) irreversible or reversible with great difficulty.

(iii) the adsorbate forms a true bond with the adsorbent forming:

(a) a true chemical compound capable of existing in the bulk state.

(b) a surface compound for which an analogous species is known to exist as a crystal or in solution with the same molecular configuration.

(c) a surface compound for which no analogous compounds have been isolated.

In physical adsorption, the adsorbate is generally held in the outer electrical double layer. Any ion or molecule may adsorb irrespective of type, size of molecule, or magnitude of charge since only overall electrical neutrality is important.

As a result, physically adsorbed species do not selectively adsorb.

In chemisorption, the adsorbate enters the adsorbent lattice through a chemical reaction in the inner Helmholtz layer. The extent of chemisorption depends on the size of the adsorbate ions and the extent to which they approximate the size of the adsorbent crystal lattice, the solubility of the surface compounds and the structure of the adsorbent surface. Because of these factors, chemisorption has been found to be highly selective.

Adsorption Isotherms

An adsorption isotherm is the relationship between the adsorbate and one of the variables which affect the adsorption at constant temperature. Several theories have been postulated to describe and explain adsorption isotherms. The most important theories will be considered below.

(i) Langmuir Equation

Langmuir[18], in 1918, developed one of the first and most important equations based on theory. He assumed maximum adsorption was one monolayer and considered a dynamic equilibrium state such that the rate of adsorption equals the rate of desorption. Thus, the rate of adsorption will be proportional to the pressure of the gas as indicated in equation (1).

$$v = \frac{abP}{1 + b\,P} \qquad (1)$$

Where v is the volume of gas adsorbed, P is the equilibrium gas pressure, a is the volume of gas adsorbed for monolayer coverage and b is a constant related to the heat of adsorption. In linear form equation (1) becomes:

$$\frac{1}{v} = \frac{1}{abP} + \frac{1}{a} \qquad (2)$$

For adsorption from dilute solutions, equation (1) can be written as:

$$\frac{1}{x/m} = \frac{1}{abC} + \frac{1}{a} \qquad (3)$$

where C is the equilibrium adsorbate concentration, x/m is the amount adsorbed per unit amount of adsorbate, and a,b are constants.

Langmuir made several simplifying assumptions. These include:

(a) The heat of adsorption is independent of the fraction of surface covered.

(b) The maximum coverage is one monolayer.

(c) No lateral interactions occur between adsorbed species.

With these assumptions, the Langmuir equation is seldom used to describe physical adsorption, where multilayer

formation is common. It has been found to describe chemisorption systems adequately.[19,20]

(ii) Freundlich Equation

Equation (4), attributed to Freundlich[21], is based on empirical considerations only and has been used to describe many systems.

$$v = kP^n \qquad (4)$$

In equation (4), v is the volume adsorbed; P is the pressure of adsorbate and k,n are constants. For adsorption from solution, equation (4) is written in the following form:

$$x/m = kC^n \qquad (5)$$

where x/m is weight adsorbed per unit weight of adsorbent, C is equilibrium concentration of adsorbate in solution. In linear form equation (5) becomes:

$$\log x/m = \log k + n \log C \qquad (6)$$

and, a plot of log x/m vs log C will be linear with slope n and intercept log k.

(iii) The B.E.T. Equation

Brunauer, Emmett, and Teller[22] extended Langmuir's

theory to include multilayer adsorption. The derivation of the B.E.T. equation is based on the same kinetic model proposed by Langmuir, and the assumption that in physical adsorption, the forces of condensation predominate. The general form of the B.E.T. equation is:

$$v = \frac{v_m\, bP}{(P_o - P)\ (1 + (b-1)\frac{P}{P_o})} \tag{7}$$

or in linear form:

$$\frac{P}{v(P_o - P)} = \frac{1}{v_m b} + \frac{b-1}{v_m b} \cdot \frac{P}{P_o} \tag{8}$$

where P is the pressure of adsorbate, P_o is the saturation pressure, v is the volume adsorbed, v_m is the volume adsorbed at monolayer coverage, and b is a constant related to the heat of liquifaction. Plotting $\frac{P}{v(P_o - P)}$ against $\frac{P}{P_o}$, a straight line is obtained with intercept $\frac{1}{v_m b}$ and slope $\frac{b-1}{v_m b}$.

While the B.E.T. equation has been found to be very reliable, several theoretical criticisms have been made. These include:

(a) heat of vaporization was assumed to be equal for all layers following the first and equal to the heat

of vaporization of the bulk liquid.

(b) interaction between adsorbed molecules is ignored.

Cook[23] extended the B.E.T. theory by including the interaction of the adsorbate molecules. Other modifications have been made by Harkins and Jura[24], Anderson and Hall[25], and Keenan[26].

The B.E.T. equation can be modified to describe adsorption from solution[25-28]. Equation (8) becomes:

$$\frac{C}{(x/m)(C_o-C)} = \frac{1}{(x/m)_m b} + \frac{b-1}{(x/m)_m b} \cdot \frac{C}{C_o} \qquad (9)$$

where x/m is the amount adsorbed per unit weight of adsorbent, C is the concentration of adsorbing species, C_o is the saturation concentration or, if micelles are formed, the critical micelle concentration, $(x/m)_m$ is the value of x/m at monolayer coverage, and b is constant as before.

DODECYLAMINE

Amines are organic derivatives of ammonia in which hydrogen atoms are replaced by aliphatic, aromatic or heterocyclic radicals. Replacing one, two, or three hydrogen atoms results in primary, secondary or tertiary amines. Dodecylamine ($CH_3(CH_2)_{11}NH_2$) is a primary amine with an aliphatic radical. Long chain amines are relatively insoluble in water and, for

use in flotation, are converted to salt form, usually to the chloride or acetate.

Three forms of the amine are present in aqueous solutions - RNH_3^+, RNH_2 (sol'n), and RNH_2 (ppt.), where R indicates the organic radical. The ratio of these species in solution is determined by the following equilibria:

$$RNH_2 + H_2O \rightleftharpoons RNH_3^+ + OH^- \qquad (10)$$

from which[29]:

$$K_1 = \frac{[OH^-]\ [RNH_3^+]}{[H_2O]\ [RNH_2]} = 4.3 \times 10^{-4} \qquad (11)$$

$$H_2O \rightleftharpoons H^+ + OH^- \qquad (12)$$

for which:

$$K_w = 1.02 \times 10^{-14} \quad \text{at } 25^oC \qquad (13)$$

and:

$$RNH_3^+ \rightleftharpoons RNH_2 + H^+ \qquad (14)$$

for which:

$$K_2 = \frac{[H^+]\ [RNH_2]}{[RNH_3^+]} = 2.4 \times 10^{-11} \qquad (15)$$

The most recent value[30] for the solubility of RNH_2

is:

$$[RNH_2]_{max} = 2 \times 10^{-5} \text{ mole/l} \qquad (16)$$

If this concentration of RNH_2 is exceeded, the concentration of RNH_3^+ can be found from equation (14) as follows:

$$[RNH_3^+] = \frac{2 \times 10^{-5}[H^+]}{2.4 \times 10^{-11}} = \frac{[H^+]}{1.2 \times 10^{-6}} \qquad (17)$$

and the precipitated amine can be calculated from:

$$[RNH_2](\text{ppt.}) = [\text{total amine}] - [RNH_3^+] - [RNH_2](\text{sol'n}) \qquad (18)$$

The relative concentrations of $[RNH_3^+]$, $[RNH_2]$ (sol'n) and $[RNH_2]$(ppt.) were first calculated by Kellogg and Vasquès-Rosas.[31]

STARCH

Starch is a polymeric carbohydrate, known as a polysaccharide, composed of many glucose units.

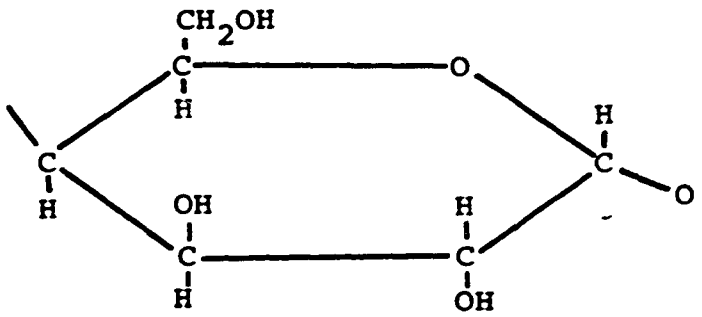

Two types of starches are recognized, known as amylose

and amylopectin. Amylose, with a molecular weight as high as 10^8, has a linear structure which is in the shape of a helix.[32] Amylopectin, with a molecular weight in the order of 10^5 - 10^6, is a branched structure, whose exact arrangement is a matter of conjecture.[33] In amylose, the glucose units are formed by 1 - 4 linkages whereas in amylopectin they are joined by 1 - 4 and 1 - 6 linkages. Amylose is highly soluble in water whereas amylopectin is relatively insoluble.

Quartz - Amine

Adsorption of amines on quartz has been studied by many workers.[34-49] Unfortunately, many discrepancies exist in literature and several theories have been postulated concerning the mechanism of adsorption. Several workers contend that only physical adsorption occurs and amine is adsorbed in the outer electrical double layer.[34-37] Gaudin and Morrow[34] and Gaudin and Bloecher[35] found the adsorption completely reversible, indicative of physical adsorption.[36] Somasundaran et al.[37] found that the cohesive energy per CH_2 group in the hydrocarbon chain was independent of chain length for primary amines and thus concluded adsorption only occurs in the outer electrical double layer.

Sutherland and Wark[38] and Danilov[39] support an ion exchange mechanism whereby the dissociated amine ion is exchanged for a cation on the surface. Taggart and Arbiter[40]

are of the opinion that an insoluble hydrophobic salt is formed on the quartz surface. Lidstrom[41], using potentiometric techniques, found the adsorption of amines on silicates obeyed chemical laws. He concludes that below pH 9, aminium ions react with ions on the silicate surface, while at higher pH's the reaction occurs between free amine and the silicate surface.

The adsorption of amines on quartz has been found to obey the Freundlich equation.

$$\Gamma = KC^n \qquad (19)$$

where Γ is the amount of adsorbed amine, C is equilibrium concentration, and K and n are constants.

Somasundaran et al.[36] and Gaudin[37] found this relationship to hold at low concentrations, while at higher concentrations adsorption increases rapidly. This phenomenon is explained in terms of the hemi-micelle hypothesis.[37] When the concentration at the surface reaches a critical value, the critical hemi-micelle concentration, the hydrocarbon chains associate with each other through Van der Waal forces. This phenomenon is analogous to the formation of micelles in solution. Calculations indicate that at the critical hemi-micelle concentration, the concentration of amine in the double layer is very close to the critical micelle concentration in the bulk solution.[42]

Sandvik et al.[43] found that adsorption obeyed the Freundlich equation up to the critical micelle concentration. They also found that increasing the length of the hydrocarbon chain increased the slope of the $\log \Gamma$ - log C plot suggesting that the hydrocarbon chain influenced the quartz-amine bond.

Sandvik also found that the method of preparation of quartz had a marked effect on adsorption. Infra-red studies show that the surface changes continually on drying due to dehydration. If drying is carried out at temperatures above 400°C, rehydration is very difficult. Due to dehydration, amine adsorption increases as temperature of drying increases. This is explained in terms of competition between water and amine for the surface sites. If rehydration is difficult, amine is easily adsorbed, while, if rehydration can occur easily, water is adsorbed on the surface, and consequently fewer surface sites are available for amine adsorption.

It is generally agreed that adsorption increases with pH,[41-47] with an increase of approximately tenfold between pH 8 and pH 10. This rapid increase is a result of the association of the adsorbed amine (hemi-micelle formation).

Amines are good collectors for quartz.[30,36,39-41] Optimum recovery occurs between pH 8 and pH 10. Recoveries as high as 100% have been reported with between 5 and 10% monolayer coverage.[36]

Recent work has introduced the concept of adsorption of amine on quartz surface by means of transfer from the air-liquid interface to the air-solid interface[48,49] to account for such high recoveries at low adsorption densities. Using surface tension measurements and applying the Gibb's equation, it was shown that the adsorption density at the liquid-air and the air-solid interface is much greater than at the solid-liquid interface.[48] When a particle becomes attached to a bubble, complimentary adsorption can occur on the mineral surface. Preliminary tests[49,50] support this hypothesis.

QUARTZ-AMINE-STARCH

The most promising flotation scheme for concentrating hematite appears to be cationic flotation of quartz, using amines as collectors, and depression of hematite with starches.[51-55] Anionic flotation of hematite gives good metallurgical results but reagent costs are high.[51]

The interaction of starch and amine in solution and on mineral surfaces, is not clearly understood. This is due, in part, to the difficulty in determining the exact nature of the starch in solution. Starch degradates in solution and as a result the exact molecular weight is unknown. The probable mechanism of adsorption of starch on quartz is thought to be a combination of hydrogen bonding between starch and surface hydroxide layer of quartz, and electrostatic forces.[53]

It has been reported that starch has little effect on adsorption of amine on quartz.[56] On the other hand, dodecylamine has been shown to enhance starch adsorption[56] up to a critical amine concentration. Further amine additions decrease starch adsorption.

Much evidence is available which indicates that a starch-amine complex may be formed in solution. Starch is known to adsorb organic solvents[57] and divalent and trivalent ions from solution.[58] The amylose helix is capable of expansion to permit inclusion of foreign molecules.[59] The depressant effect of starch in oleate flotation of calcite has been attributed to starch-oleate complexing.[60] Amine derivatives of amylose, amylopectin, potato and corn starch have been reported.[61] Adsorption isotherms of starch, amine and starch-amine combinations on hematite have been explained on the basis of amine-starch complex formation.[62]

III. STATEMENT OF INTENT

Several workers have studied the quartz-amine-starch system[51-56] with its applicability to the concentration of hematite ores by reverse flotation. Many of the discrepancies which exist in the literature are due to variations in mineral sources, laboratory techniques, and reagent sources and preparation..

It was felt that an extensive study of the adsorption characteristics of dodecylamine and starch on quartz and its relationship to floatability may help to correlate much of the published data. A comparison between this study and a similar study with hematite recently completed in this laboratory is made.

Tritium tagged amine and carbon-14 tagged starch were used in this study. Analysis for amine and starch in the test solutions was carried out by simultaneous scintillation counting of tritium and carbon-14. The amine concentrations studied were in the range zero to 10^{4} μmole/l. The starch concentrations used were in the range zero to 1000 mg/l. The pH of the test solutions studied varied from 2 to 12.

IV. EXPERIMENTAL

MATERIALS AND CHEMICALS

Quartz

The quartz was crushed from 6 inch diameter to -20 mesh using laboratory jaw and gyratory crushers. The crushed material was ground dry in an Abbé ball mill for 10 minutes. The ground quartz was screened using Tyler standard sieves. The -400 mesh fraction was discarded and the +325 mesh fraction was recycled for further grinding. The -325, +400 mesh fraction was wet screened to insure the removal of all the -400 mesh material. This product was passed through a Davis tube (Dings model "TT") to remove any magnetic material. The heavier non-magnetic material was removed on a Haultain Superpanner. The remaining product was cleaned in 10% hydrochloric acid solution for a minumum of 12 hours. The final product was washed with conductivity water until no acid was present in the wash water as indicated by pH measurements. The quartz was dried at 150^{o}C, mixed well and stored under moderate vacuum (approximately 100 Torr) to protect against atmospheric contamination. This procedure is similar to that used by Partridge[62], Smith[63], and Oko[64].

X-ray diffraction analysis confirmed the presence of

quartz and no other crystalline materials. Spectographic analysis gave the impurities shown in Table 1.

TABLE I

QUARTZ ANALYSIS

Impurity	Percent
Fe	$\approx$.002
Cu	$<$.003
Al	$<$.003
Mg	trace
Mn	trace

The specific surface area was 4273 cm^2/gm as determined by the B.E.T.. The surface area available to positive ions, determined with 1-hexadecylpyridinium bromide at pH 8, 9.7 and 12, was 592 cm^2/gm, 1734 cm^2/gm, and 2748 cm^2/gm respectively. Details are presented in Appendix III.

Dodecylamine

The dodecylamine was obtained from Aldrich Chemical Co. and was subsequently purified by Partridge[62]. A one gram sample was sent to Amersham-Seale Co. for tritiation.

Since dodecylamine is only slightly soluble in water, it was converted to the more soluble acetate salt for subsequent use.[65] The salt was made by dissolving a known amount of amine in benzene and adding a stoichiometric amount

Of glacial acetic acid. On cooling to 12°C, dodecylammonium acetate precipitated from solution. The product was filtered, washed with clean benzene and dried under vacuum to constant weight. The yield was approximately 85% of theoretical. Two batches of tritium tagged amine were used with specific activities of 47 μCi/gm and 354 μCi/gm.[62] The melting point of the product was 68.4 ± 0.2°C [62] as compared to the published range of 68.5°C - 69.0°C.[64] The phase change occurred over a very narrow temperature range indicating a high purity product.

Starch

Soluble starch (corn starch) was purchased from British Drug House Ltd. for use in this study. The starch was dried at 150°C to constant weight and stored in a dessicator.

A second starch, tagged with carbon-14 was obtained from Amersham-Seale Corp. This starch was isolated from tobacco leaves which had been allowed to photosynthesize in a $^{14}CO_2$ atmosphere for 12 hours. The specific activity is given as 26 μCi/mg. It is assumed that any difference in the two starches would be insignificant after the extensive degradation which occurs during causticization.

Conductivity Water

Double distilled, nitrogen saturated water was used in

all experiments. The water was distilled in a "Precision" brand laboratory still, and redistilled in an all-Pyrex Yoe-type still (Corning Model AG-2). Carbon dioxide, which forms insoluble carbonates with amine, was removed by bubbling high purity nitrogen until the pH became constant, at approximately 7.2.

Nitrogen

Nitrogen, (grade L) obtained from Canadian Liquid Air Ltd., was certified 99.99% pure, and no further purification was required before use.

Sodium Hydroxide

A saturated solution of sodium hydroxide was made and allowed to stand for two weeks. Finely divided carbonates settled out and the pure solution was siphoned off, diluted with conductivity water and the normality determined by titration against reagent grade oxalic acid.[62]

Standard Activity Solutions

Two standards, one tritium and one carbon-14 were required to calibrate the scintillation solution.

(i) Tritium Standard

A solution of exactly 10^{-3} molar amine was prepared using tritiated amine acetate with specific

activity of 354 μCi/gm on May 15, 1970. The activity of the solution was found to be F x 1.9348 x 10^5 dpm/cc where F is a correction factor for decay after assay date.

(ii) Carbon-14 Standard

Two carbon-14 standards were prepared. The first was made using ^{14}C-benzoic acid. The benzoic acid was mixed with 100% excess 1 N NaOH and heated at 50°C for approximately 12 hours. The solution was diluted to 100 ml and had a specific activity of 3.1185 x 10^4 dpm/cc.

A second series was prepared using ^{14}C tagged starch used in the adsorption tests. A weighed portion was causticized and diluted to give a solution with a specific activity of 8.648 x 10^3 dpm/cc. Excellent agreement between the two series was obtained in calibrating the scintillation solution.

Other Reagents

All other reagents used were of the highest purity generally available. These include:

Acetic Acid	C.P. Reagent Grade
Hydrochloric Acid	C.P. Reagent Grade
and the components of the scintillation solution	
1-4 Dioxane	Cert. A.C.S.
P.P.O. (2,5 diphenyloxazole)	Scintillation Grade
Naphthalene	Recrystallized from alcohol

EXPERIMENTAL PROCEDURES

Starch-Amine-Solution Preparation

Stock solutions of tritiated amine were prepared, as required, at concentrations of 10^{-1}, 10^{-2}, 10^{-3}, and 10^{-4} molar. The high activity amine acetate (354 μCi/gm) was used to prepare the stock solutions at 10^{-3} and 10^{-4} molar concentrations. The 10^{-2} molar solution was prepared using the low activity amine acetate (47 μCi/gm). The 10^{-1} molar solution was made using an arbitrary mixture of tritiated amine and untagged amine. The stock solutions were diluted by a factor of ten for the adsorption tests.

Starch solutions were prepared immediately prior to each test. A solution, ten times as concentrated as the test solutions, was prepared. The required amount of untagged starch was weighed and a small amount of tagged starch was then added. The amount of tagged starch used was in the order of 0.5 mg. The starch solutions were causticized using the following procedure.

A 3% (w/w) solution of starch in 0.5 N NaOH was heated in a water bath at 100°C for 15 minutes. The solution was rapidly cooled to room temperature and diluted to 100 ml. This procedure is similar to that used by Iwasaki[52,53] and Partridge.[62]

To prepare the test solutions,10 ml of the starch and amine solutions were combined with approximately 50 ml of conductivity water. The pH was adjusted using HCl or NaOH and the contents of the beaker washed into a 100 ml volumetric flask and diluted to the final concentration. This was sufficient solution to run a test in duplicate.

Adsorption

The adsorption tests were carried out in Pyrex glass vials with an average volume of 48.0 $\pm$ 0.1 cc. When filled with two grams of quartz, the average volume remaining, was 47.3 $\pm$ 0.1 cc.

Two grams of quartz was accurately weighed into each vial. The vials were then filled with the appropriate solution, capped with rubber serum stoppers, the remaining air bubbles being removed with a syringe. The vials were rotated end over end at 16 r.p.m. to equilibrium. Preliminary tests indicated that 10 hours was sufficient time for equilibrium to be established (see Appendix II).

Following each test, the quartz was allowed to settle and three 1 ml samples were taken from each vial for scintillation counting. Triplicate samples were also taken of the initial solution to determine the initial activity. Adsorption on the mineral surface was taken as the difference between the

initial and final concentrations. Adsorption on the vials was assumed to be negligible as the surface area of the smooth vials was small compared to the surface area of the quartz. The final pH of each solution was measured using the Metrohm model E-300 pH meter.

Flotation

A modified Hallimond tube designed, constructed and described by Partridge[62] was used for the flotation tests. A schematic drawing of the cell is shown in Fig. 2. The products from the adsorption tests were used as feed for the flotation tests. A mercury manometer was used for accurate pressure readings. The nitrogen gas flow was controlled by a needle valve and measured by a #1 Gilmont spherical flow-meter. The nitrogen flow rate used was 20 cc/min. at S.T.P. The gas control system is shown schematically in Fig. 3. The flotation time was 30 seconds. Both sink and float products were filtered, dried and weighed.

The cell was washed well with distilled water between each test and left immersed in dilute HCl solution between each series of tests.

FIGURE 2

SCHEMATIC DRAWING OF

FLOTATION CELL

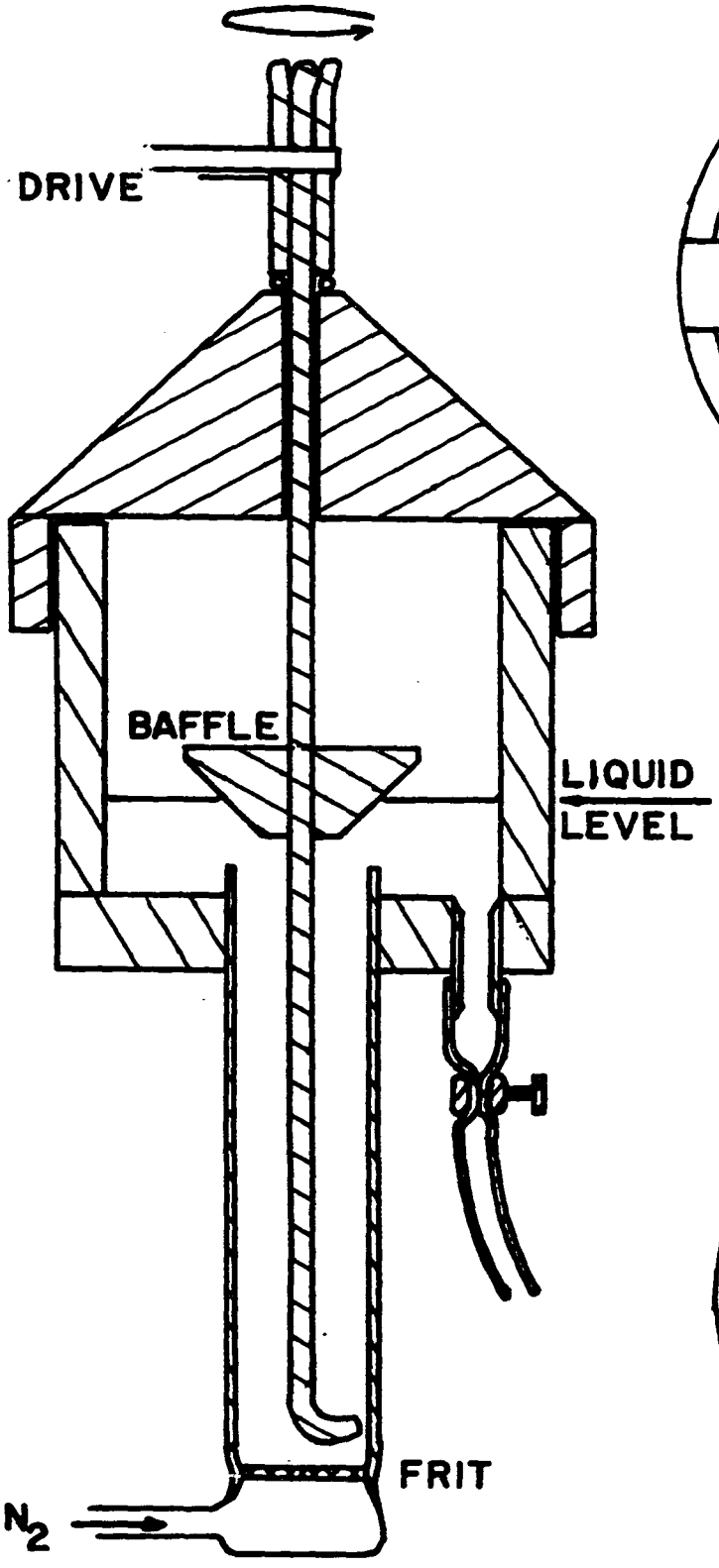

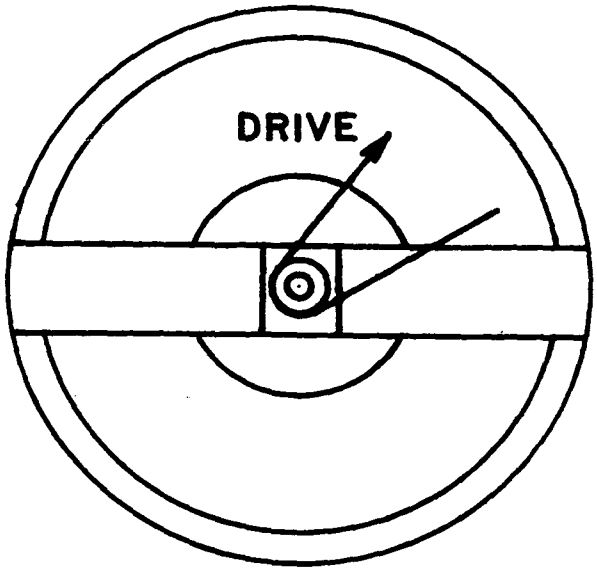

UPPER SECTION PLAN

1 cm

LOWER SECTION PLAN

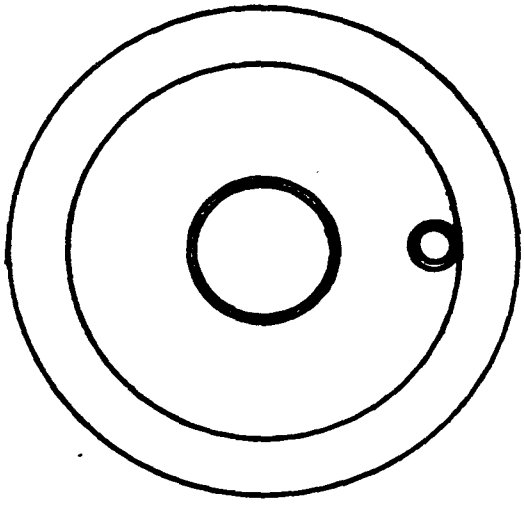

SECTION THROUGH CELL ASSEMBLY

FIGURE 3

GAS CONTROL SYSTEM FOR

FLOTATION CELL

C - Nitrogen Cylinder
R - Pressure Regulator
M - Mercury Manometer
F - Flowmeter
N - Needle Valve
S - 3 - Way Stopcock
B - Ball Joint

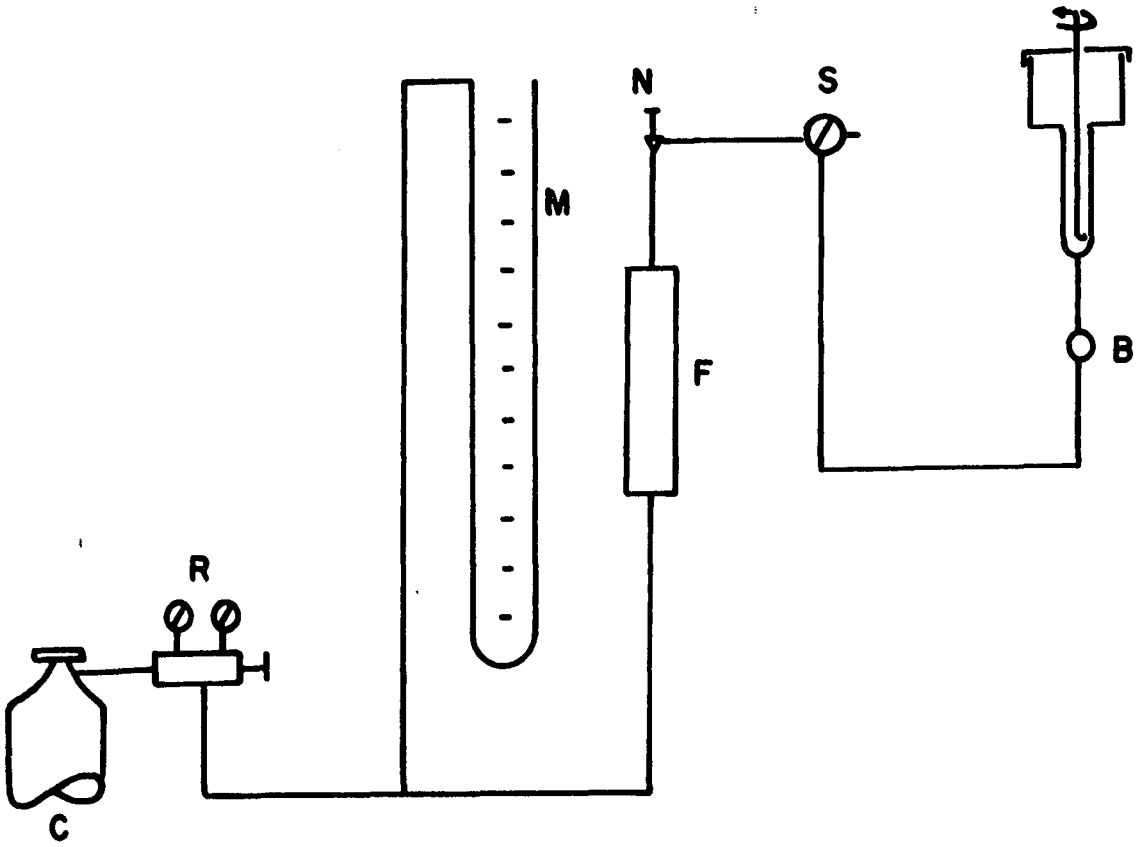

V. EXPERIMENTAL RESULTS

ADSORPTION

The adsorption density of amine is shown as a function of amine concentration at pH 4, 7 and 10 (Fig. 4-6). In dilute acidic solutions, the slope of the log Γ - log C plot is linear with slope of approximately 0.67. In concentrated solutions the slope increases to approximately 1.20. Starch additions increase the slope in dilute amine solutions and decrease the slope in concentrated amine solutions. Small starch additions enhance amine adsorption in dilute solutions but decrease amine adsorption in concentrated amine solutions. In alkaline solutions, amine adsorption decreases with increasing starch additions.

Amine adsorption is plotted as a function of starch concentration at pH 4, 7, 10 and 12 (Fig. 7-10). For dilute acidic amine solutions, amine adsorption is seen to increase with starch additions up to 400 mg/l and was decreased at 1000 mg/l starch. In concentrated amine solutions, even small amounts of starch decreased amine adsorption. The adsorption of amine is decreased with increasing starch concentration in alkaline solutions.

The effect of pH on amine adsorption at constant starch concentrations is shown in (Fig. 11-14). In general, adsorption

FIGURE 4

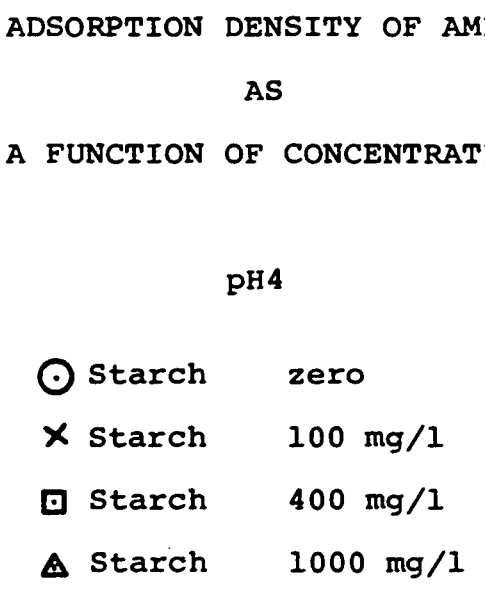
ADSORPTION DENSITY OF AMINE
AS
A FUNCTION OF CONCENTRATION
pH4
Starch zero
Starch 100 mg/l
Starch 400 mg/l
Starch 1000 mg/l

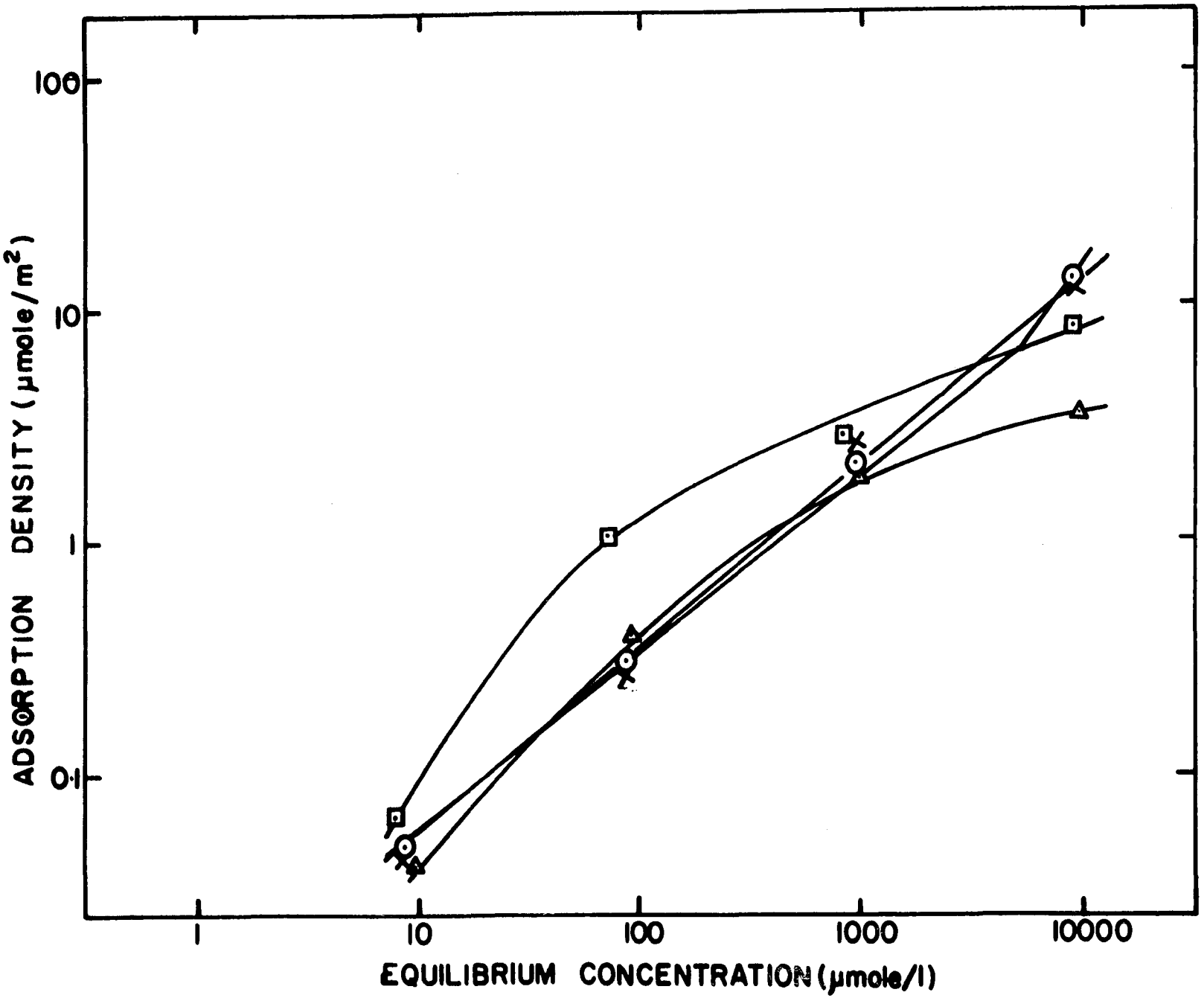
100
10
1
0.1
ADSORPTION DENSITY (μmole/m²)
1
10
100
1000
10000
EQUILIBRIUM CONCENTRATION (μmole/l)

FIGURE 5

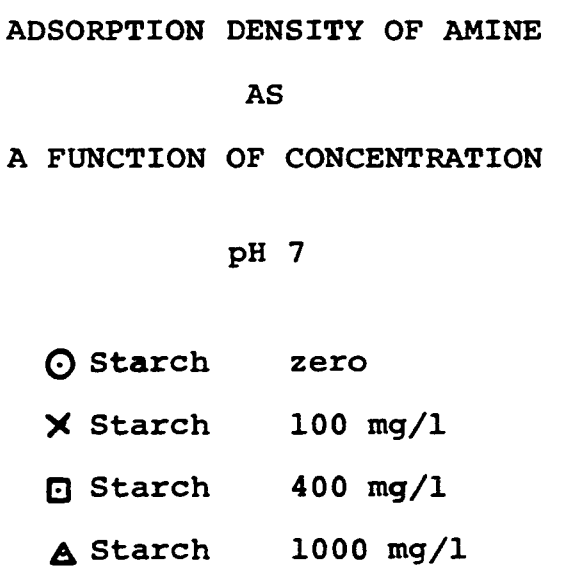
ADSORPTION DENSITY OF AMINE
AS
A FUNCTION OF CONCENTRATION
pH 7
⊙ Starch zero
✕ Starch 100 mg/l
⊡ Starch 400 mg/l
△ Starch 1000 mg/l

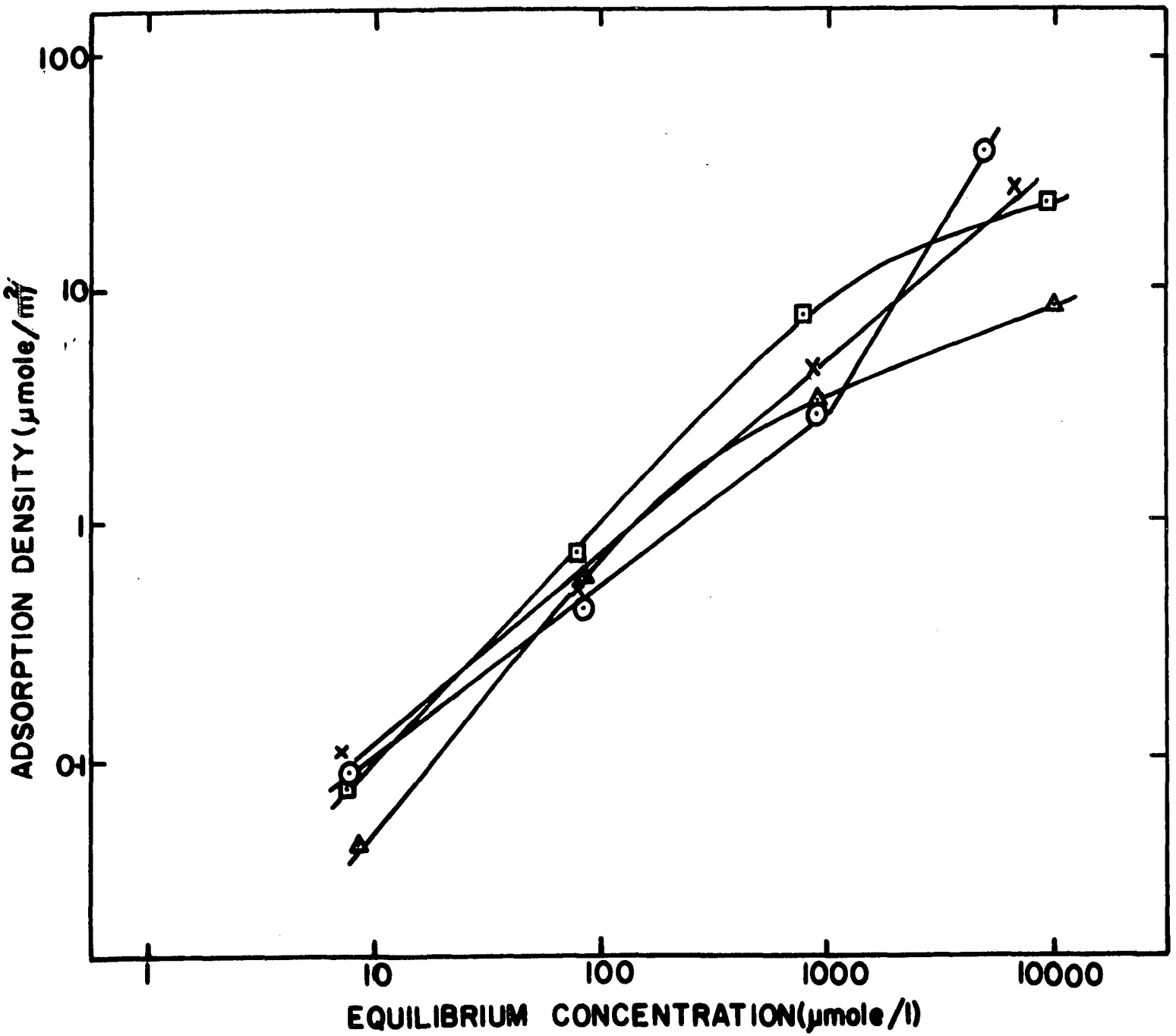
100
10
1
0.1
ADSORPTION DENSITY (μmole/m²)
1
10
100
1000
10000
EQUILIBRIUM CONCENTRATION(μmole/l)

FIGURE 6

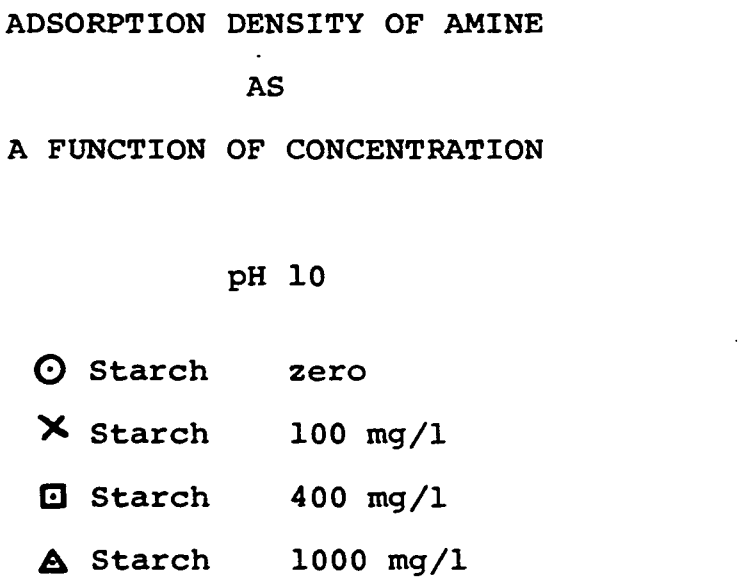
ADSORPTION DENSITY OF AMINE
AS
A FUNCTION OF CONCENTRATION
pH 10
Starch zero
Starch 100 mg/l
Starch 400 mg/l
Starch 1000 mg/l

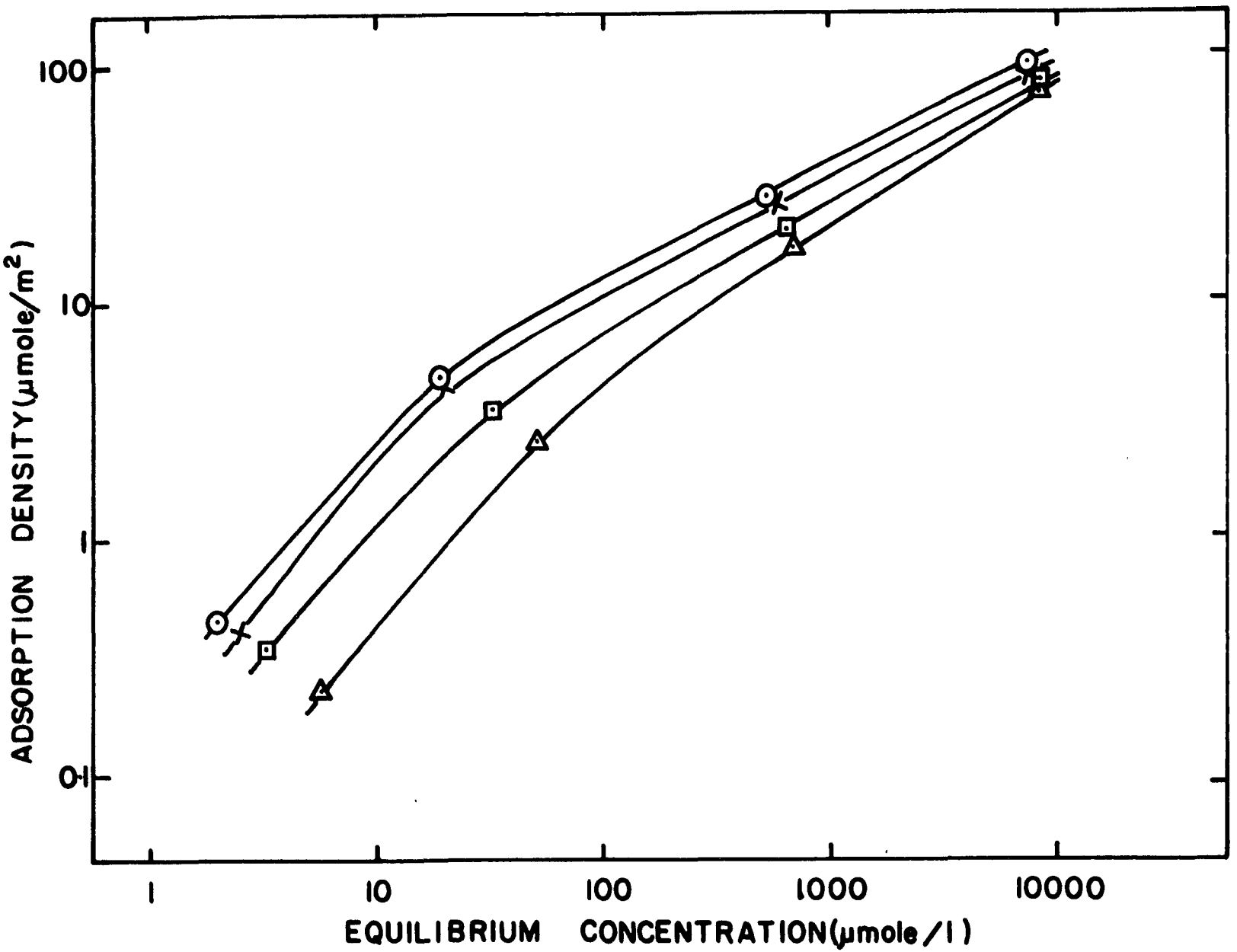
100
10
1
0.1
ADSORPTION DENSITY(μmole/m²)
1
10
100
1000
10000
EQUILIBRIUM CONCENTRATION(μmole/l)

FIGURE 7

ADSORPTION DENSITY OF AMINE

AS A FUNCTION OF

INITIAL STARCH CONCENTRATION

Amine - 10 μmole/l

× pH 4

⊙ pH 7

⊡ pH 10

△ pH 12

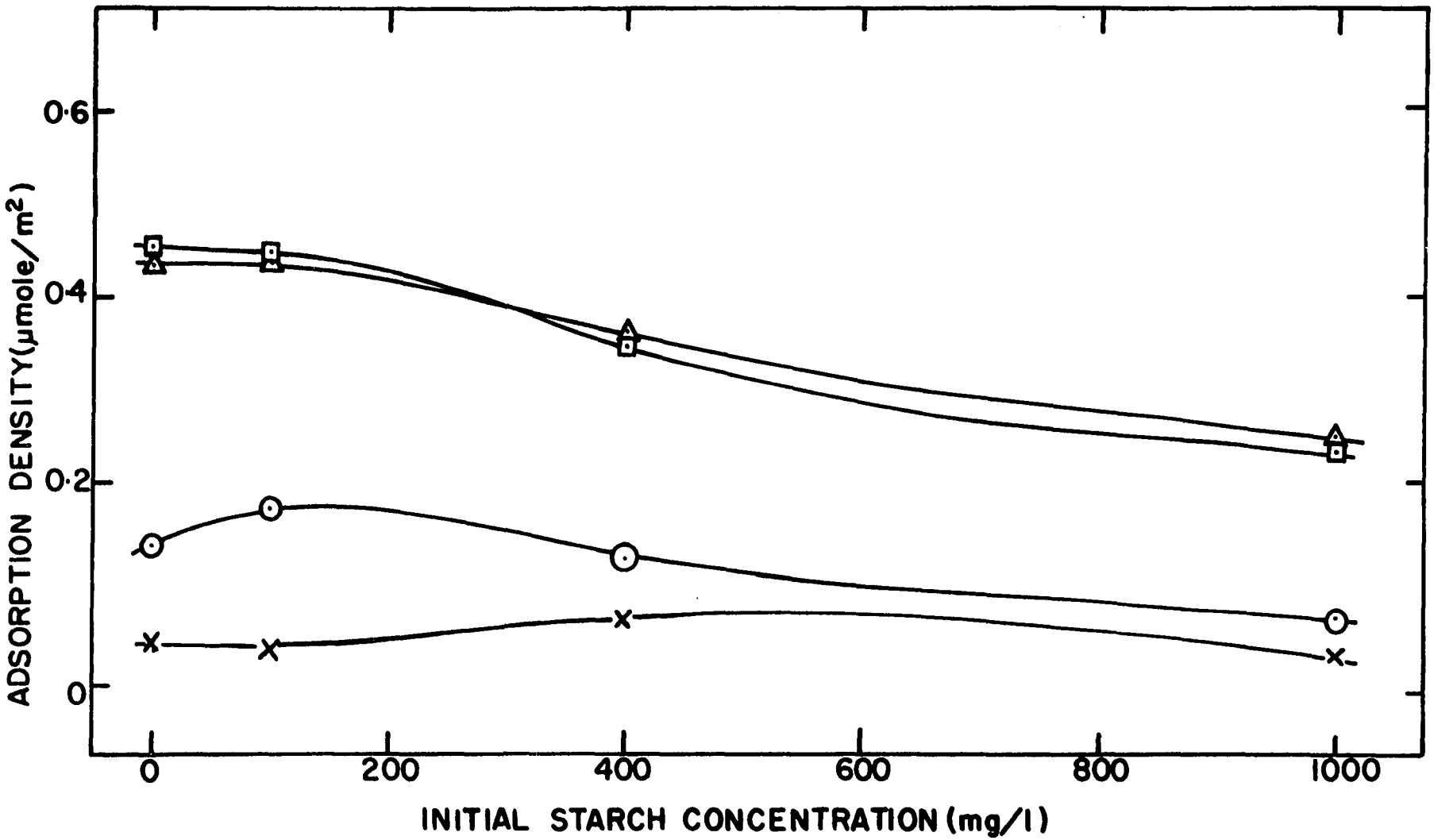
0·6
0·4
0·2
0
ADSORPTION DENSITY(μmole/m²)
0
200
400
600
800
1000
INITIAL STARCH CONCENTRATION (mg/l)

FIGURE 8

ADSORPTION DENSITY OF AMINE

AS A FUNCTION OF

INITIAL STARCH CONCENTRATION

Amine - 100 μmole/l

pH 4

pH 7

pH 10

pH 12

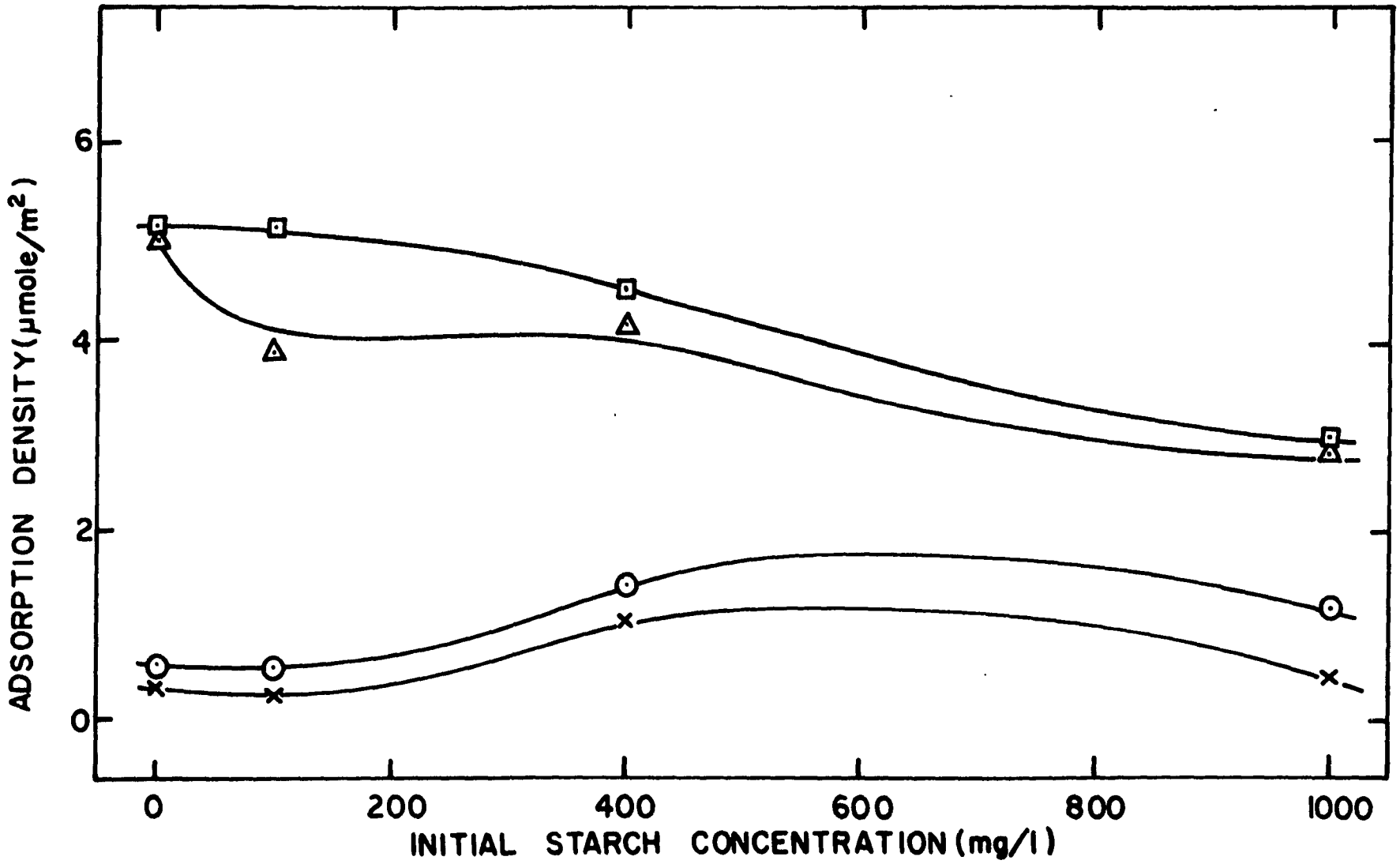
ADSORPTION DENSITY (μmole/m²)
6
4
2
0
0
200
400
600
800
1000
INITIAL STARCH CONCENTRATION (mg/l)

FIGURE 9

ADSORPTION DENSITY OF AMINE

AS A FUNCTION OF

INITIAL STARCH CONCENTRATION

Amine - 1000 μmole/l

× pH 4

⊙ pH 7

⊡ pH 10

△ pH 12

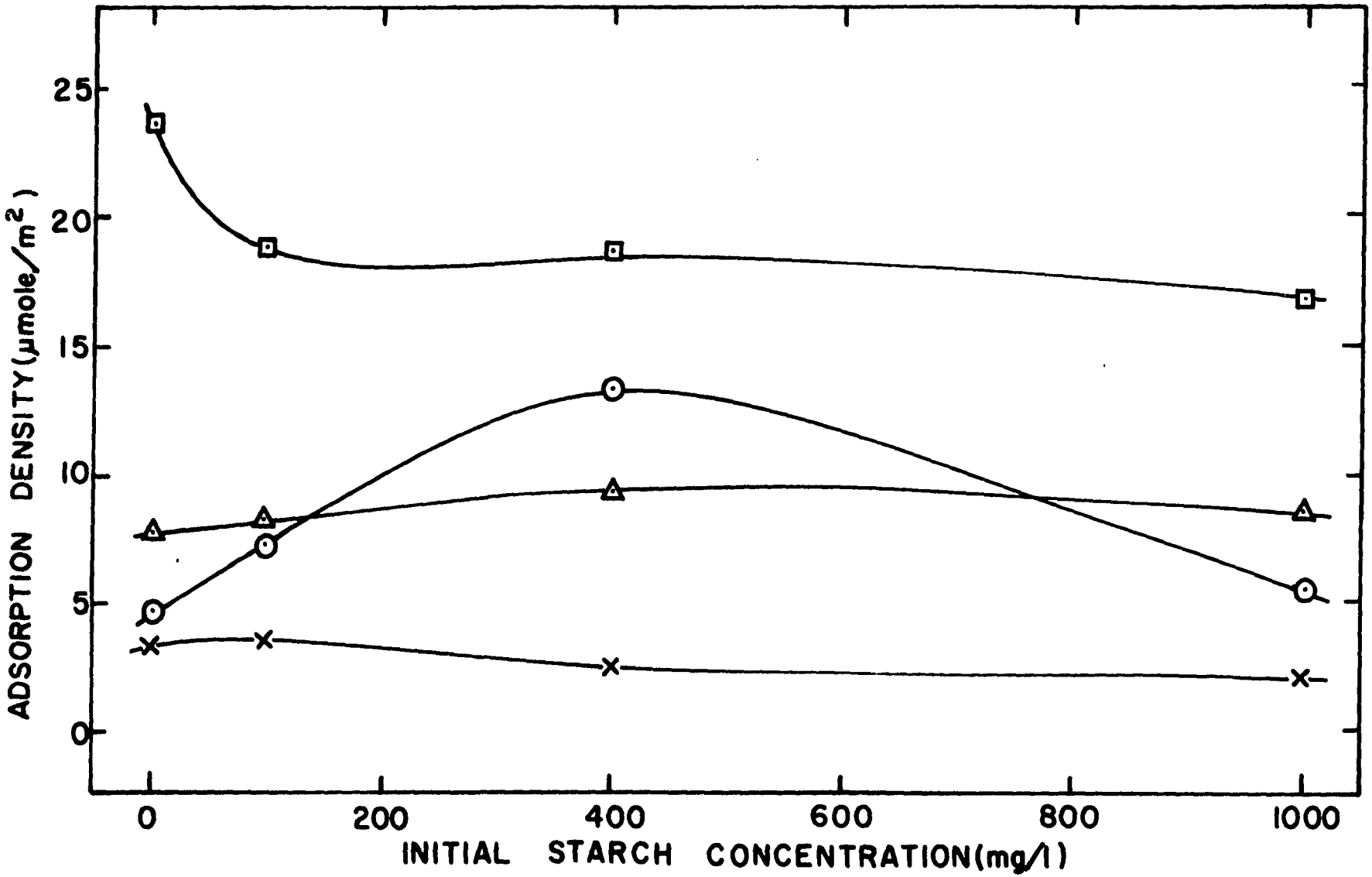
ADSORPTION DENSITY (μmole/m²)
25
20
15
10
5
0
0
200
400
600
800
1000
INITIAL STARCH CONCENTRATION(mg/l)

FIGURE 10

ADSORPTION DENSITY OF AMINE

AS A FUNCTION OF

INITIAL STARCH CONCENTRATION

Amine - 10,000 μmole/l

× pH 4

⊙ pH 7

⊡ pH 10

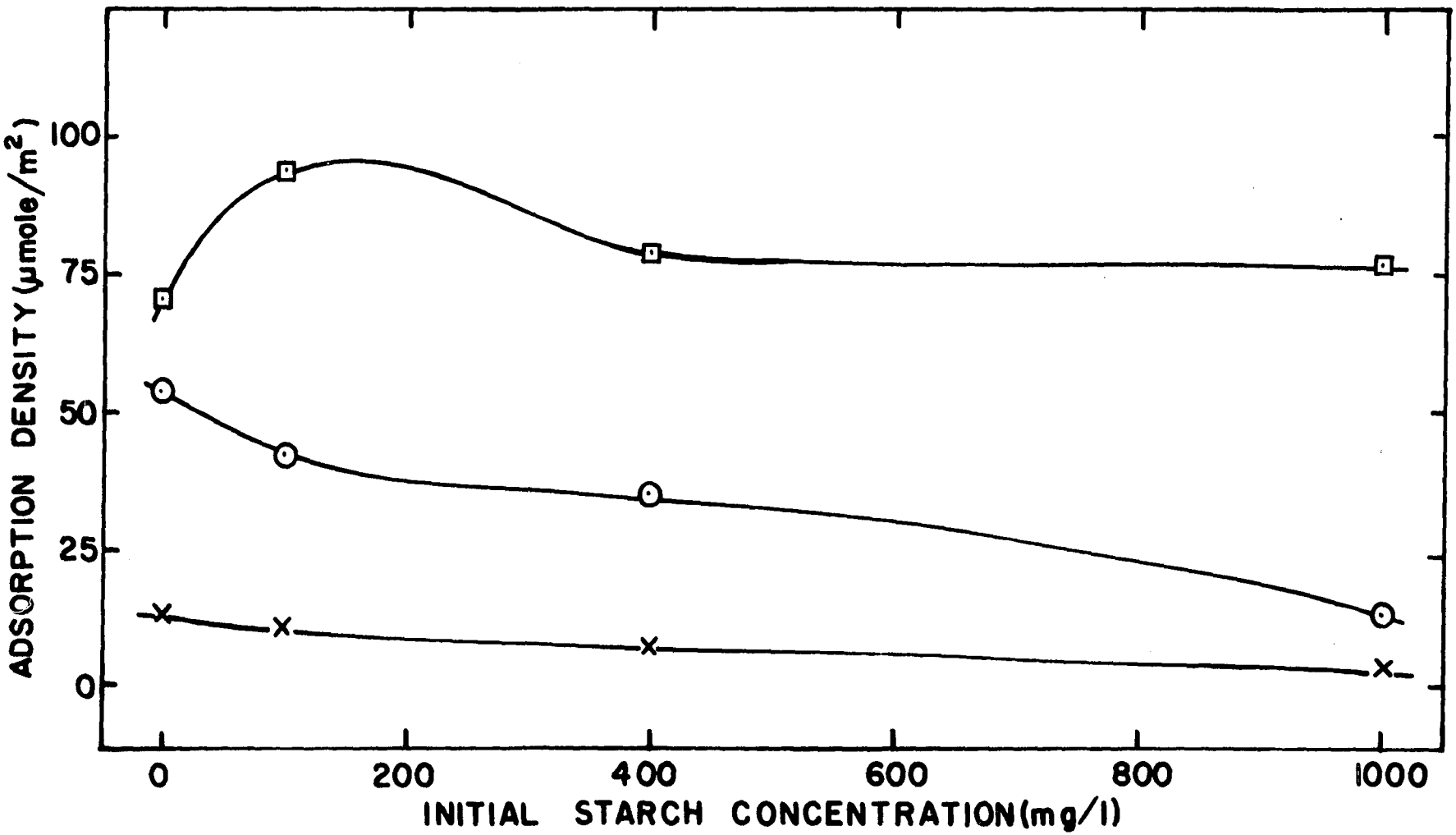
ADSORPTION DENSITY (μmole/m²)
100
75
50
25
0
0
200
400
600
800
1000
INITIAL STARCH CONCENTRATION (mg/l)

FIGURE 11

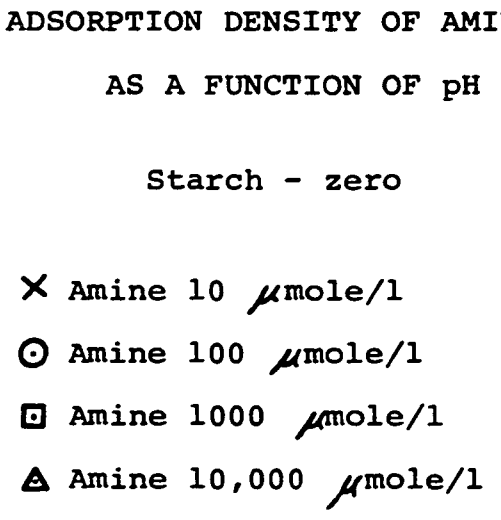
ADSORPTION DENSITY OF AMINE
AS A FUNCTION OF pH
Starch - zero
Amine 10 μmole/l
Amine 100 μmole/l
Amine 1000 μmole/l
Amine 10,000 μmole/l

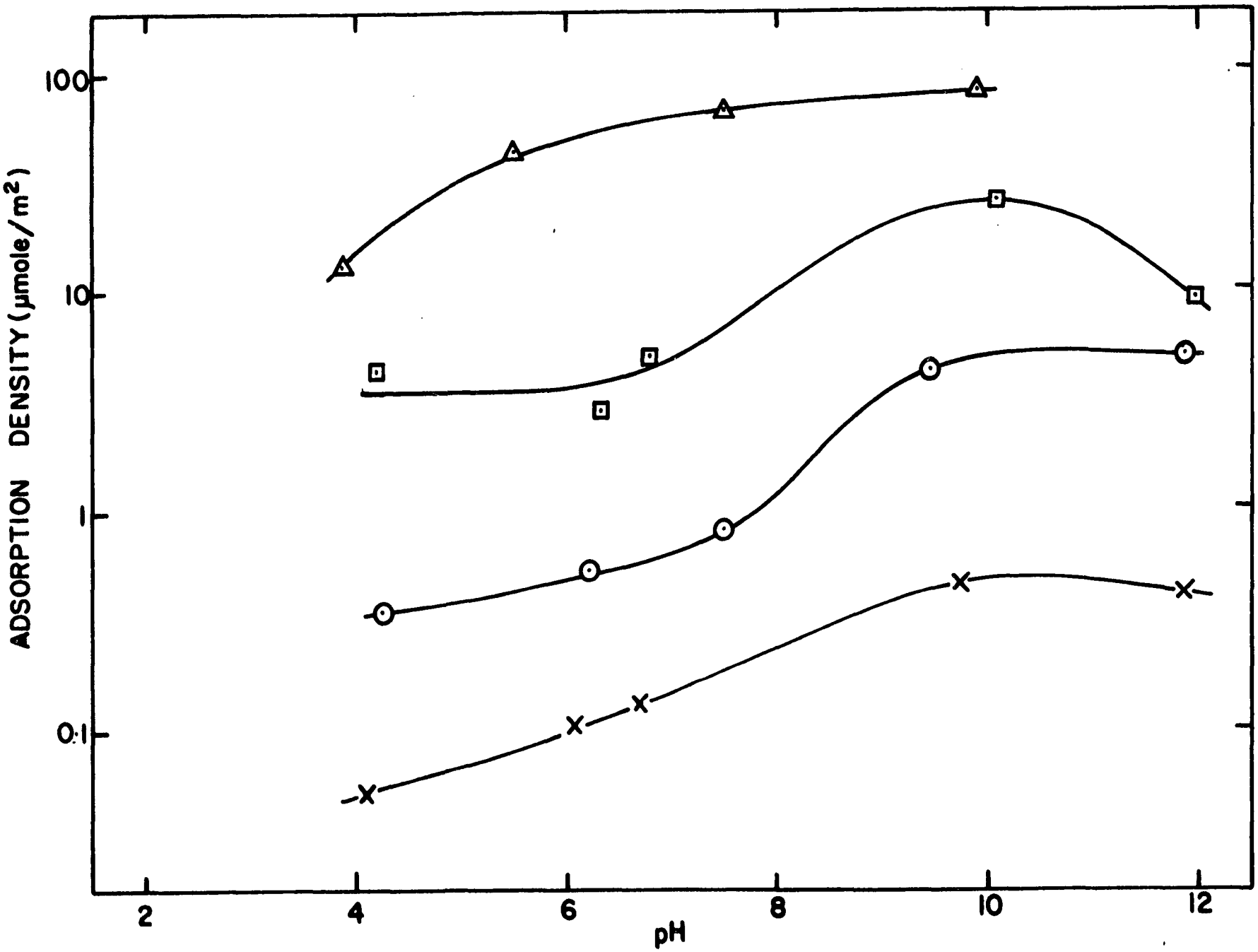
ADSORPTION DENSITY (μmole/m²)
100
10
1
0.1
2
4
6
8
10
12
pH

FIGURE 12

ADSORPTION DENSITY OF AMINE

AS A FUNCTION OF pH

Starch - 100 mg/l

× Amine 10 μmole/l

⊙ Amine 100 μmole/l

⊡ Amine 1000 μmole/l

△ Amine 10,000 μmole/l

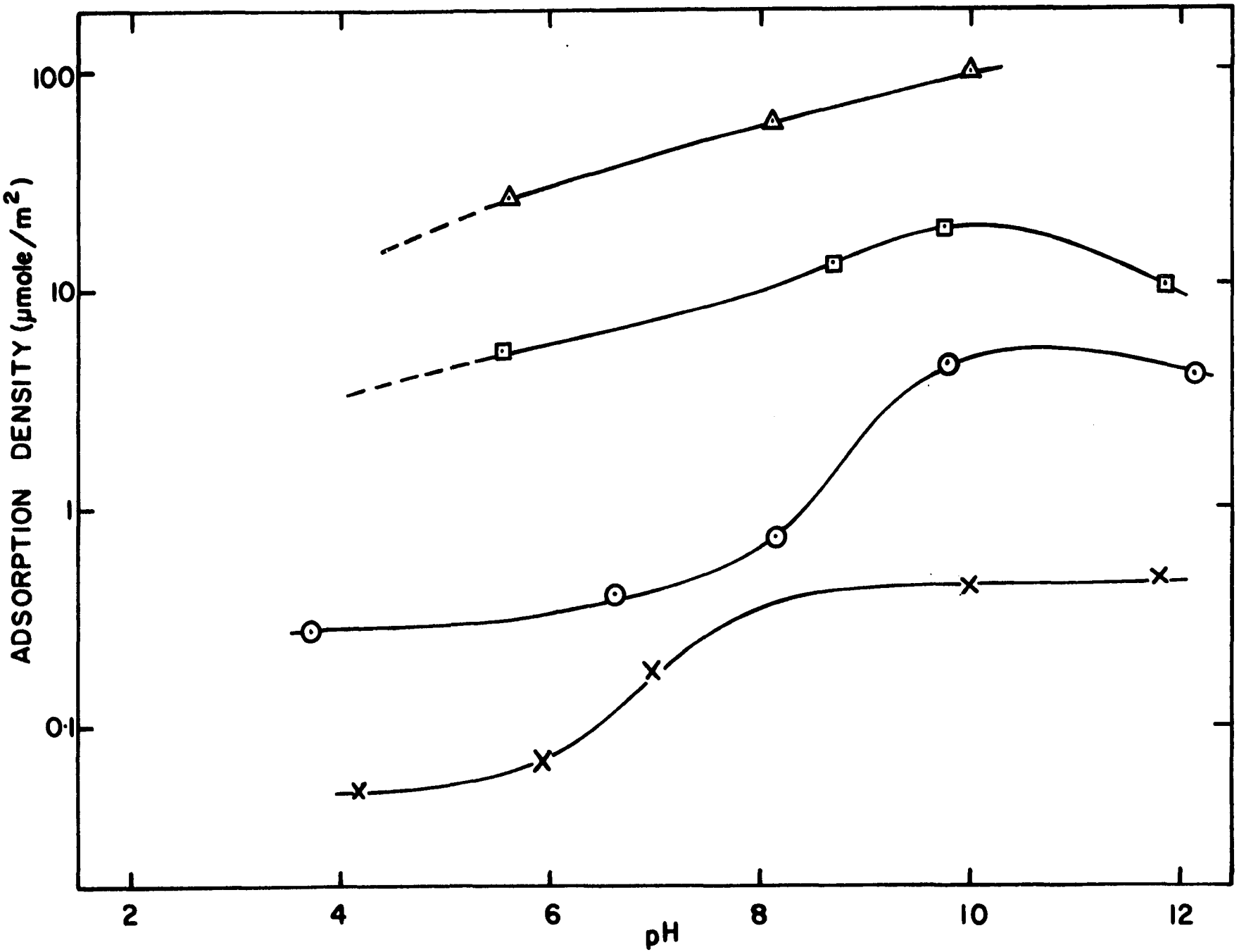
ADSORPTION DENSITY (μmole/m²)
100
10
1
0·1
2
4
6
8
10
12
pH

FIGURE 13

ADSORPTION DENSITY OF AMINE

AS A FUNCTION OF pH

Starch - 400 mg/l

× Amine 10 μmole/l

⊙ Amine 100 μmole/l

⊡ Amine 1000 μmole/l

◬ Amine 10,000 μmole/l

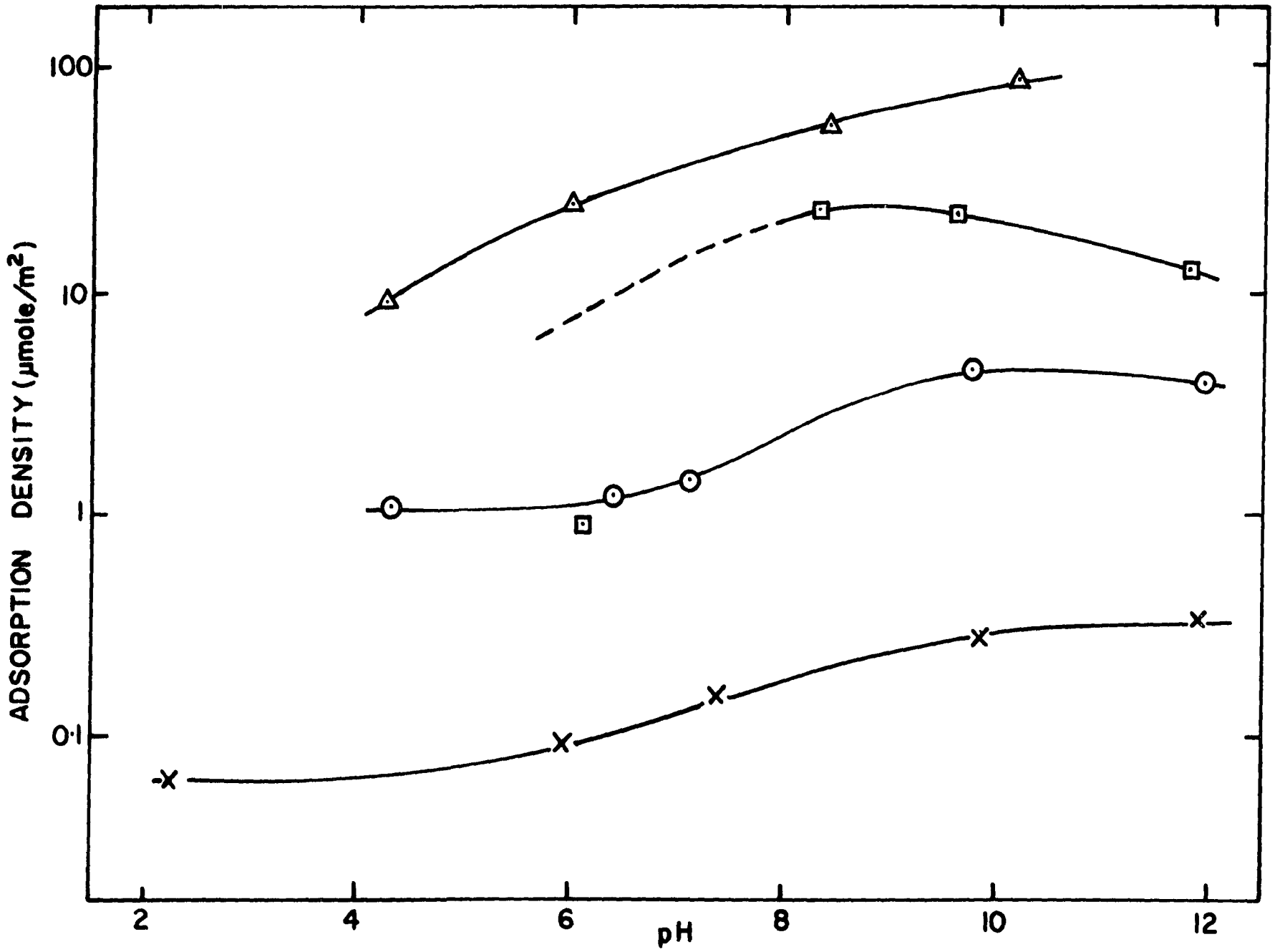
ADSORPTION DENSITY (μmole/m²)
100
10
1
0·1
2
4
6
8
10
12
pH

FIGURE 14

ADSORPTION DENSITY OF AMINE

AS A FUNCTION OF pH

Starch - 1000 mg/l

✕ Amine 10 μmole/l

⊙ Amine 100 μmole/l

⊡ Amine 1000 μmole/l

◬ Amine 10,000 μmole/l

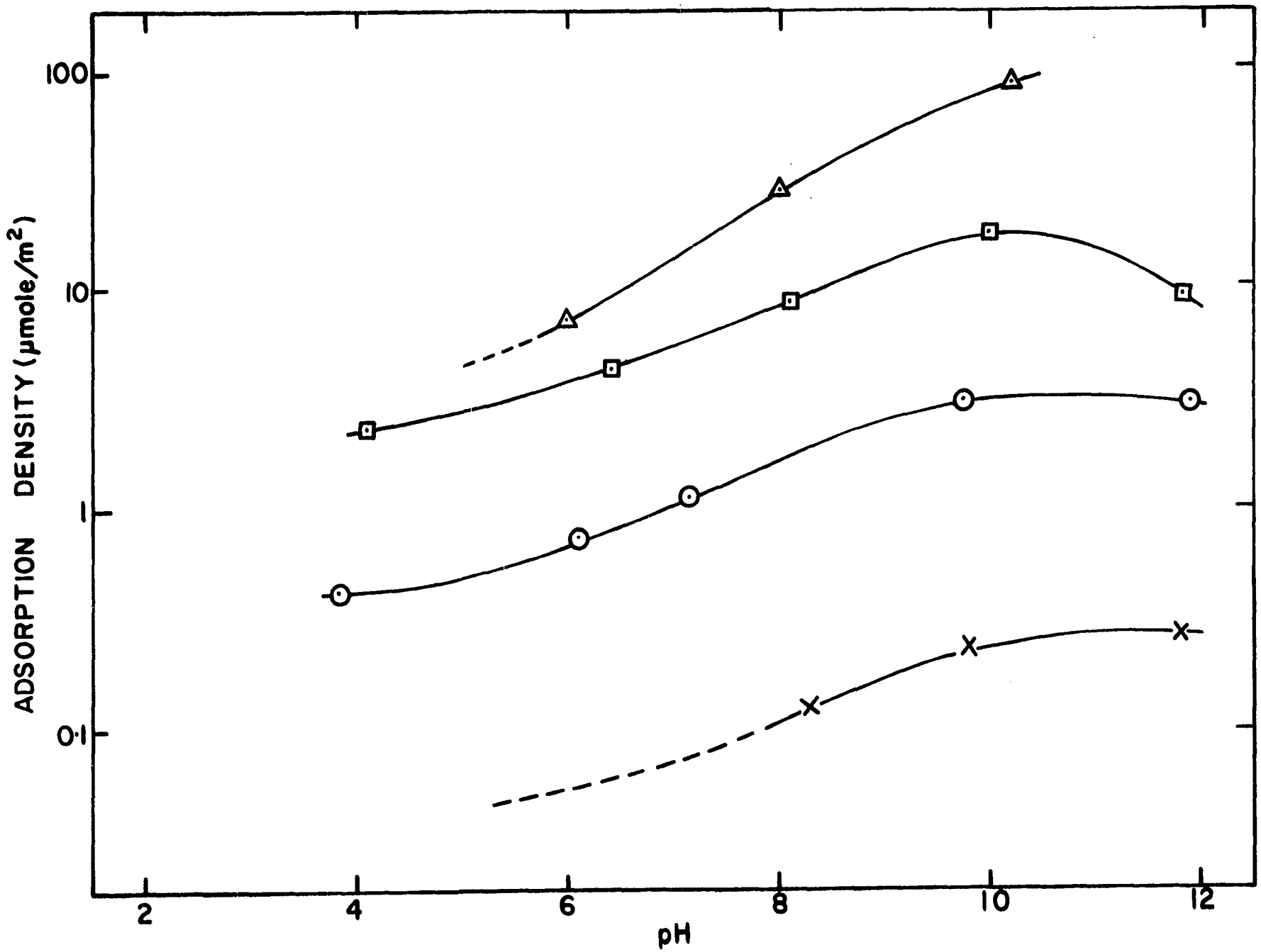
100
10
1
0.1
ADSORPTION DENSITY (μmole/m²)
2
4
6
8
10
12
pH

increased slowly with pH up to approximately pH 8. Between pH 8 and 10, adsorption density of amine increased approximately four fold. Between pH 10 and 12, amine adsorption remained constant in dilute amine solutions, but decreased in more concentrated solutions.

In neutral and acidic solutions, starch adsorption, in the absence of amine, was very low and appeared to be masked by experimental error. Adsorption density of starch is plotted as a function of pH and amine concentration (Fig. 15-16). The adsorption of starch obtained for 100 mg/l starch appeared to be very low and comparable to the experimental errors. Increasing amine concentration enhanced starch adsorption up to 100 μmole/l amine. At higher amine concentrations, adsorption of starch decreased becoming negligible at 10,000 μmole/l amine. Starch adsorption increased with pH with a sharp increase between pH 10 and pH 12.

FLOTATION

The flotation results are shown as a function of pH and amine concentrations at constant starch additions (Fig. 17-20) and as a function of pH and starch concentration at constant amine additions (Fig. 21-24).

In general, floatability increased with amine concentrations up to 1000 μmole/l amine and decreased at 10,000 μmole/l. Floatability reached a maximum between pH 8 and 10 and

FIGURE 15

ADSORPTION DENSITY OF STARCH

AS A FUNCTION OF

AMINE CONCENTRATION AND pH

Starch - 400 mg/l

⊙ Amine zero

× Amine 10 μ mole/l

⊙ Amine 100 μ mole/l

△ Amine 1000 μ mole/l

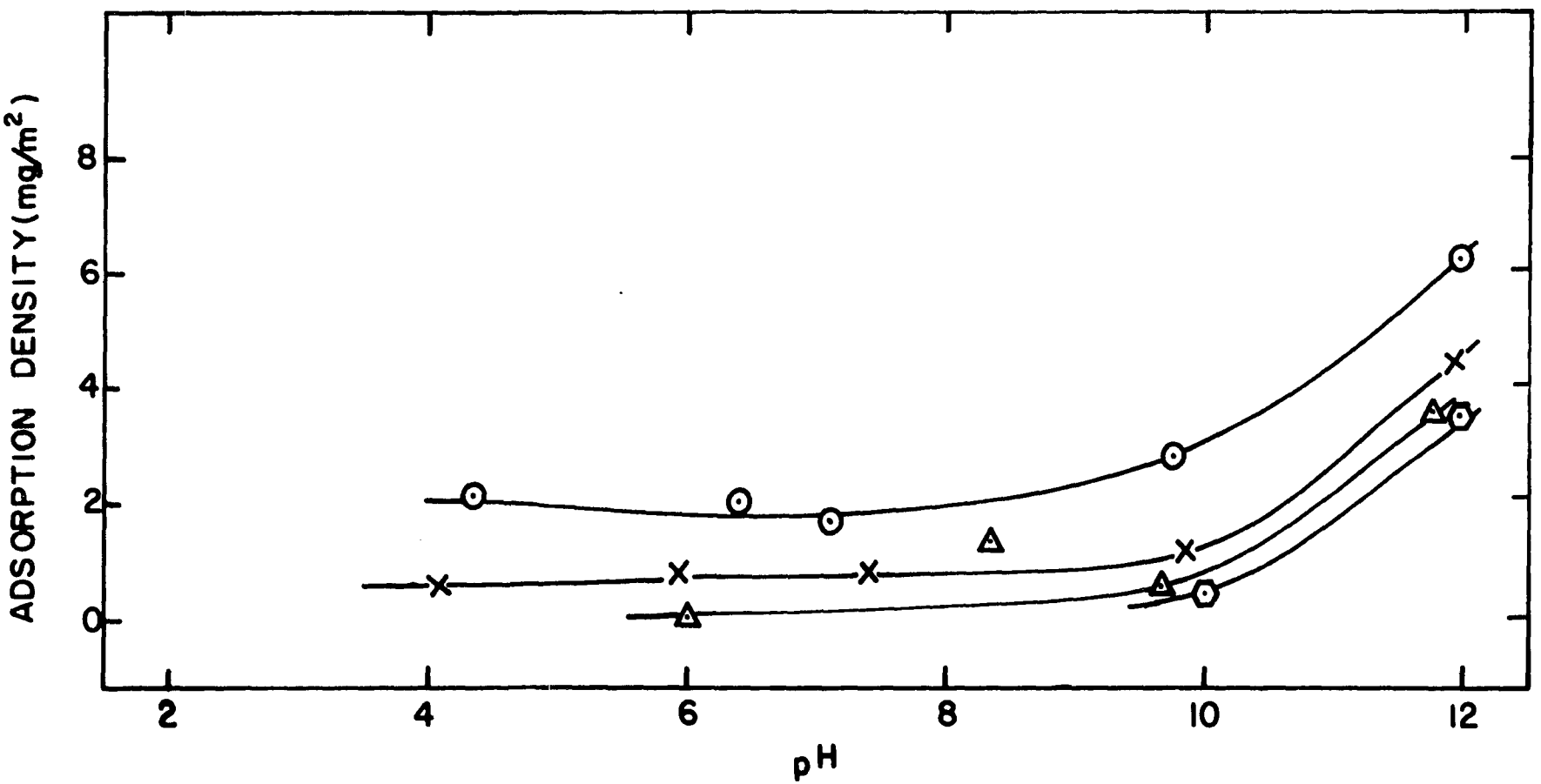
ADSORPTION DENSITY(mg/m²)
0
2
4
6
8
2
4
6
8
10
12
pH

FIGURE 16

ADSORPTION DENSITY OF STARCH

AS A FUNCTION OF

AMINE CONCENTRATION AND pH

Starch - 1000 mg/l

⊙ Amine zero

× Amine 10 μmole/l

⊙ Amine 100 μmole/l

⊡ Amine 1000 μmole/l

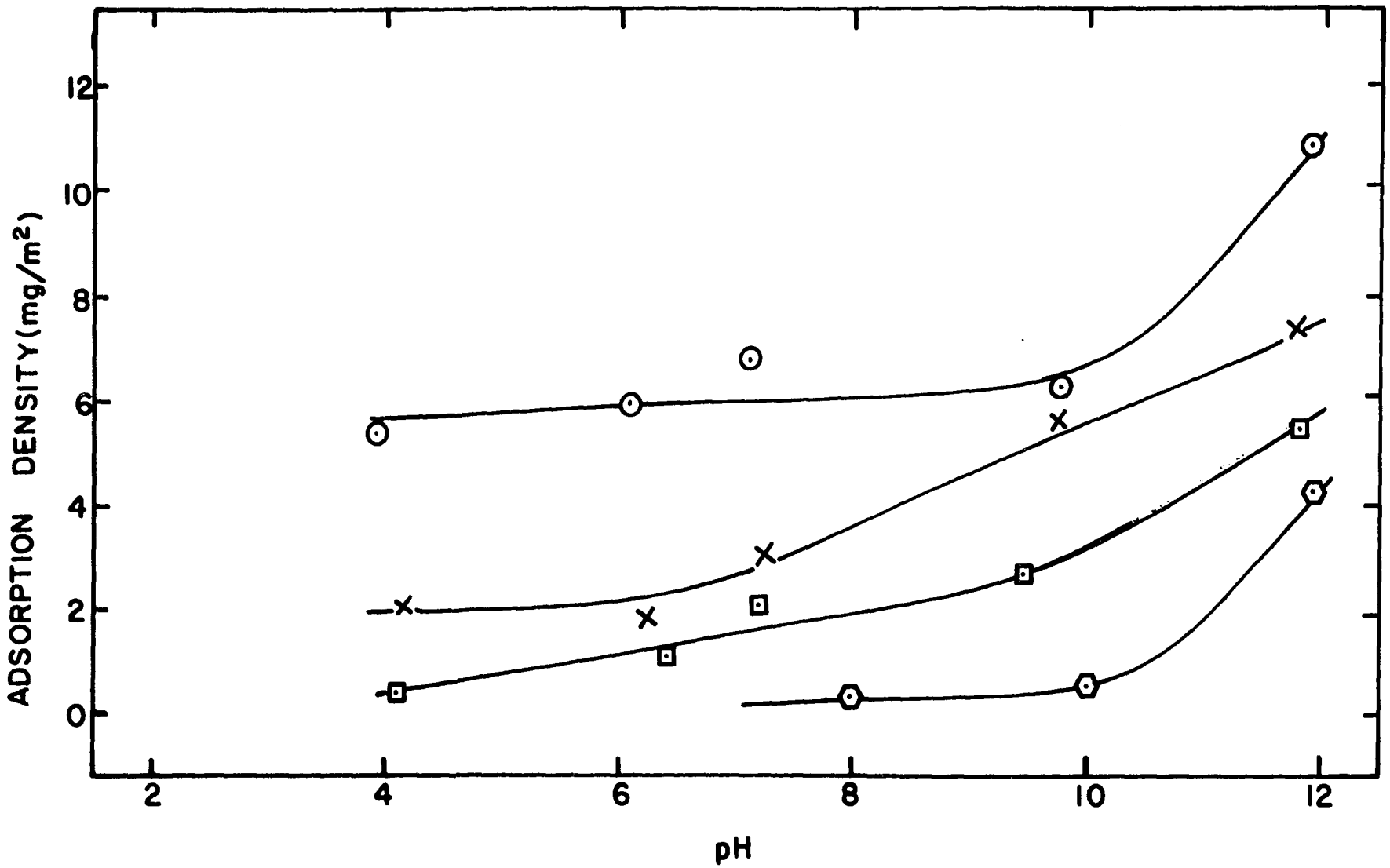
ADSORPTION DENSITY (mg/m²)
0
2
4
6
8
10
12
2
4
6
8
10
12
pH

FIGURE 17

FLOATABILITY AS A FUNCTION OF

AMINE CONCENTRATION AND pH

Starch - zero

⬡ Amine zero

✕ Amine 10 μmole/l

⊡ Amine 100 μmole/l

⊙ Amine 1000 μmole/l

△ Amine 10,000 μmole/l

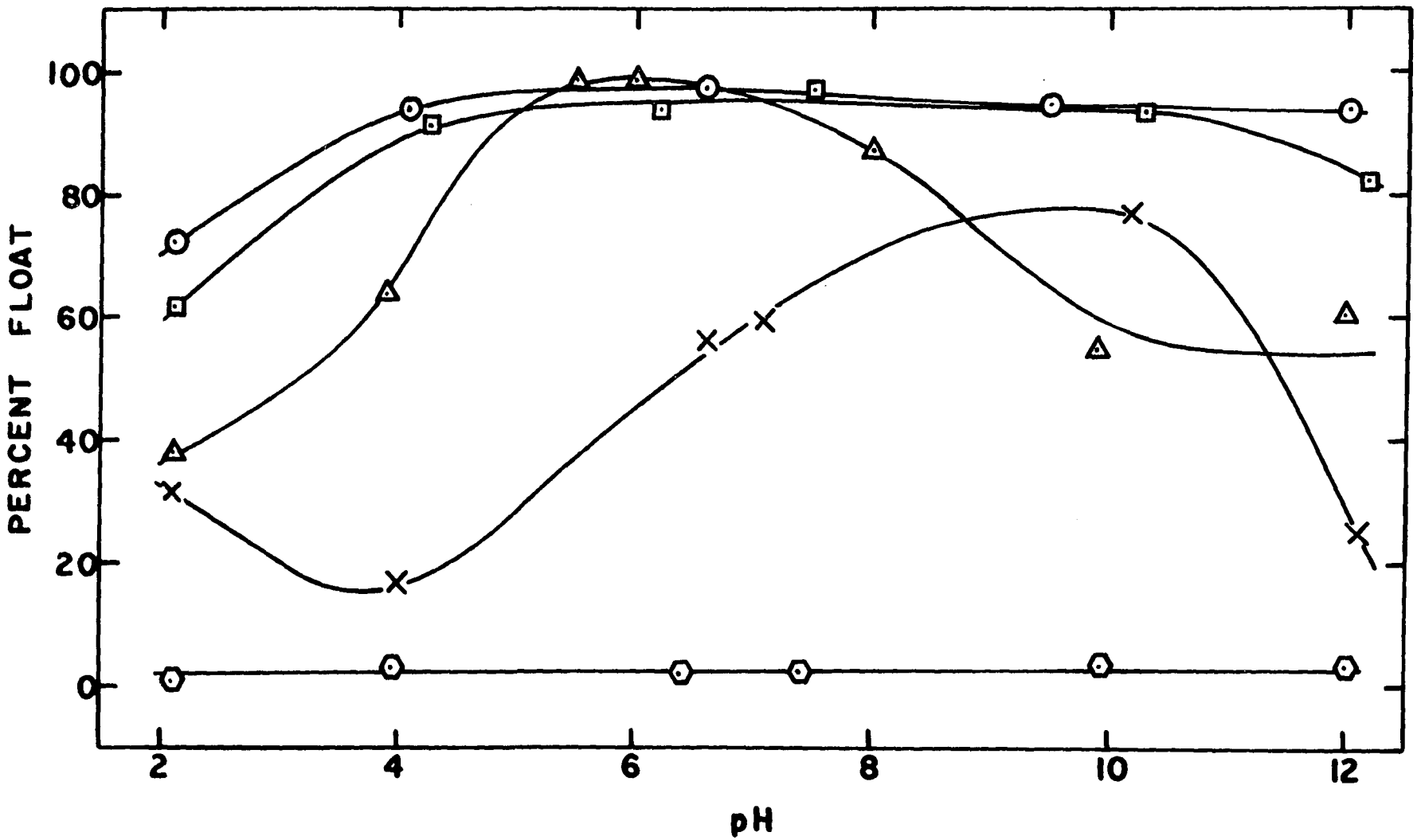
PERCENT FLOAT
100
80
60
40
20
0
2
4
6
8
10
12
pH

FIGURE 18

FLOATABILITY AS A FUNCTION OF

AMINE CONCENTRATION AND pH

Starch - 100 mg/l

- Amine zero
- Amine 10 μmole/l
- Amine 100 μmole/l
- Amine 1000 μmole/l
- Amine 10,000 μmole/l

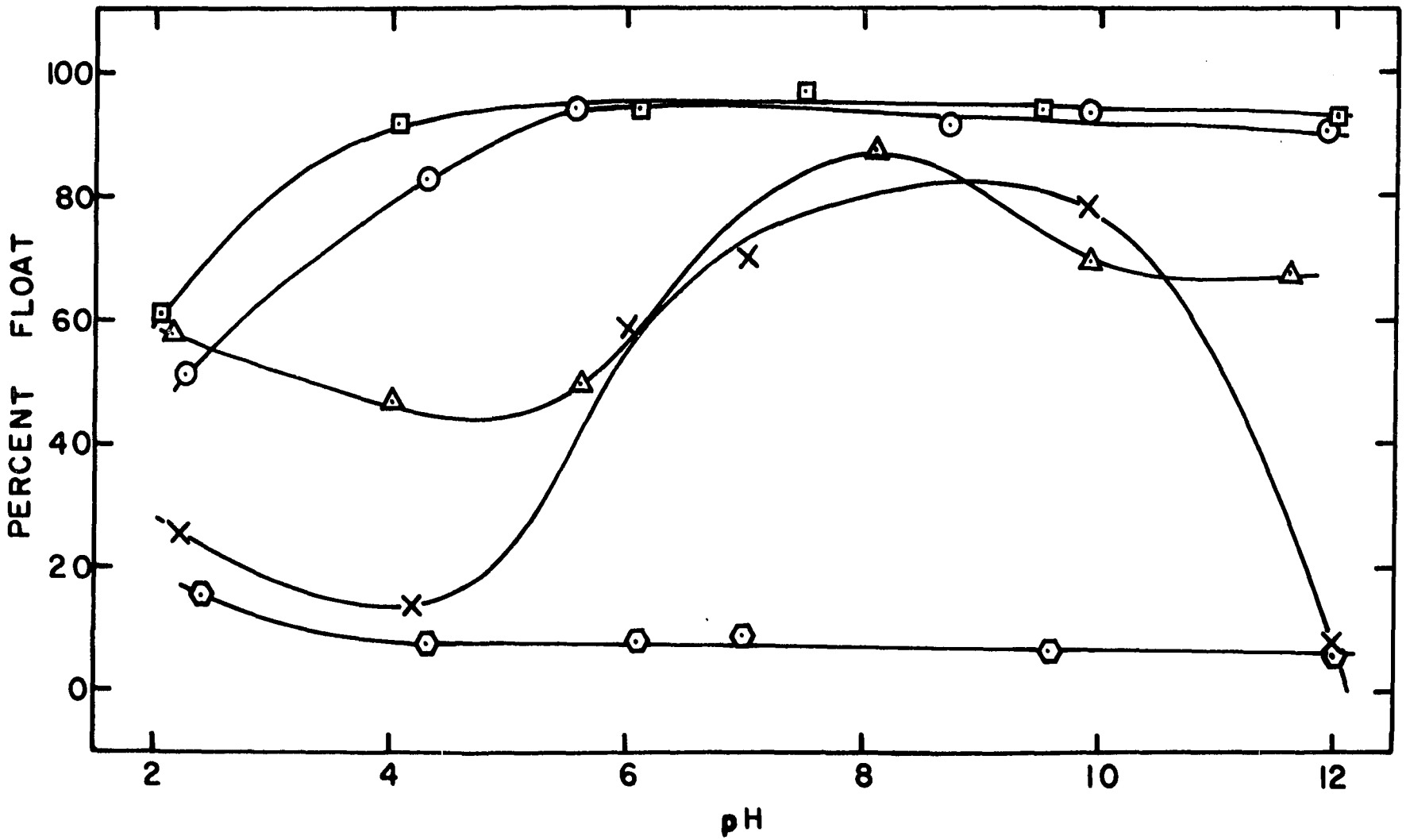
PERCENT FLOAT
100
80
60
40
20
0
2
4
6
8
10
12
pH

FIGURE 19

FLOATABILITY AS A FUNCTION OF
AMINE CONCENTRATION AND pH

Starch = 400 mg/l

⊙ Amine zero

× Amine 10 μmole/l

⊡ Amine 100 μmole/l

⊙ Amine 1000 μmole/l

△ Amine 10,000 μmole/l

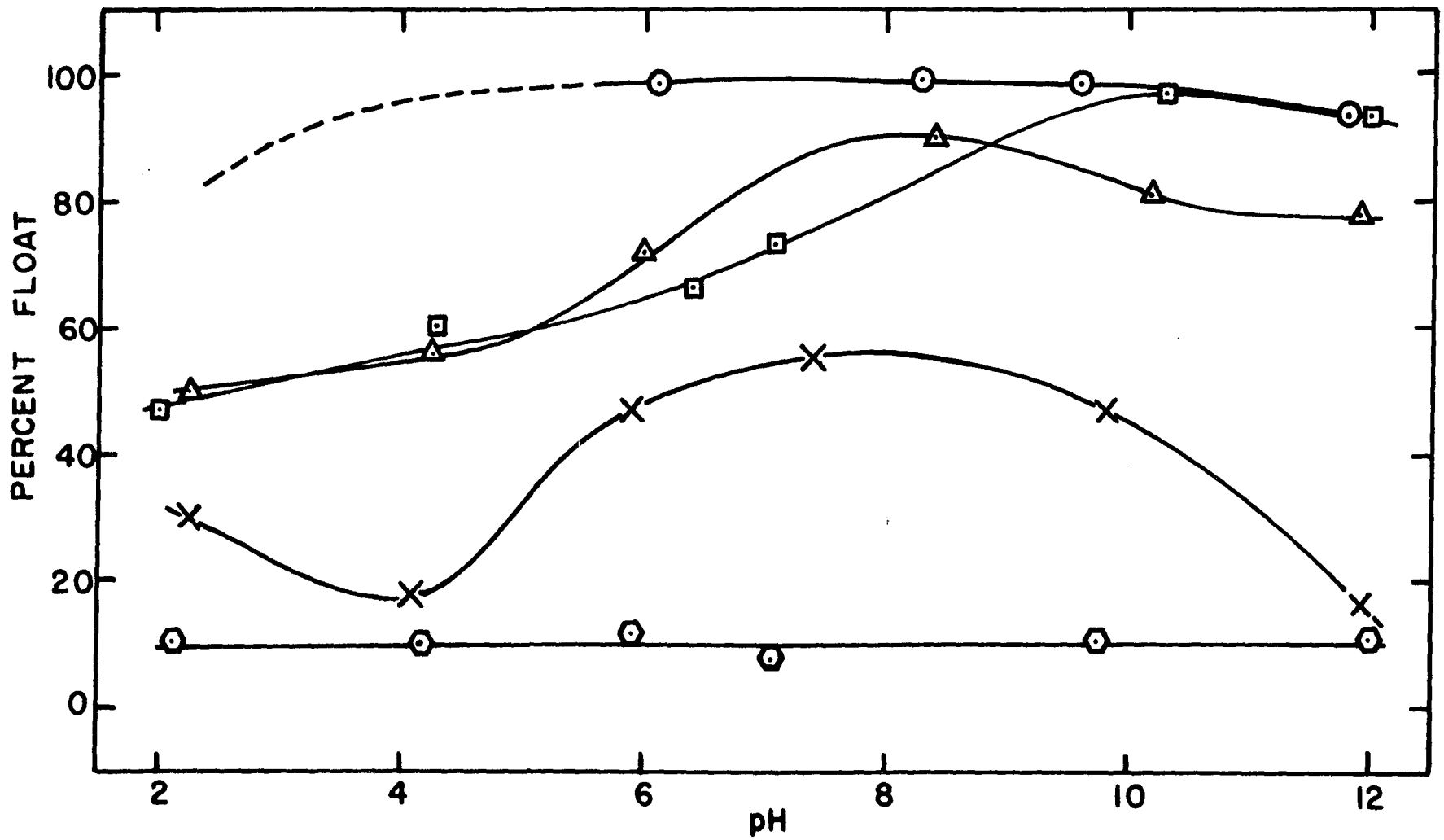
PERCENT FLOAT
100
80
60
40
20
0
2
4
6
8
10
12
pH

FIGURE 20

FLOATABILITY AS A FUNCTION OF

AMINE CONCENTRATION AND pH

Starch - 1000 mg/l

- Amine zero
- Amine 10 μmole/l
- Amine 100 μmole/l
- Amine 1000 μmole/l
- Amine 10,000 μmole/l

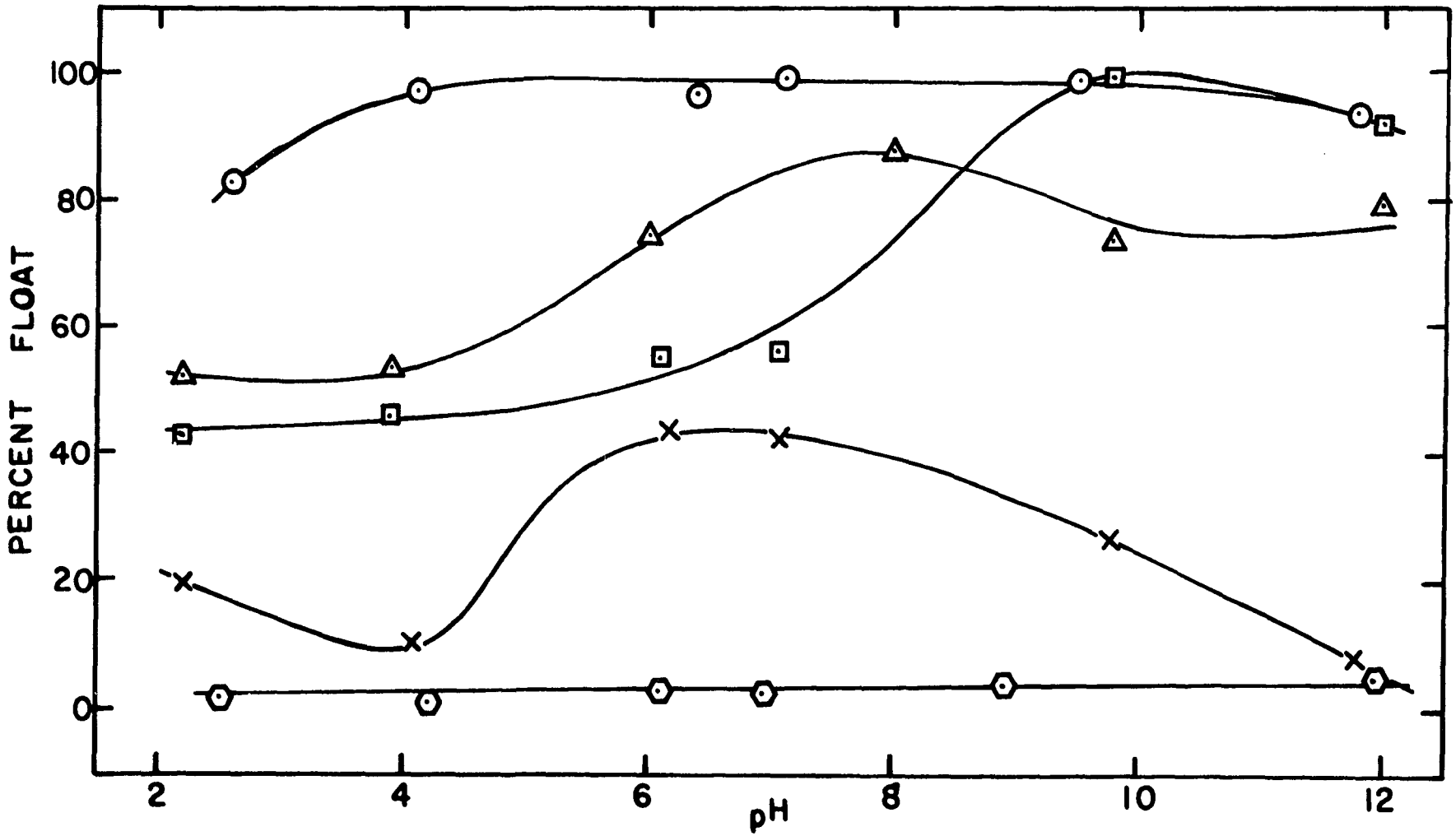
PERCENT FLOAT
100
80
60
40
20
0
2
4
6
8
10
12
pH

FIGURE 21

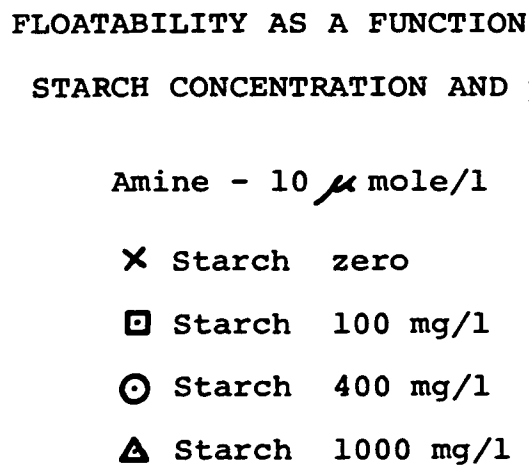
FLOATABILITY AS A FUNCTION OF
STARCH CONCENTRATION AND pH
Amine - 10 μ mole/l
Starch zero
Starch 100 mg/l
Starch 400 mg/l
Starch 1000 mg/l

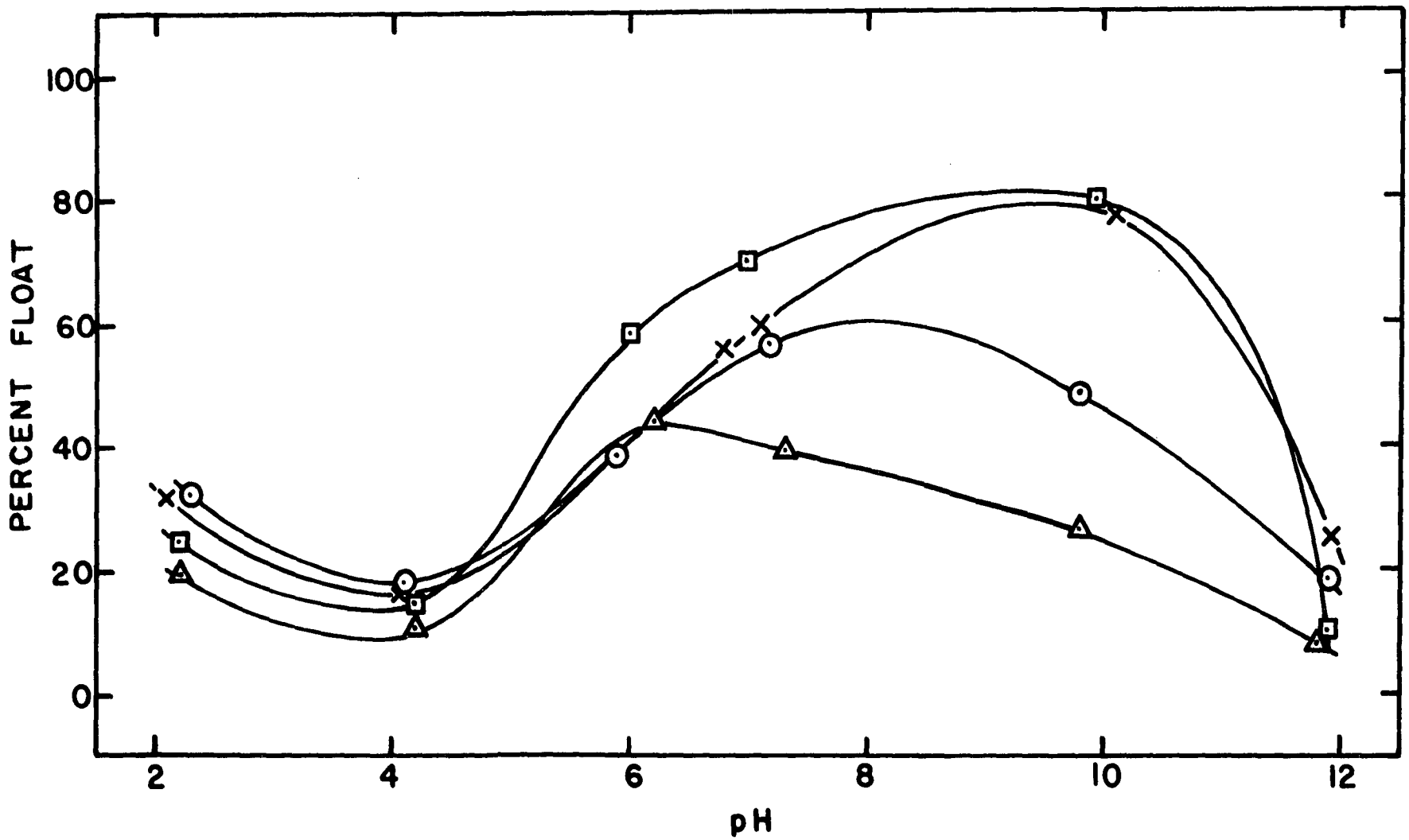
PERCENT FLOAT
100
80
60
40
20
0
2
4
6
8
10
12
pH

FIGURE 22

FLOATABILITY AS A FUNCTION OF
STARCH CONCENTRATION AND pH

Amine - 100 μ mole/l

✕ Starch zero

⊡ Starch 100 mg/l

⊙ Starch 400 mg/l

△ Starch 1000 mg/l

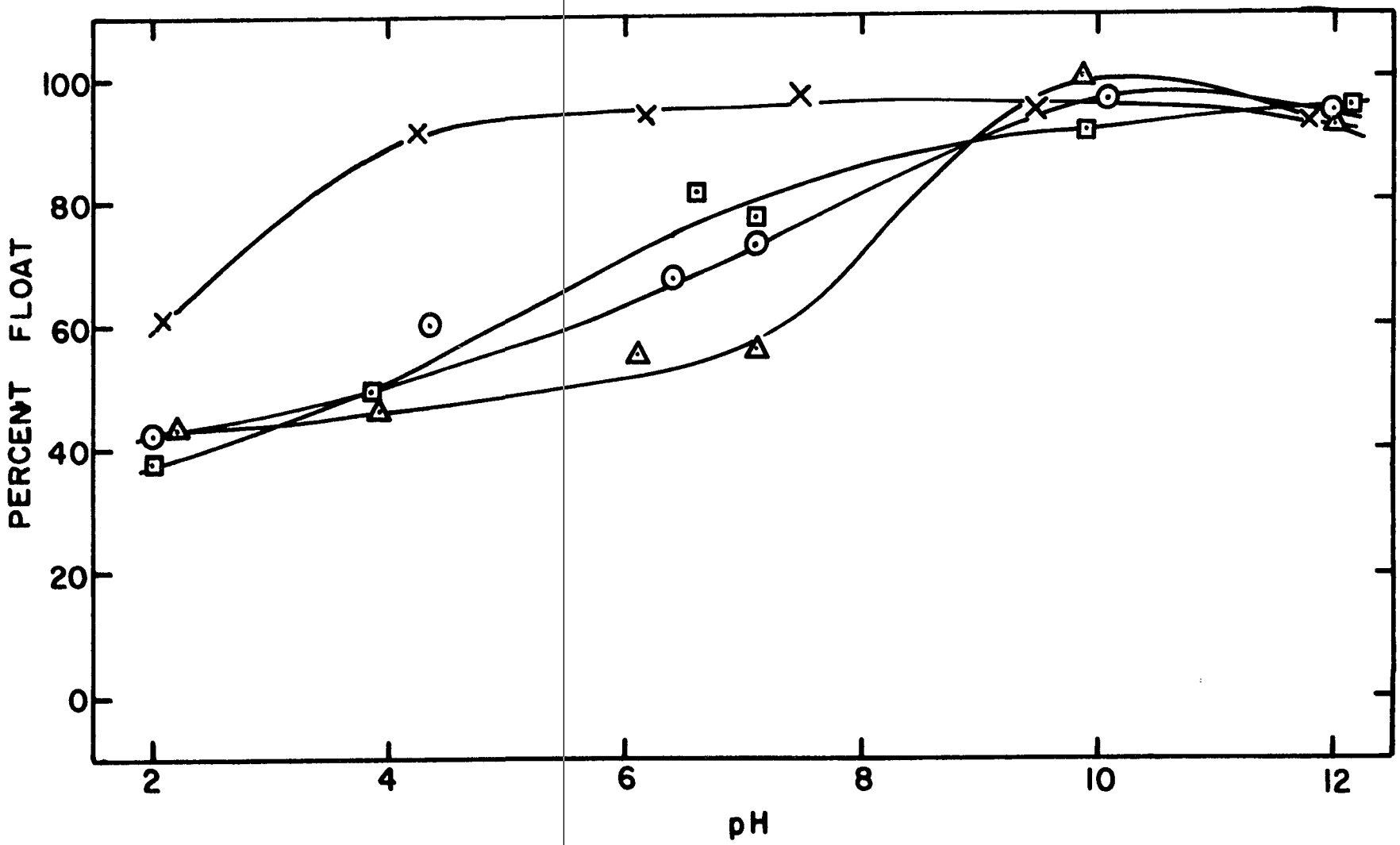
PERCENT FLOAT
100
80
60
40
20
0
2
4
6
8
10
12
pH

FIGURE 23

FLOATABILITY AS A FUNCTION OF
STARCH CONCENTRATION AND pH

Amine - 1000 μ mole/l

× Starch zero

⊡ Starch 100 mg/l

⊙ Starch 400 mg/l

△ Starch 1000 mg/l

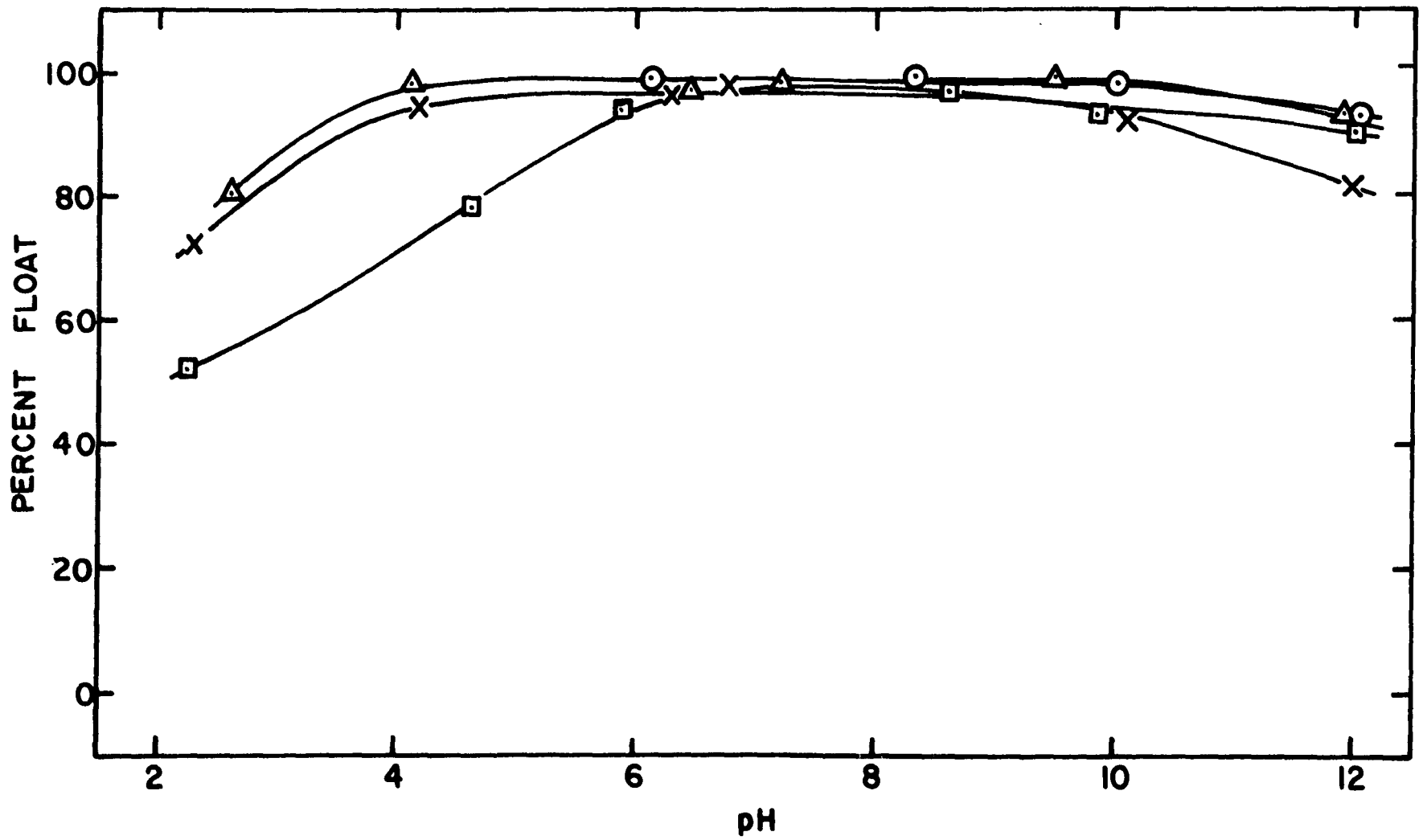
PERCENT FLOAT
100
80
60
40
20
0
2
4
6
8
10
12
pH

FIGURE 24

FLOATABILITY AS A FUNCTION OF

STARCH CONCENTRATION AND pH

Amine - 10,000 μ mole/l

✕ Starch zero

⊡ Starch 100 mg/l

⊙ Starch 400 mg/l

△ Starch 1000 mg/l

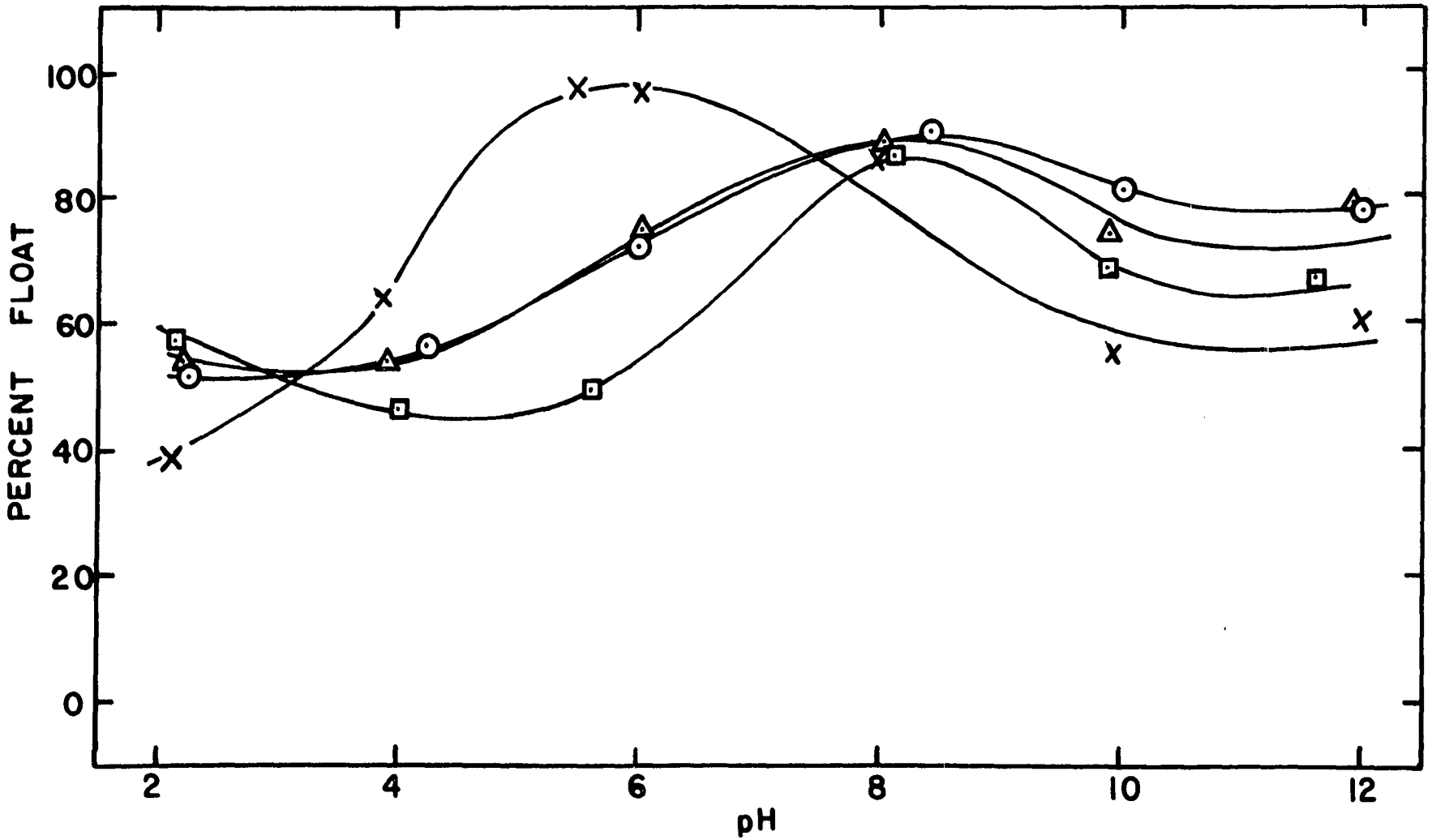
PERCENT FLOAT
100
80
60
40
20
0
2
4
6
8
10
12
pH

decreased in more acidic or alkaline solutions for amine concentrations of 1,000 μ mole/l. or less. With 10,000 μ mole/l amine, the flotation maximum was observed at approximately pH 6.

The depressant effect of starch increased with increasing starch concentration (Fig. 21-24). The effect of starch also depended on the initial amine concentration. In the most dilute amine solution, the maximum depressent effect of starch occurred between pH 8 and 10 and had virtually no effect on floatability for pH<7 (Fig. 21). In 100 μ mole/l amine solutions, the maximum depression occurred in near neutral solutions and starch had no effect at pH>9 (Fig. 22). Starch additions up to 1000 mg/l had no effect on floatability with 1000 μ mole/l amine (Fig. 23). A similar effect is noted with amine concentration of 10,000 μ mole/l (Fig. 24). The scatter observed in Fig. 24 is attributed to excessive frothing, due to high amine concentration, which occurred during the flotation test. A secondary flotation peak was observed under low amine, low pH conditions (Fig. 21). As the pH decreased, floatability decreased, reaching a minimum at pH 4 and increased at pH 2. This secondary flotation peak was observed with 10 μ mole/l amine and all starch concentrations studied.

VI. DISCUSSION

AMINE ADSORPTION

Although these experiments were not designed to produce adsorption isotherms of amine, four points can be obtained at any pH level. Isotherms have been drawn at pH 4, 7 and 10 (Fig. 25). In neutral or acidic solutions, the slope of $\log \Gamma$ - log C plot is linear in dilute solutions. At pH 10, adsorption increases with concentration and appears to be approaching a maximum in concentrated solutions. The isotherms shown in Fig. 25 should be considered with some reservation as only four points are available, all interpolated from the $\log \Gamma$ - pH curves.

The possible mechanisms for adsorption of amine on negatively charged quartz surface are:

(1) amine ions may react with OH^- in the diffuse layer forming oxyamine compounds:

$$OH^- + RNH_3^+ \rightleftharpoons OH_3NR^- + H^+$$

(2) an exchange reaction between amine ion and H^+ in the diffuse layer.

(3) amine ions may adsorb directly on the surface and reduce the net negative charge.

(4) specific adsorption of unionized amine in the Stern layer.

FIGURE 25

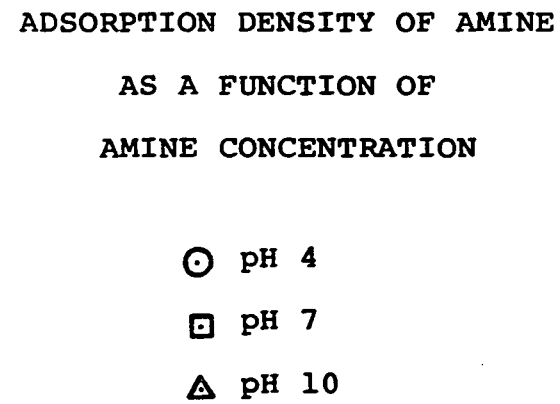
ADSORPTION DENSITY OF AMINE
AS A FUNCTION OF
AMINE CONCENTRATION
pH 4
pH 7
pH 10

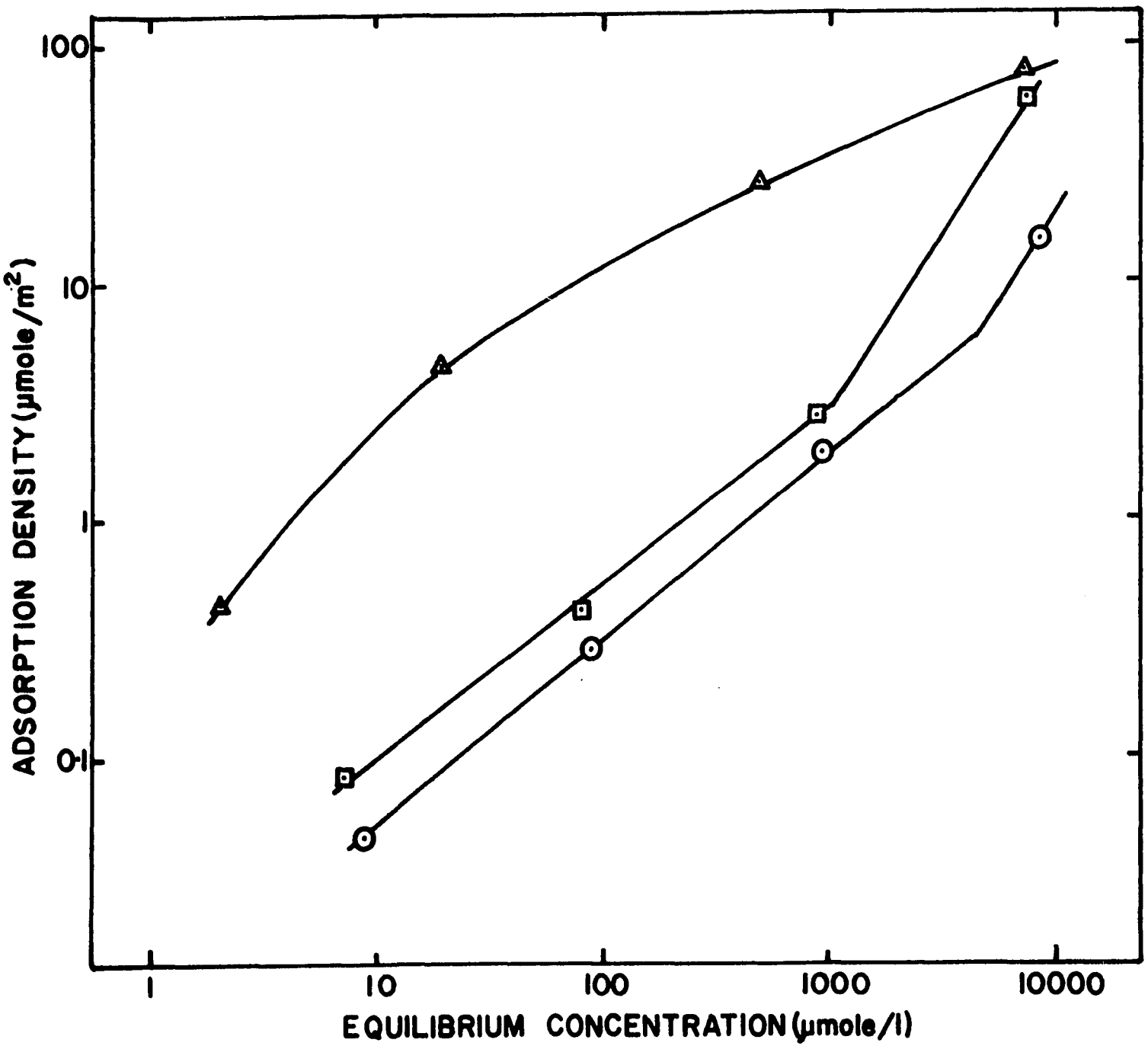
100
10
1
0.1
ADSORPTION DENSITY (μmole/m²)
1
10
100
1000
10000
EQUILIBRIUM CONCENTRATION (μmole/l)

The first three reactions result in the liberation of H^+ into the bulk solutions. No consistent pH shift was noted after adsorption in this study. The fourth reaction will only be significant at pH 8 when the concentration of RNH_2 becomes significant.

By assuming that H^+ and OH^- are the potential determining ions and RNH_3^+ is adsorbed in the diffuse layer, Morrow[66] showed that the adsorption density will be proportional to the square root of the concentration of amine in the bulk solution at constant pH.

$$\Gamma_{RNH_3^+} = K\sqrt{C} \qquad (20)$$

where $\Gamma_{RNH_3^+}$ is the adsorption density of RNH_3^+, C is the equilibrium concentration of amine and K is a constant.

If RNH_2 or RNH_3^+ chemisorption occurs at the solid surface, the adsorption will conform to the Freundlich equation in dilute solution and low surface coverage and:

$$\Gamma_m = K'C_m \qquad (21)$$

where Γ_m is the adsorption density of chemisorption ions or adsorbed molecules, C_m is the concentration of free amine in the solution and K' is a constant.

If both the above mechanisms are occurring, then

$$\Gamma_t = \Gamma_{RNH_3^+} + \Gamma_m \quad (22)$$

$$= K\sqrt{C} + K'C_m \quad (23)$$

where Γ_t is total amine adsorbed.

Further, since C_m is related to C by the dissociation constant for amine, at constant pH then

$$\Gamma_t = K\sqrt{C} + K''C \quad (24)$$

The rapid increase in adsorption in concentrated solutions has been attributed to the formation of hemi-micelles[37]. The critical hemi-micelle concentration is related to the critical micelle concentration. Recent work[67] has shown that the critical micelle concentration of dodecylammonium acetate decreases with increasing pH. The rapid increase in adsorption with concentration at pH 10 may reflect the low critical micelle concentration of dodecylamine in alkaline solutions.

The effect of pH on the adsorption of amine (Fig. 11) is similar to other published data[41-45]. The rapid increase in adsorption which occurs between pH 8 and pH 10 has been attributed to hemi-micelle formation[37]. The plateau between pH 10 and pH 12 reflects the increasing competition of Na^+ ions, from NaOH used for pH control, for available adsorption sites[44].

It is significant to note the marked similarity in the shape of the log Γ - pH curves with those obtained by Partridge[62] for adsorption of dodecylamine on hematite. A similar phenomenon was observed by Smith[63] with adsorption of dehydroabietylamine on quartz, hematite, rutile and baddeleyite. Since the zero-point-of-charge varies considerably for the minerals (approximately pH 2 for quartz to approximately pH 8 for hematite) solution properties appear to be more significant than the surface properties of the minerals.[31,63]

STARCH ADSORPTION

Adsorption of starch in the absence of amine was low and masked by experimental scatter below pH 10, but was the same order of magnitude as other published data.[53] More extensive work[53,55,56] indicates Langmuir type adsorption, with an approach to monolayer coverage. Adsorption has been found to decrease with increasing pH.[52,53,56] Starch adsorption is thought to depend on a balance between hydrogen bonding and electrostatic forces.[53] As the pH is increased, protons will be stripped from the starch molecule and will increase its negative charge. Electrokinetic studies[53] have shown that the negative charge on starch increases with pH up to pH 10 and decreases rapidly at higher pH levels. Starch adsorption on hematite is greater than on quartz suggesting some selectivity.[68] This fact has been used to selectively flocculate hematite from hematite-quartz

mixtures.[69]

AMINE-STARCH ADSORPTION

The mutual adsorption effects of amine and starch can only be explained if an amine-starch complex is formed in solution. There are four possible mechanisms which could result in the formation of a complex. These are:

(1) electrostatic attraction between RNH_3^+ and the negative starch molecule.

(2) Van der Waal forces between the hydrocarbon chain of ionized amine and starch.

(3) hydrogen bonding.

(4) a combination of the above mechanisms.

There are two possible forms the complex could assume. First, amine may enter the amylose helix and its hydrophobic characteristics would be masked by the starch. The second possibility is the amine adsorbing on amylose or amylopectin and thus mask the hydrophilic nature of the starch. Proteins can be precipitated by forming electrovalent bonds at their ionized sights with surface active agents.[53] Amylose is known to form specific precipitates with surface active agents, such as sodium dodecyl sulphate and fatty acids, by inclusion in the helix.[70,71] The addition of dodecylamine to starch solutions (British Gum 9084) decreases the viscosity of the solution. This is thought to reflect the formation of binary compounds.[53]

The mechanisms of formation of the starch-amine complex and the extent to which complexing occurs will be pH dependant. It has been shown that the negative surface charge of starch increases with pH up to pH 10 and decreases at higher pH levels.[53] Thus, electrostatic attraction between RNH_3^+ and starch increases with pH and is a maximum at pH 10.

Since hydrogen bonds are weakened as the pH is increased, the extent to which complexing occurs by hydrogen bonding decreases with increasing pH. The weakening of hydrogen bonds has a marked effect on amylose. The helix becomes unstable and at pH 11 becomes flexible. At approximately pH 12, the hydroxyl groups dissociate and the helix stretches out.[72] At high pH, amine-starch complexes, where amine is held within the amylose helix, are precluded.

Solution properties of amine also may play a role in complex formation. As the pH is increased above pH 8, the ratio of $[RNH_3^+]$ to $[RNH_2]$ decreases rapidly. With RNH_2 becoming increasingly significant, with the decrease in electrostatic attraction between RNH_3^+ and starch and with the decreasing hydrogen bond strength in alkaline solutions, it may be assumed that RNH_2-starch complex will predominate at high pH. The most probable mechanism of RNH_2-starch complex formation would be Van der Waal forces.

Therefore, the RNH_3^+-starch complex will predominate at low pH and RNH_2-starch complex at higher pH. Adsorption

of amine and starch will depend on the relative amount of amine, starch, and amine-starch complex in solution.

Thus, at low pH, small amounts of amine enhance starch adsorption and small starch additions enhance amine adsorption. The increased starch adsorption is due to the formation of a hydrophobic RNH_3^+-starch complex. The increased amine adsorption may be due to the large size of the starch molecule. Starch will adsorb on the quartz surface, but will extend into the solution. Thus the effective surface available for amine is increased. This is shown schematically in Fig. 26.

In dilute amine solutions, as the starch concentration is increased, the ratio of RNH_3^+ to starch in the complex will be decreased and the concentration of starch will be greater than the concentration of amine or amine-starch complex. Therefore, amine adsorption decreases with high starch additions. In concentrated amine solutions, the amounts of amine present will be greater than the amount of starch or starch-amine complex. Thus, the adsorption of the amine will decrease corresponding to a decrease in effective amine concentration due to complex formation. The adsorption of the complex will decrease (corresponding to a decrease in starch adsorption) since most of the available adsorption sites are occupied by amine.

In alkaline solution, complexing appears to be at a minimum and competition between amine and starch governs

FIGURE 26

SCHEMATIC DRAWING OF
AMINE ADSORPTION, STARCH ADSORPTION
AND AMINE-STARCH COMPLEX ADSORPTION

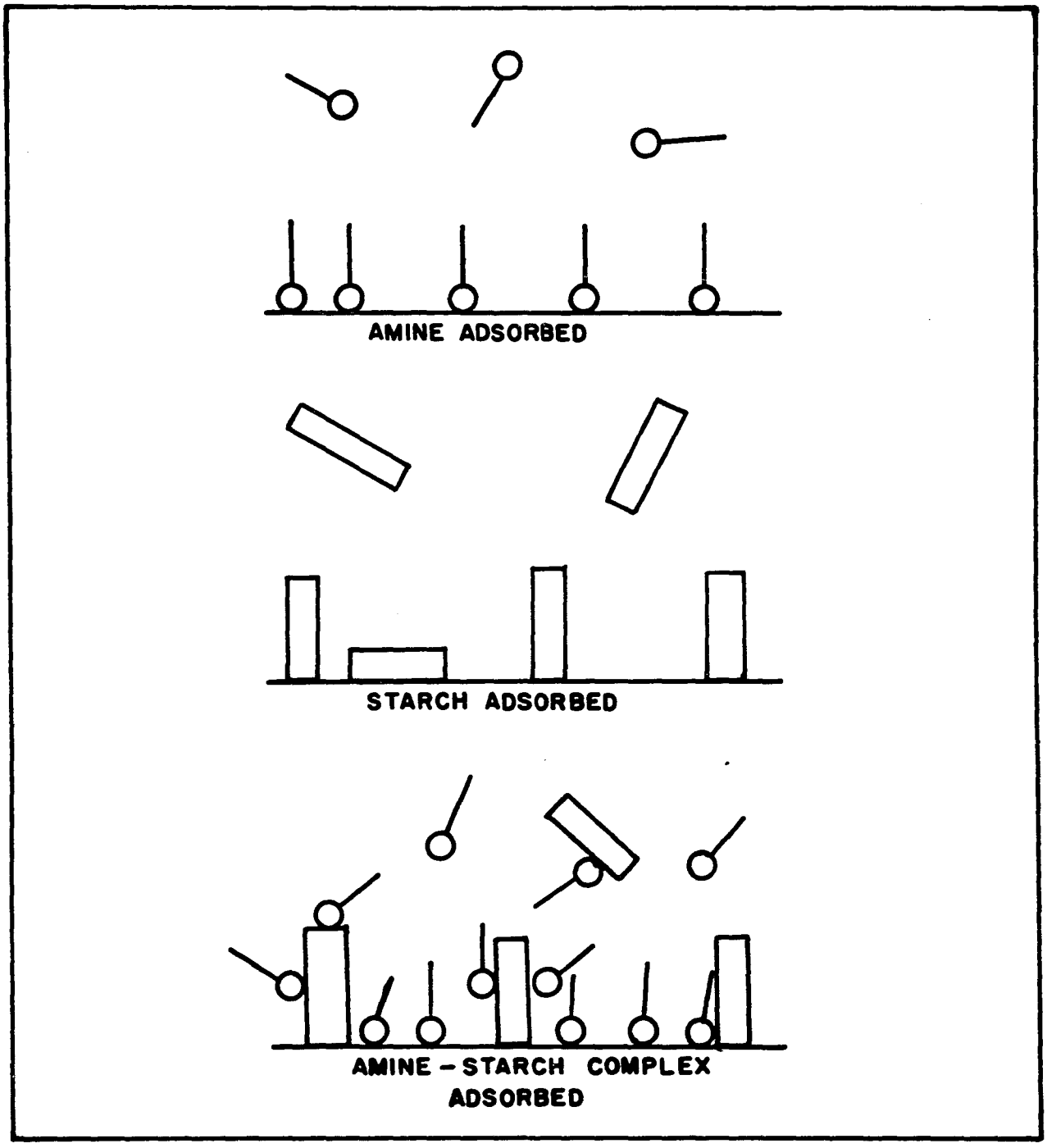
AMINE ADSORBED
STARCH ADSORBED
AMINE – STARCH COMPLEX
ADSORBED

amine adsorption. Thus, increasing starch concentration decreases amine adsorption. The increase in starch adsorption in dilute amine solutions results from the effect of amine on the zeta potential of quartz. It has been shown[42,53] that amine adsorption can change the sign of the zeta potential from negative to positive. The concentration required to effect this change decreases as the pH is increased. In alkaline solutions only dilute amine concentrations are required. Under these conditions, electrostatic attraction between starch and the mineral surface, or more correctly the adsorbed amine layer, is increased, enhancing starch adsorption.

FLOTATION

The depressant effect of starch was small but can be related to the relative adsorption density of amine and starch. At 10 μmole/l amine, starch had no effect on floatability at pH<7 but had a depressant effect in alkaline solution, due to increased starch adsorption at higher pH values. With 100 μmole/l. amine, the maximum depressant effect of starch occurred between pH 5 and pH 9. Floatability was not effected at pH>9 since the amount of amine adsorbed is large compared to starch adsorption. At higher amine concentrations, the effect of starch can be considered negligible. In the two regions where starch depresses quartz (10 μmole/l amine, pH<7 and 100 μmole/l amine,

pH>8), the relative amounts of amine and starch adsorbed is approximately equal. The effect of starch on floatability can be seen by comparing Fig. 27 and Fig. 28.

The poor floatability observed at low amine concentration results from insufficient collector adsorption to overcome the natural hydrophilic nature of the surface. At high amine concentration, the depressant effect can be attributed to the formation of an adsorbed layer of amine on the bubble (bubble armouring).[72]

The secondary flotation peak observed at low pH, low amine conditions, is attributed to the collecting ability of the acetyl radical. A similar secondary flotation peak has been reported for the hematite-dodecylamine system.[62] Acetic acid has been found to act as a collector with hematite, recovery increasing with increasing acetic concentration.[62]

A comparison of the relative floatability of hematite and quartz can be made using the results of Partridge.[62] The relative floatability of the two minerals at various amine-starch concentrations is shown in Fig. 29. Both minerals have similar flotation characteristics, with optimum floatability occurring at approximately pH 10, resulting from the similar amine adsorption characteristics. Starch is a more effective depressant for hematite than for quartz. For example, at 10 μmole/l amine, 100 mg/l starch

FIGURE 27

PER CENT FLOATABILITY CONTOURS

AS A FUNCTION OF

AMINE CONCENTRATION AND pH

Starch - zero

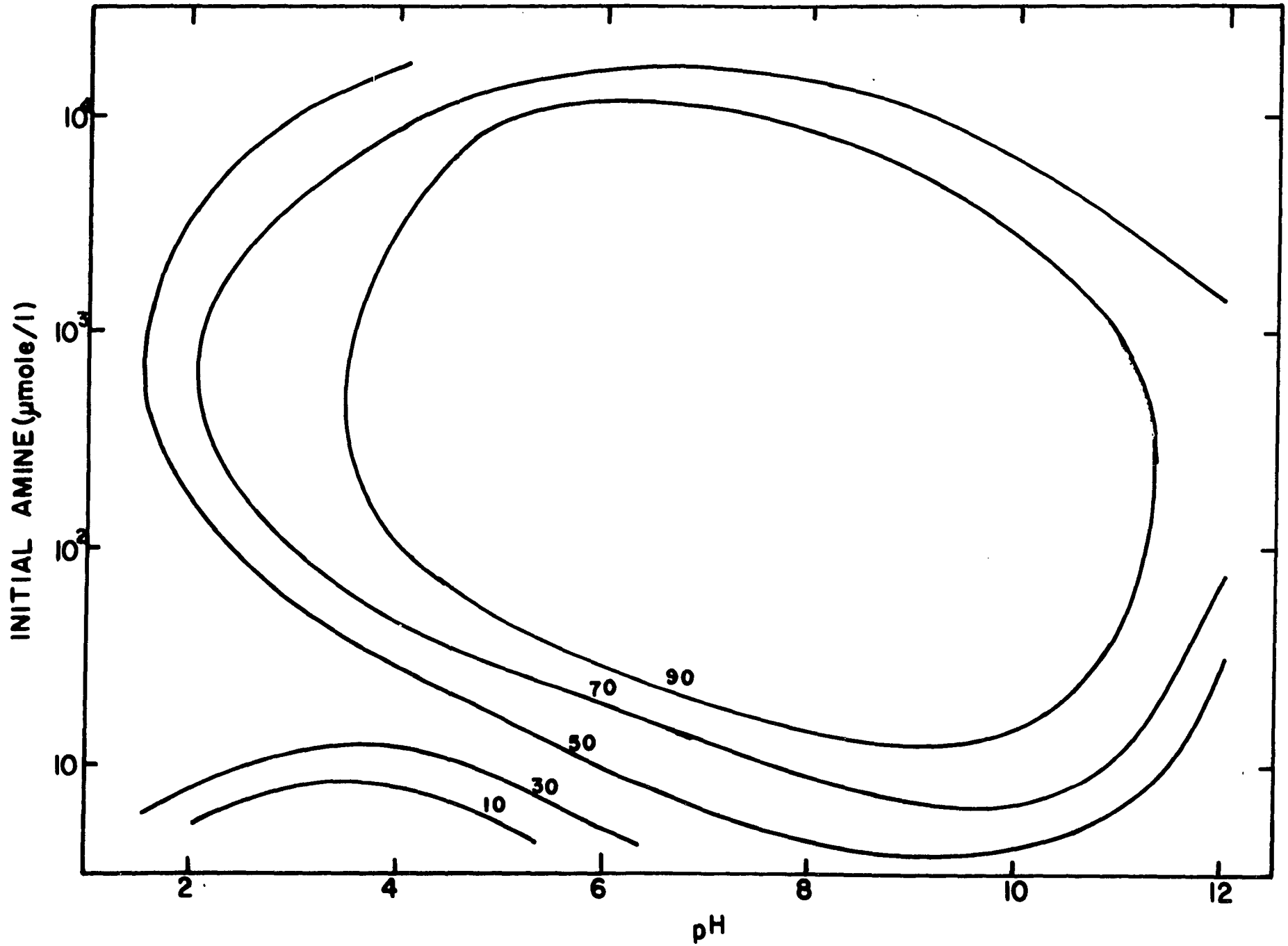
INITIAL AMINE (μmole/l)
10⁴
10³
10²
10
2
4
6
8
10
12
pH
90
70
50
30
10

FIGURE 28

PER CENT FLOATABILITY

AS A FUNCTION OF

AMINE CONCENTRATION AND pH

Starch - 1000 mg/l

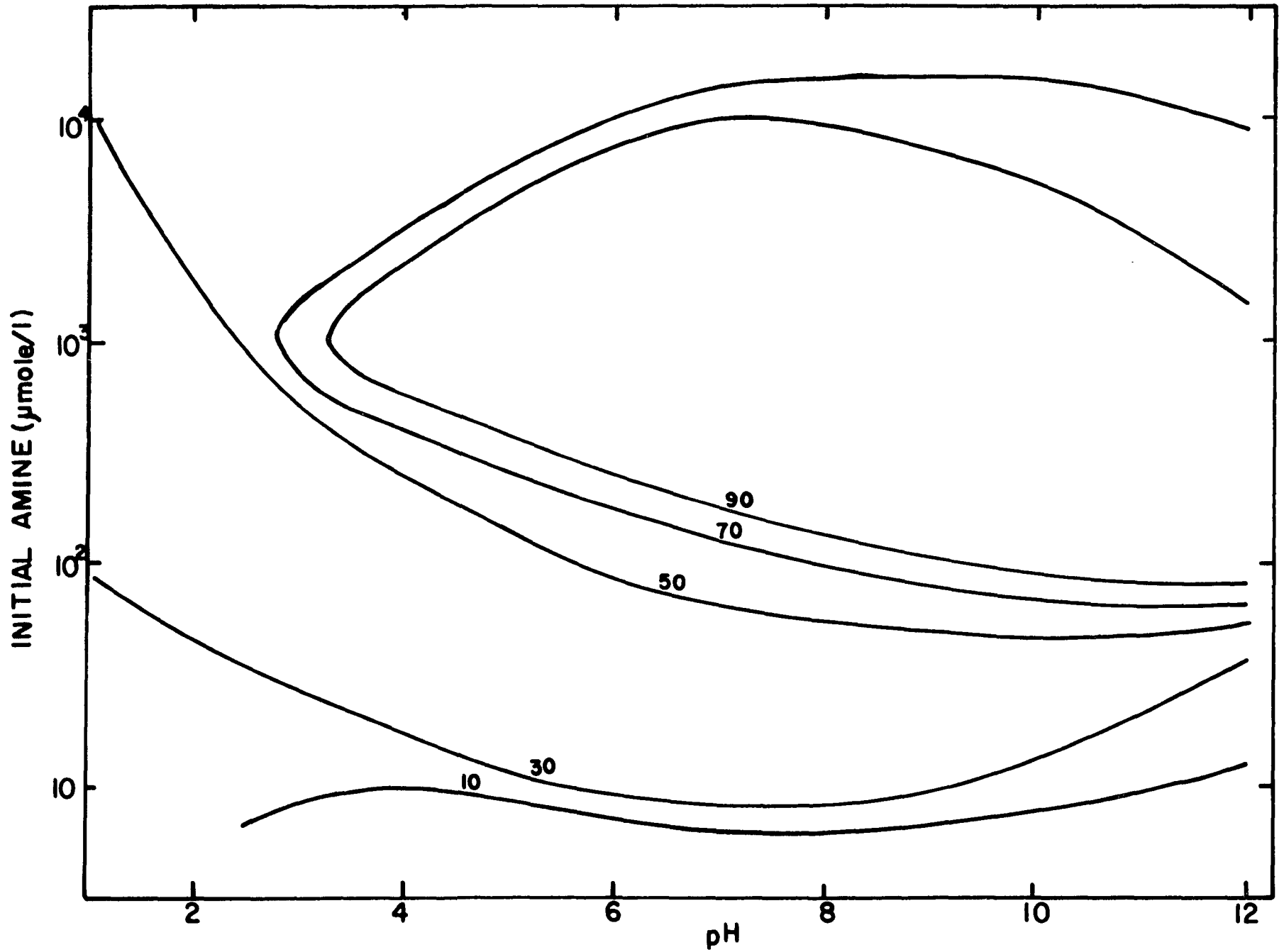
INITIAL AMINE (μmole/l)
10⁴
10³
10²
10
90
70
50
30
10
2
4
6
8
10
12
pH

FIGURE 29

FLOATABILITY AS A FUNCTION OF

AMINE CONCENTRATION, STARCH CONCENTRATION AND pH

—— Quartz

---- Hematite (Partridge)

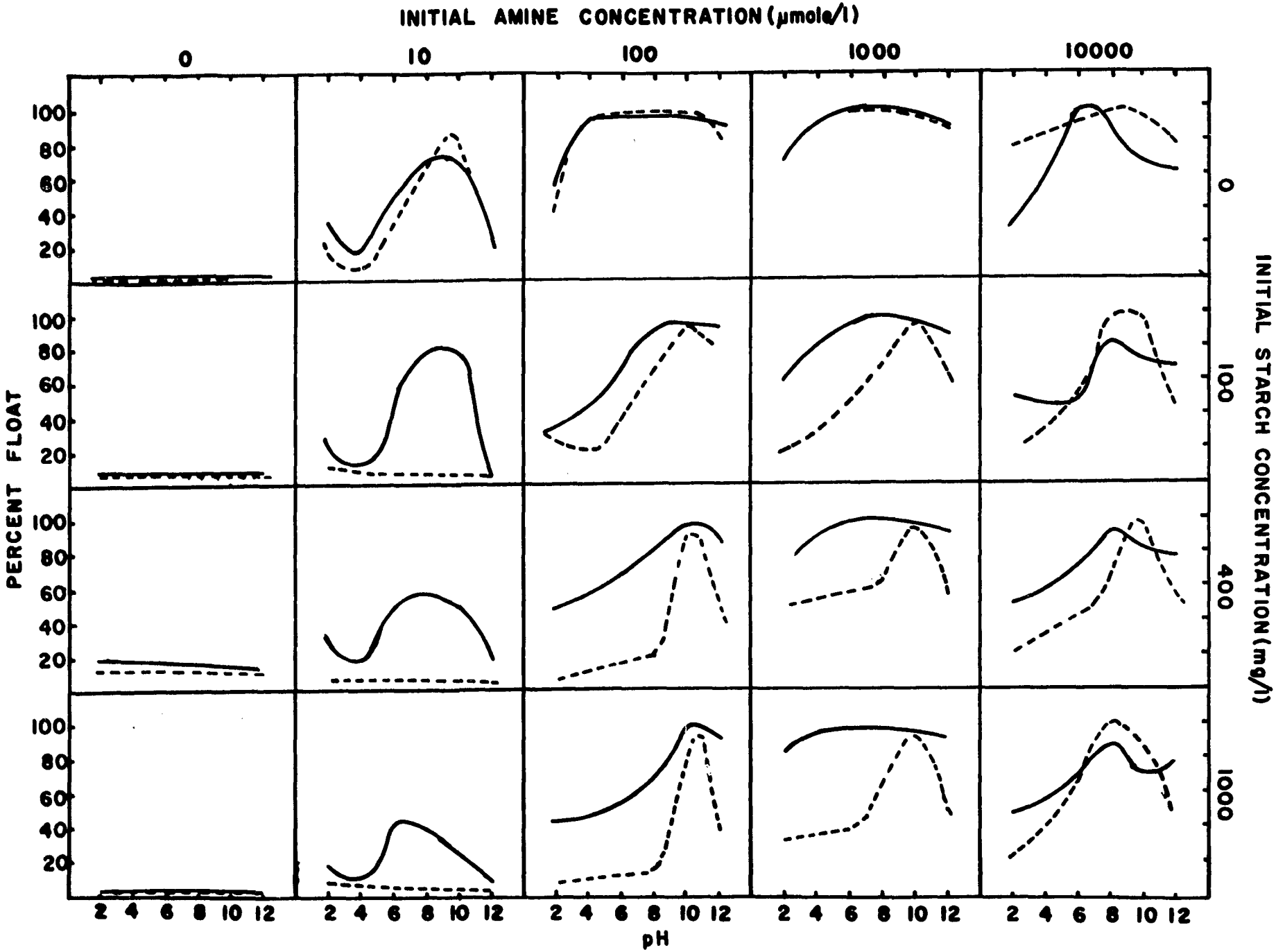
INITIAL AMINE CONCENTRATION (μmole/l)
0
10
100
1000
10000
PERCENT FLOAT
INITIAL STARCH CONCENTRATION (mg/l)
0
100
400
1000
100
80
60
40
20
2 4 6 8 10 12
pH

completely depresses hematite but had little effect on quartz floatability. This suggests that quartz can be effectively floated from hematite between pH 6 and pH 10.

Differential flotation tests were carried out using samples containing 50% quartz and 50% hematite with 10 μmole/l amine and 100 mg/l starch. The hematite was the same as that used by Partridge.[62] The results are shown in Table (2). Optimum separation of quartz from hematite occurred in near neutral solutions. The results of the differential flotation test were reasonably consistent with the flotation results of pure quartz and pure hematite.

Several conclusions can be drawn from the results. First, quartz can be separated from hematite using amine as a collector and starch as a depressant. The process may be effective in neutral or slightly alkaline solutions. Second, the interaction of amine and starch suggests that conditioning with starch prior to collector addition may decrease reagent costs. Starch-amine complexing will reduce the effectiveness of starch as a depressant and of amine as a collector. Smith[63] found that conditioning with starch and KOH before collector addition greatly improved the metallurgical results. It is difficult to apply the results directly to industrial practice. The inevitable presence of foreign ions in industrial mills may effect the flotation process. The effect of iron oxides other than

TABLE (2)

Differential flotation tests.

50% hematite - 50% quartz

Product	% wt.	Assay		Distribution		pH
		$\%Fe_2O_3$	$\%SiO_2$	$\%Fe_2O_3$	$\%SiO_2$	
Float	49.5	37.6	62.4	34.8	65.5	6.0
Sink	51.5	68.4	31.6	65.2	34.5	
Float	31.3	32.2	67.8	18.4	47.1	6.0
Sink	68.7	65.4	34.6	81.6	52.9	
Float	31.0	25.0	75.0	15.0	48.9	7.7
Sink	69.0	65.0	35.0	85.0	51.1	
Float	20.5	25.0	75.0	9.5	33.0	7.6
Sink	79.5	60.6	39.4	90.5	67.0	
Float	11.3	27.2	72.8	7.5	16.9	9.8
Sink	88.7	54.4	45.6	92.5	83.1	
Float	10.1	35.0	65.0	6.4	14.2	9.9
Sink	89.9	55.6	44.4	93.6	85.8	

hematite (magnetite, siderite) and gangue materials other than quartz on the process must also be investigated. Slimes may also have a detrimental effect on flotation.

SURFACE AREA AND ADSORPTION

Surface area determination by the B.E.T. method represents an absolute value. This will include all cracks and pores accessible to the nitrogen molecule. Surface areas determined by adsorption of dyes from solution represent the total surface available to the dye molecule, and will generally be smaller than the B.E.T. surface area. The presence of adsorption sites of the same charge as the dye molecule and competition from the solvent and other ions in solution tend to reduce dye adsorption. The surface of cracks or pores which are smaller than the dye molecule will not be measured.

The available surface area of quartz was found to be pH dependent, increasing with increasing pH. (Fig. 30) This can be explained in terms of competition between pyridinium ions and hydrogen ions. Increasing pH reduces the concentration of hydrogen ions in solutions. Thus, increasing pH will increase adsorption of pyridinium ions and increase the available surface area.

The adsorption density of amine, calculated as a per cent of available surface, is approximately constant up to pH 10

FIGURE 30

AVAILABLE SURFACE AREA

AS A FUNCTION OF pH

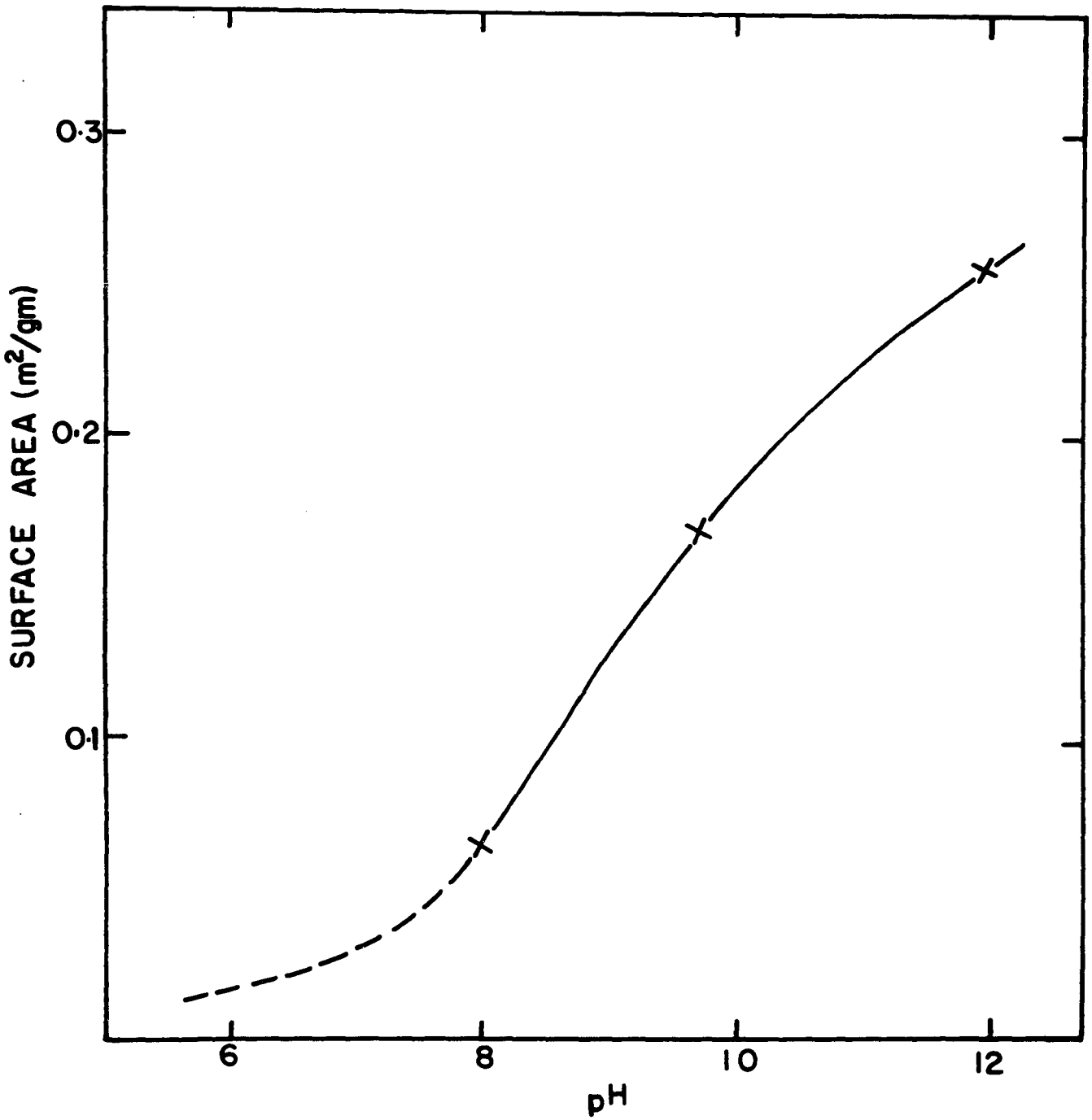
0·3
0·2
0·1
SURFACE AREA (m²/gm)
6
8
10
12
pH

at constant amine concentration. These calculations are shown in Table (3).

TABLE (3)

INITIAL CONCENTRATION	% MONOLAYER of AVAILABLE SURFACES				% MONOLAYER of B.E.T. SURFACE AREA			
mole/l	pH 6	pH 8	pH 10	pH 12	pH 6	pH 8	pH 10	pH 12
10	20.7	27.8	14.6	8.9	1.0	3.9	6.5	5.7
100	99.5	92.5	113.	90.0	4.6	13.0	50.5	58.4
1000	135.	390.	665.	180.	6.2	55.0	289.	115.

Competition between RNH_3^+ and other positive ions for available adsorption sites is qualitatively supported by the results. The maximum capacity of quartz to adsorb amine decreases with decreasing pH. The per cent coverage of available surface remains approximately constant up to pH 10 but the specific adsorption of amine decreases with decreasing pH.

Above pH 10,adsorption density in terms of available surface decreased considerably. This may be attributed to decreasing ratio of RNH_3^+ to RNH_2 in solution. At pH 12, the concentration of RNH_3^+ can be considered negligible. Increasing competition of Na^+ ions may also be a factor.

SUGGESTIONS FOR FUTURE WORK

1) A study of the relative flotation rates of quartz and hematite would be useful to determine the effectiveness of the flotation process.

2) The effect of Ca^{++}, Fe^{++} and other divalent or trivalent ions on starch and amine adsorption on quartz and hematite should be investigated.

3) A study of the properties of starch-amine solutions, such as surface tension and conductivity, may help elucidate the adsorption mechanisms.

4) An investigation of adsorbed starch-amine using infra-red methods may clarify the nature of amine-starch complexing.

5) A study of the electrokinetic properties of quartz and hematite in alkaline solutions of amine and starch may clarify the adsorption mechanism.

6) The relative depressing effect of the two starch fractions, amylose and amylopectin, should be investigated.

7) An investigation of colloidal depressants other than starch would be useful although cost would be an important factor.

APPENDIX I

QUARTZ ANALYSIS

QUARTZ ANALYSIS

A) Spectrochemical Analysis

Semi-quantitative analysis of the final cleaned quartz, performed by Mr. G. Capuano, was obtained by spectrochemical methods. The spectrum of quartz and of silicic acid, of known composition,were obtained. The two spectrums were taken using the same exposure conditions. The approximate impurity levels of the quartz were determined by comparing the intensity of the spectral lines with those obtained from silicic acid. While the method is approximate, it was sufficient to establish that the impurity levels were low enough to have a negligible effect on subsequent experiments. The details can be found in Table (4).

TABLE 4

Quartz Analysis

Experimental Conditions - Exposure Time - 30 sec.

Intensity - Hi

Wave Form - ½

Impurity	Silicic Acid	Quartz	Reference Spectral Line (A^{O})
Fe	.002%	$\approx$ .002%	
Cu	.003%	$<$ .003%	2933, 3968, 3273
Al	.003%	$<$ .003%	3082, 3092
Mg	trace	trace	2881, 2852
Mn	trace	--	

TABLE 4 con't

Impurity	Silicic Acid	Quartz	Reference Spectral Line (A^{o})
Cl	.005%	--	
SO_4	.003%	--	

B) X-ray Diffraction Analysis

The sample was scanned using a Phillips Diffractometer. The peaks obtained were compared to ASTM file card 5-0490. All peaks were identified as part of the quartz pattern. The results are recorded in Table (5).

TABLE 5

X-RAY IDENTIFICATION OF QUARTZ

Conditions: Cu Target; Ni Filter

40 kv, 20 ma.

2θ OBSERVED	I/I_o	"d" SPACING	d CARD 5-0490	DIFFERENCE	I/I_o
20.9	20	4.260	4.26	--	35
26.7	100	3.420	3.343	.077	100
36.5	10	2.461	2.458	.003	12
39.5	8	2.281	2.282	-.001	12
40.3	5	2.238	2.237	.001	6
42.4	10	2.132	2.128	.004	9
45.8	5	1.983	1.980	.003	6
50.1	20	1.821	1.817	.004	17
54.8	6	1.675	1.672	.003	7
55.2	3	1.664	1.659	.005	3
59.9	15	1.544	1.541	.003	15
64.0	3	1.455	1.453	.002	3
65.8	1	1.419	1.418	.001	<1

TABLE 5 con't

2θ OBSERVED	I/I_o	"d" SPACING	d CARD 5-0490	DIFFERENCE	I/I_o
67.6	8	1.386	1.382	.004	7
68.1	10	1.377	1.375	.002	11
68.3	11	1.373	1.372	.001	9
73.4	3	1.290	1.288	--	3
73.6	2	1.287 } 1.288			
75.6	5	1.258	1.256	--	4
75.8	3	1.255 } 1.256			
77.6	3	1.230	1.228	.001	4
77.8	1	1.228 } 1.229			
79.8	4	1.215	1.1997	.0003	5
80.0	3	1.199 } 1.201			
81.1	3	1.186	1.1838	.0022	4
81.4	5	1.182	1.1802	.0008	4
81.6	3	1.180 } 1.181			
83.8	3	1.1543	1.1530	.0002	2
84.0	2	1.1521 } 1.1532			

TABLE 5 con't

2θ OBSERVED	I/I_o	"d" SPACING	d CARD 5-0490	DIFFERENCE	I/I_o
84.9	1	1.1422 | 1.1411	1.1408	.0003	2
85.1	1	1.1400			
87.4	1	1.1158 | 1.1143	--	--	
87.7	1	1.1128			
90.8	3	1.0818 | 1.0817	1.0816	.0001	1
91.1	2	1.0816			
92.7	1	1.0645 | 1.0641	1.0636	.0005	1
93.1	1	1.0636			
94.7	1	1.0481	1.0477	.0004	2
95.1	1	1.0439 | 1.0440	1.0437	.0003	2
95.4	1	1.0440			
96.2	2	1.0348 | 1.0345	1.0346	-.0001	2
96.6	1	1.0342			
98.7	2	1.0152 | 1.0150	1.0149	.0001	2
99.1	1	1.0147			
102.2	1	0.9897	0.9896	.0001	1

TABLE 5 con't

2θ OBSERVED	I/I_o	"d" SPACING	d CARD 5-0490	DIFFERENCE	I/I_o
102.6	1	0.98695	--	--	
		.98713			
102.9	1	0.98731			
103.8	1	0.97879	--	--	
104.2	1	0.97612	0.9762	.00013	1
		.97633			
104.5	1	0.97654			
106.6	1	0.96067	0.96067	-.00006	1
		.96061			
107.0	1	0.96055			
** 114.0	1	0.91841	--	--	
114.6	2	0.91531	--	--	
		0.91576			
114.9	1	0.91603	--	--	
115.0	1	0.91327	--	--	
115.8	1	0.90925	--	--	
116.3	1	0.90677	--	--	
118.3	1	0.8972			
118.7	1	0.8975			
120.0	1	0.8894			

TABLE 5 con't

2θ OBSERVED	I/I_o	"d" SPACING
120.6	1	.8889
122.6	1	.8781
123.1	1	.8782
127.3	1	.8603
132.8	1	.8413
136.5	2	.8280
137.2	1	.8230

** Not listed on Card 5-0490 and assumed to belong to pattern for quartz.

APPENDIX II

EQUILIBRIUM TESTS FOR AMINE ADSORPTION

Equilibrium tests were run at pH 10.3 with initial amine concentration of 10 and 1000 μ mole/l amine. The results are plotted in Fig. 31 and shown in Table (6). With 1000 μmole/l amine, equilibrium was reached within one hour. In dilute amine solutions (10 μ mole/l) equilibrium was established after 10 hours agitation. To insure uniform conditions, all adsorption tests were run for 10 hours. Starch adsorption has been shown to be very rapid[9] and it was assumed equilibrium would be reached within 10 hours.

FIGURE 31

AMINE ADSORPTION AS A

FUNCTION OF TIME

⊙ Initial Amine - 10 μmole/l

× Initial Amine - 100 μmole/l

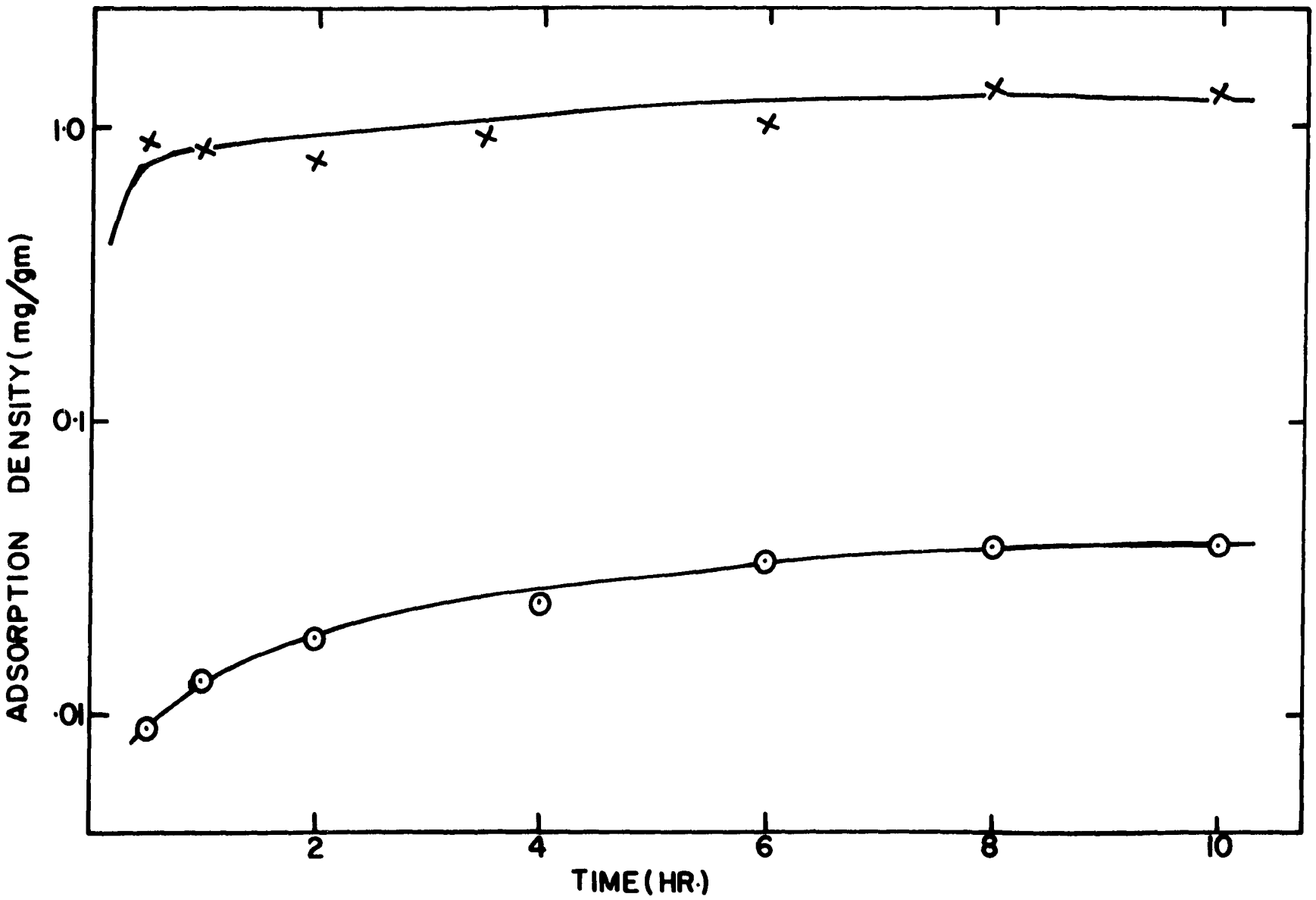
ADSORPTION DENSITY (mg/gm)
1·0
0·1
·01
2
4
6
8
10
TIME (HR·)

TABLE 6

EQUILIBRIUM TESTS FOR AMINE ADSORPTION

TIME (HOURS)	FINAL CONCENTRATION mg/l	ADSORPTION DENSITY mg/gm
	INITIAL CONCENTRATION	2.454 mg/l
0	2.454	--
½	2.059	.0093
1	1.902	.0130
2	1.646	.0191
4	1.416	.0246
6	1.029	.0337
8	0.847	.0380
10	0.832	.0384
	INITIAL CONCENTRATION 245.4 mg/l	
0	245.4	--
½	203.3	0.995
1	208.7	0.867
2	211.9	0.792
4	204.7	0.962
6	196.9	1.147
8	172.3	1.723
10	187.1	1.379

APPENDIX III

SURFACE AREA DETERMINATION

The surface area of the quartz was determined using the B.E.T. method of gaseous adsorption, described on page 11, and by adsorption of 1-hexadecylpyridinium bromide from solution.

(a) B.E.T.

In the B.E.T. surface area determination, nitrogen was adsorbed on the quartz at liquid nitrogen temperatures using the apparatus described by Salman[73]. The surface area covered by 1 cc of nitrogen at S.T.P. is taken as 4.36 M^2. Table (7) contains all the data necessary to determine the specific surface area. The B.E.T. plot, which is linear, is shown in Fig. 32. The specific surface area was determined to be 4273 cm^2/gm.

(b) Dye Adsorption

The structure[74] of the dye 1-hexadecylpyridinium bromide is shown below and

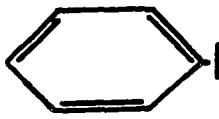

$$-[CH_2]_{25} - CH_3 - Br$$

F.W = 384.6

has a cross sectional area of $54A^{o2}$. The adsorption tests were carried out as described on page 28. The solutions were analyzed using a Perkin Elmer double seam spectrophotometer at 260 μm similar to the procedure

FIGURE 32

B.E.T. PLOT FOR NITROGEN ADSORPTION

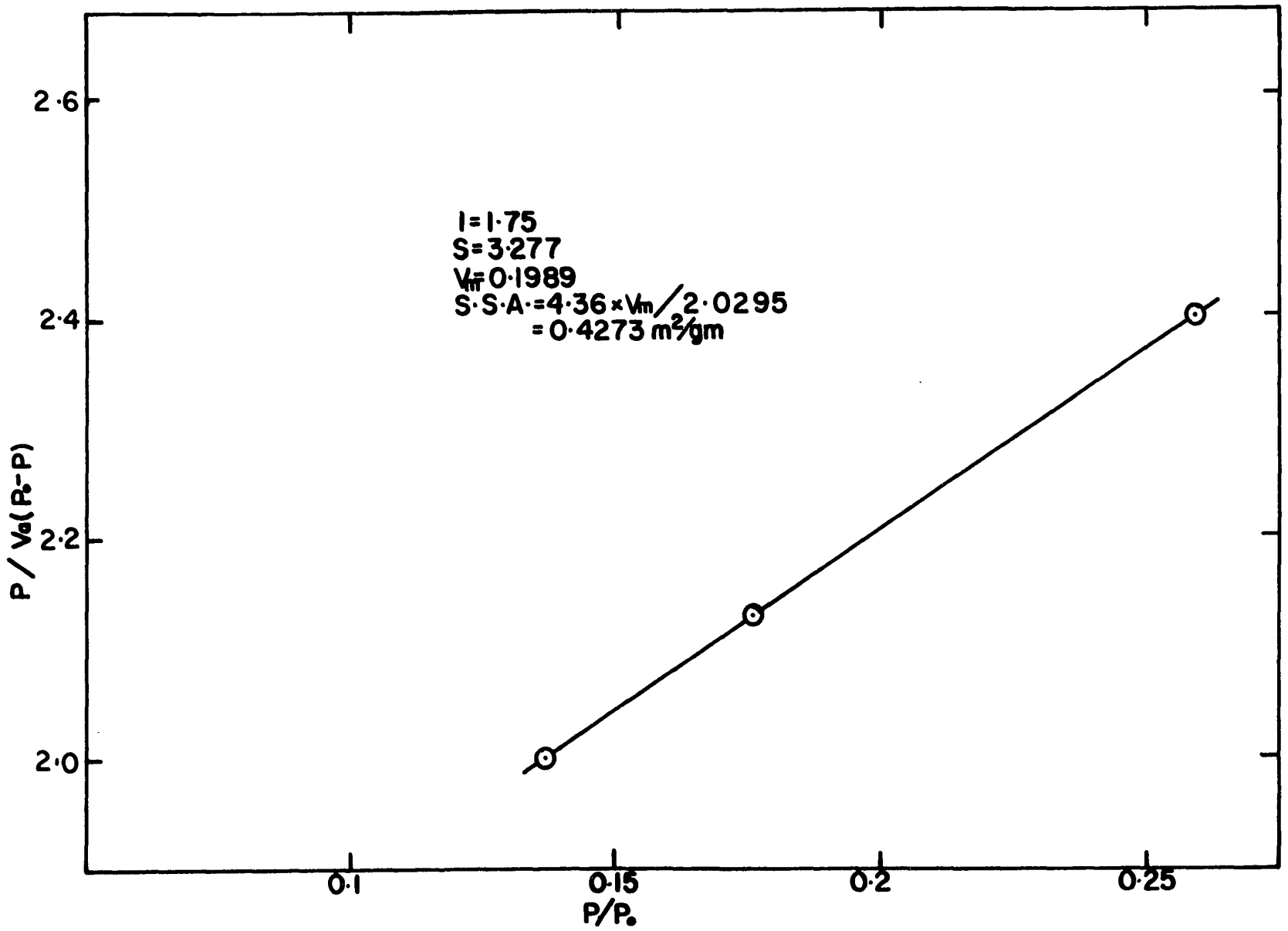
I=1·75
S=3·277
V_m=0·1989
S·S·A·=4·36×V_m/2·0295
=0·4273 m²/gm
2·6
2·4
2·2
2·0
P / Va(Ps-P)
0·1
0·15
0·2
0·25
P/Ps

TABLE 7

NITROGEN ADSORPTION DATA FOR SURFACE AREA DETERMINATION

TEST NO.	TOTAL VOLUME CC.STP.	BULB VOLUME CC.STP.	SAMPLE TUBE VOLUME CC.STP.	VOLUME ADSORBED CC.STP.	NITROGEN P_o mm Hg	BULB PRESSURE mm Hg	$\frac{P}{P_o}$	$\frac{P}{V(P_o-P)}$
1	5.1903	3.6866	1.4243	0.0794	766	104.5	.137	2.001
2	5.1903	3.2592	1.8306	0.1005	761	134.	.176	2.126
3	5.1903	2.3431	2.7014	0.1458	760	197.	.259	2.400

used by Paterson[75]. The calibration curve (Fig. 33) was linear for 1- HPB concentrations up to 80 mg/l. Equilibrium tests were run with initial concentration of 50 mg/l at pH 11. Equilibrium was established in three hours (Fig. 34). A series of tests were run at pH 7 to 13 to determine the variation in adsorption with pH (Fig. 35). Above pH 13, the solutions turned yellow and analysis by u.v. methods was impossible.

The adsorption isotherm of 1-HPB was determined at pH 8, 9.7 and 12. The results are shown in Fig. 36. The isotherms were found to be L3 type according to the classification of Giles[76]. The distinct plateau was taken as monolayer. The available surface was 2748, 1734, and 592 cm^2/gm at pH 12, 9.7 and 8 respectively. The modified B.E.T. equation was also used to determine the available surface area. The saturation concentration of 1-HPB was taken as the critical micelle concentration of 1-HPB, (7.0×10^{-4} M/l at 25^oC)[77]. The surface areas obtained using the modified B.E.T. equation were 2307, 1693 and 670 cm^2/gm at pH 12, 9.7 and 8 respectively. The B.E.T. plots are shown in Fig. 37. The results obtained using the modified B.E.T. agree with the results using the plateau method.

The correlation between surface area determination by gas phase adsorption and adsorption from solution is

reasonable. From the discussion page 72, it is apparent that a significant amount of the surface is inaccessable to the dye molecules. Previous studies[78] found good agreement between surface area determined by 1-HPB adsorption and gas phase adsorption.

FIGURE 33

CALIBRATION CURVE FOR

1-HEXADECYLPYRIDINIUM BROMIDE

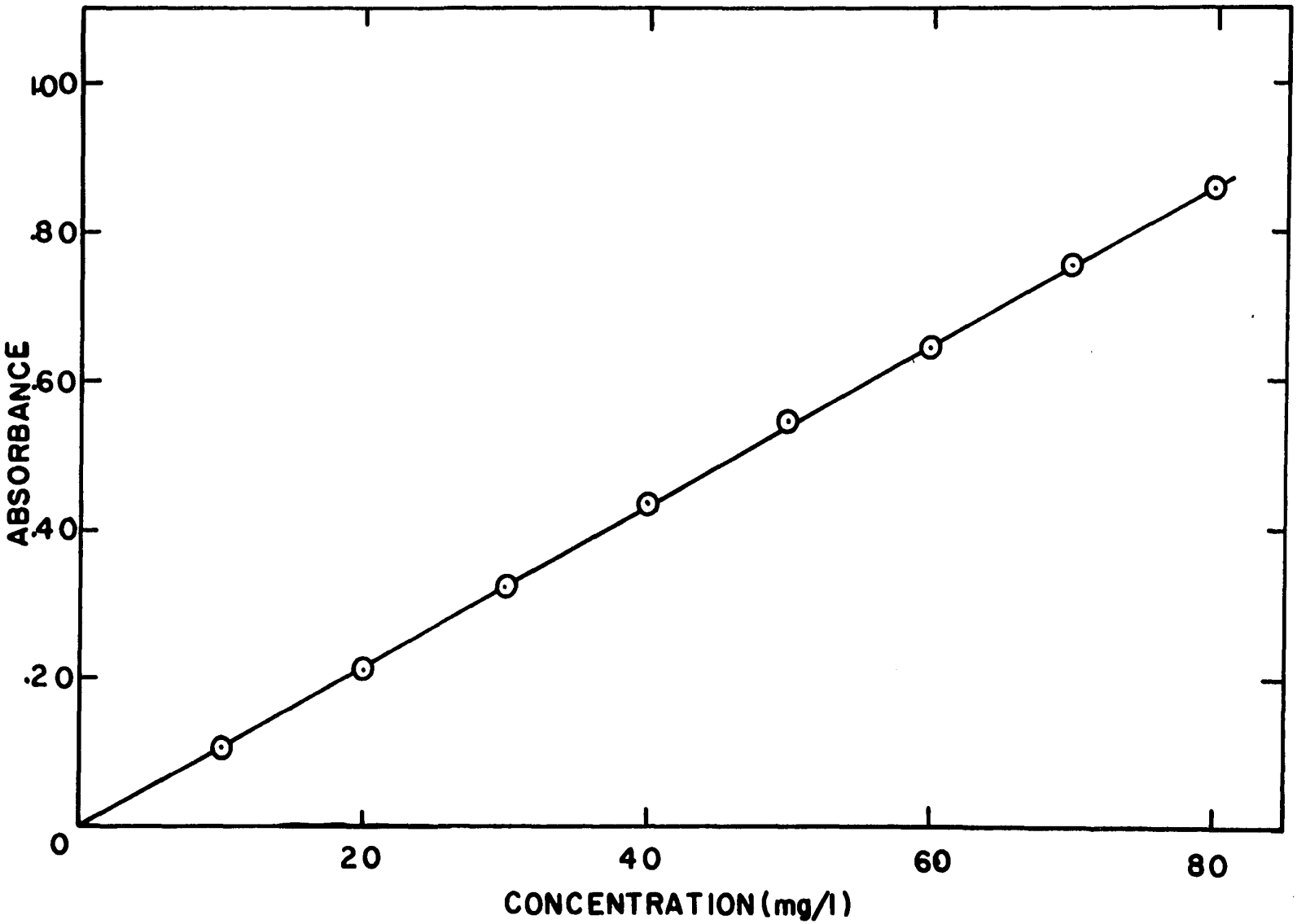
1.00
.80
.60
.40
.20
0
ABSORBANCE
20
40
60
80
CONCENTRATION (mg/l)

TABLE 8

CALIBRATION CURVE 1-HPB

CONCENTRATION mg/l	log I/I_o
10	.110
20	.211
30	.321
40	.435
50	.543
60	.643
70	.751
80	.857

FIGURE 34

ADSORPTION OF 1-HPB AS A

FUNCTION OF TIME

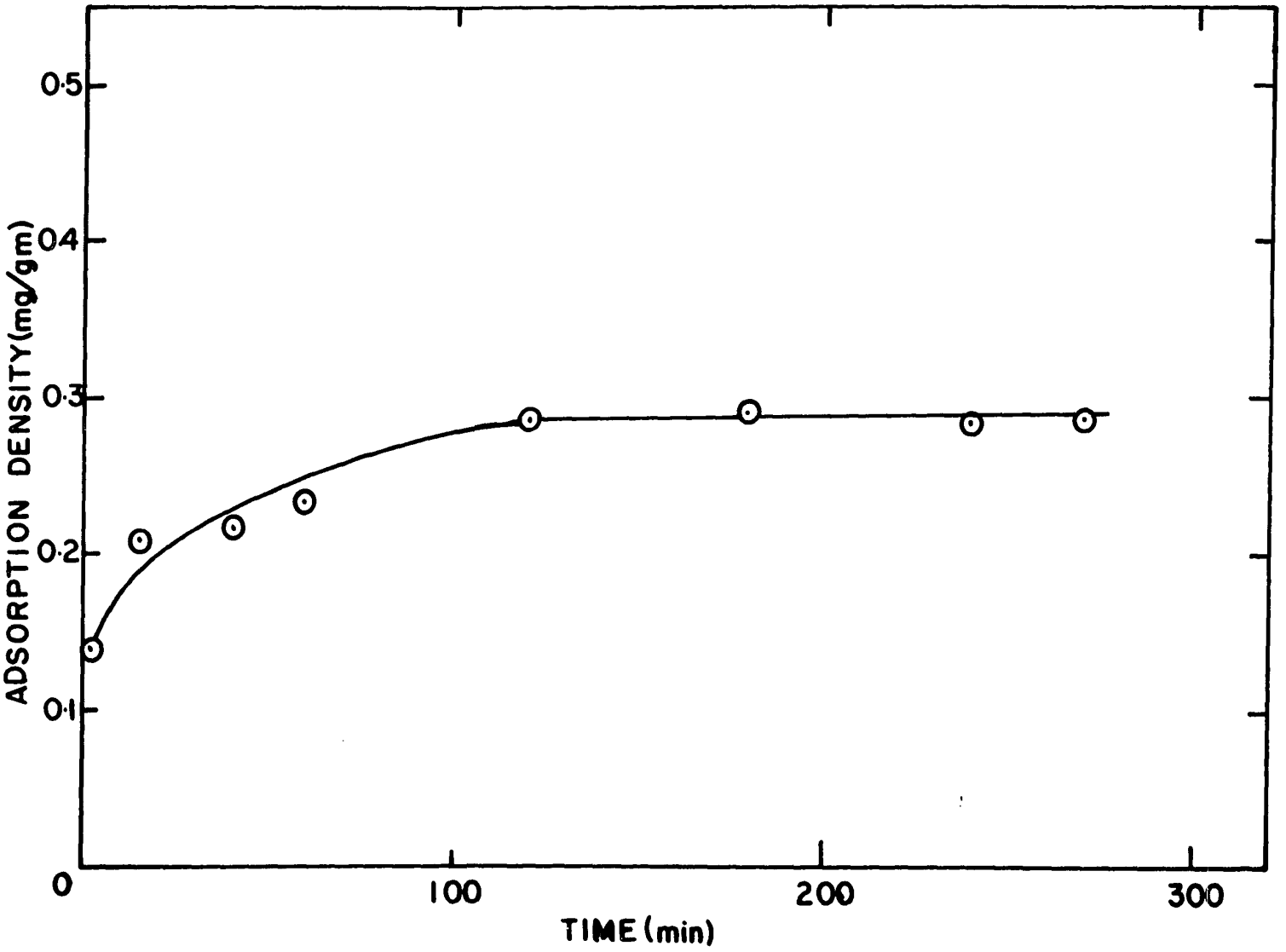
0·5
0·4
0·3
0·2
0·1
0
ADSORPTION DENSITY(mg/gm)
100
200
300
TIME (min)

TABLE 9

EQUILIBRIUM TESTS 1-HPB

INITIAL CONCENTRATION 48.85 mg/l

TIME (MIN)	FINAL CONCENTRATION (mg/l)	ADSORPTION DENSITY mg/gm
2	41.58	.1463
15	40.00	.2065
40	39.44	.2195
60	38.93	.2315
120	36.46	.2890
180	36.32	.2931
240	36.79	.282
275	36.79	.282

FIGURE 35

ADSORPTION OF 1-HPB AS A

FUNCTION OF pH

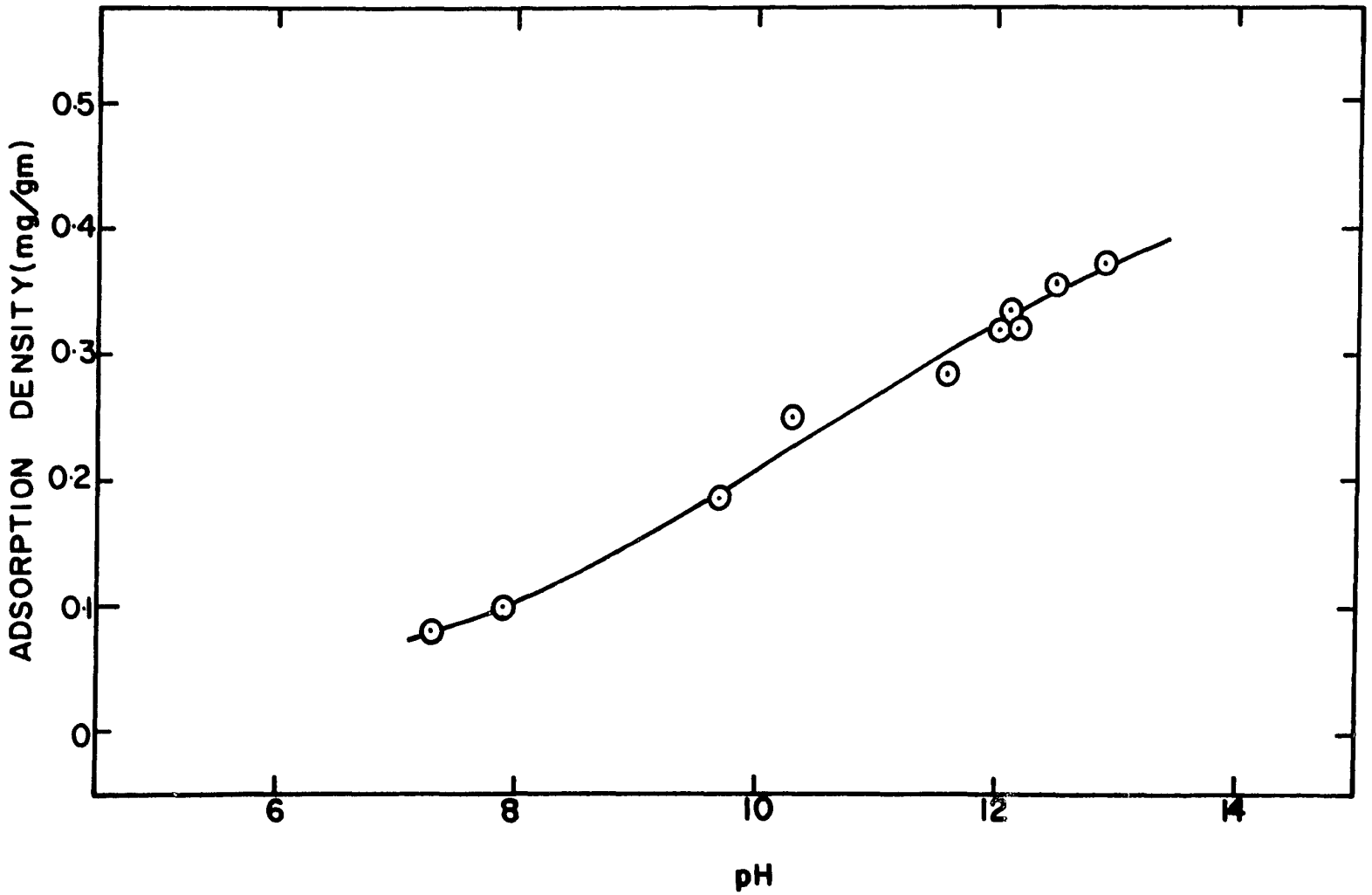
ADSORPTION DENSITY (mg/gm)
0·5
0·4
0·3
0·2
0·1
0
6
8
10
12
14
pH

TABLE 10

ADSORPTION 1-HPB AS FUNCTION OF pH

INITIAL CONCENTRATION 50 mg/l

pH	FINAL CONCENTRATION mg/l	ADSORPTION DENSITY mg/gm
7.35	45.68	.0833
7.9	44.98	.1148
9.7	41.21	.1866
10.3	38.00	.2499
11.6	35.58	.2834
12.1	33.90	.3415
12.2	33.62	.3569
12.5	33.62	.3569
12.9	31.99	.3745

FIGURE 36

ADSORPTION ISOTHERM OF 1-HPB

ON QUARTZ

X pH 8

⊙ pH 9.7

⊡ pH 12

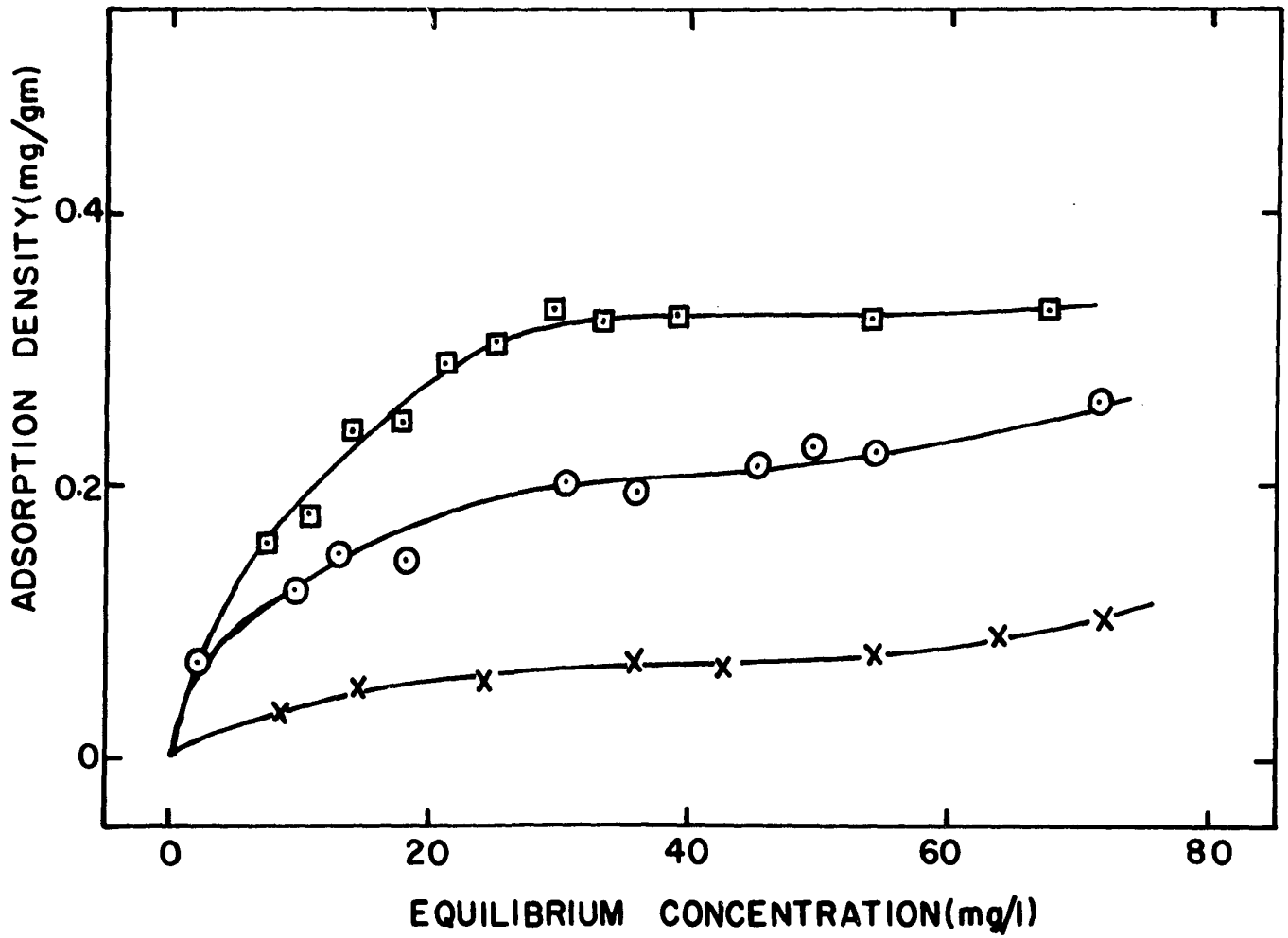
ADSORPTION DENSITY(mg/gm)
0.4
0.2
0
0
20
40
60
80
EQUILIBRIUM CONCENTRATION(mg/l)

TABLE 11

ADSORPTION OF 1-HPB AS FUNCTION OF CONCENTRATION pH 8

INITIAL CONCENTRATION mg/l	FINAL CONCENTRATION mg/l	ADSORPTION DENSITY mg/gm
9.85	8.49	.0322
19.51	17.27	.0529
26.60	24.27	.0552
39.29	36.12	.0749
45.27	42.47	.0662
57.49	54.13	.0794
67.85	63.93	.0929
77.00	72.71	.1014

TABLE 12

ADSORPTION OF 1-HPB AS FUNCTION OF CONCENTRATION pH 9.7

INITIAL CONCENTRATION mg/l	FINAL CONCENTRATION mg/l	ADSORPTION DENSITY mg/gm
5.36	2.31	.0722
14.98	9.71	.1245
19.41	13.04	.1505
24.59	18.31	.1482
39.20	30.60	.2032
44.47	36.15	.1966
49.09	41.21	.1866
54.36	45.12	.2183
59.26	49.65	.2271
68.22	58.70	.2249
82.62	71.49	.2625

TABLE 13

ADSORPTION OF 1-HPB AS FUNCTION OF CONCENTRATION pH 12

INITIAL CONCENTRATION mg/l	FINAL CONCENTRATION mg/l	ADSORPTION DENSITY mg/gm
4.53	1.85	.0633
8.78	6.47	.0546
14.14	7.40	.1593
18.31	10.72	.1793
24.31	14.05	.2424
28.47	17.94	.2488
33.74	21.36	.2925
37.90	25.15	.3012
43.82	29.68	.3342
46.96	33.37	.3211
52.97	39.20	.3253
68.32	54.60	.3242
81.57	67.76	.3286

FIGURE 37

B.E.T. PLOTS FOR 1-HPB ADSORPTION

X pH 8	S = 11.448 I = 0.634	Surface Area = 670 cm^2/gm
⊙ pH 9.7	S = 4.875 I = 0.119	Surface Area = 1693 cm^2/gm
⊡ pH 12	S = 3.628 I = 0.034	Surface Area = 2307 cm^2/gm

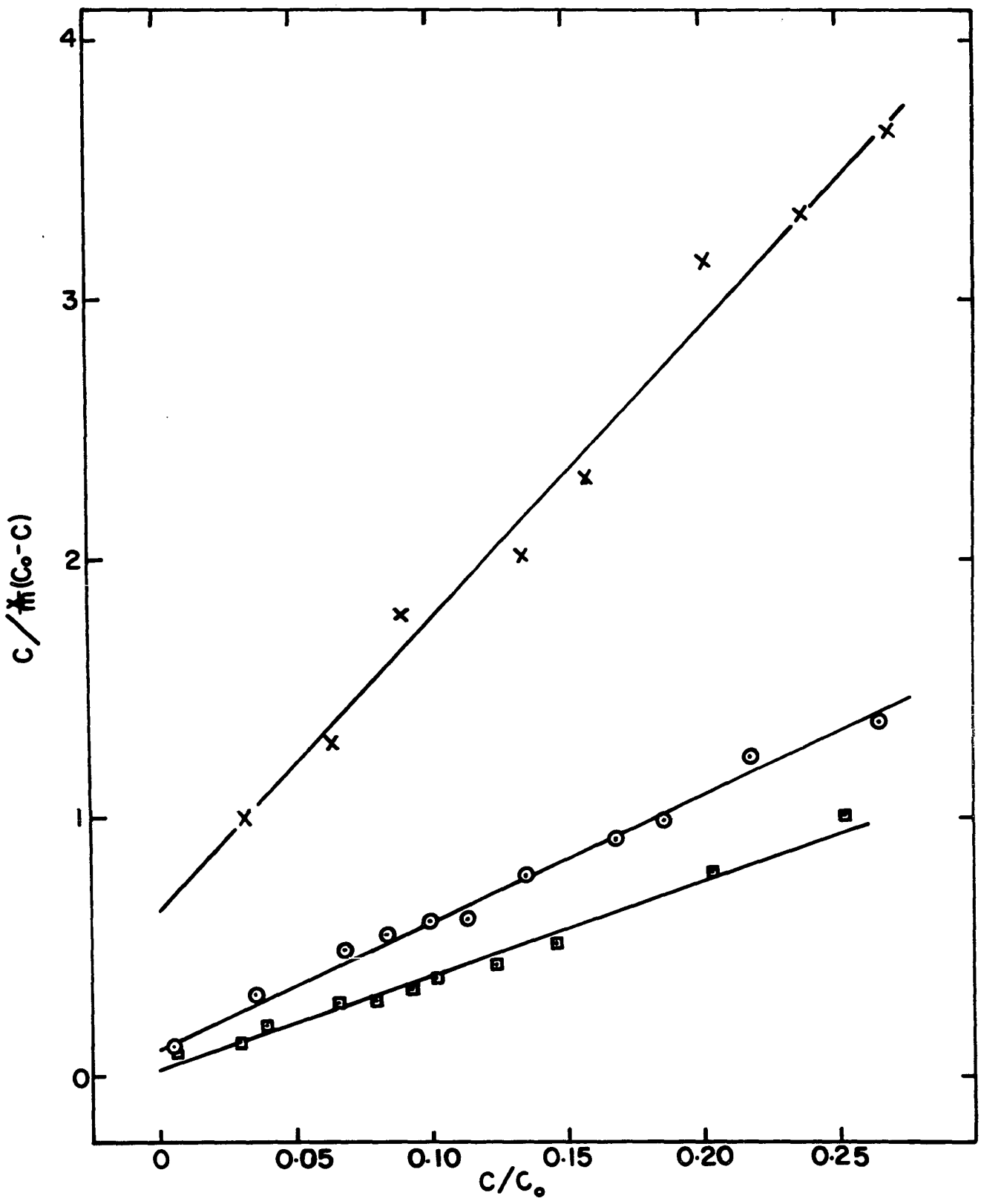
4
3
2
1
0
C/x(C₀-C)
0
0·05
0·10
0·15
0·20
0·25
C/C₀

TABLE 14

MODIFIED B.E.T. CALCULATIONS FOR 1-HPB ADSORPTION

$\frac{x}{m}$ mg/gm	$\frac{C}{\frac{x}{m}[C_o-C]}$	$\frac{C}{C_o}$
pH 8		
.0322	1.011	.0315
.0529	1.296	.0642
.0552	1.795	.0902
.0749	2.066	.1342
.0662	2.318	.1578
.0794	3.169	.2011
.9926	3.352	.2375
.1014	3.650	.2701
pH 9.7		
.0722	.1199	.0086
.1245	.3005	.0361
.1505	.3382	.0484
.1484	.4918	.0680
.1585	.5718	.0831
.1808	.6065	.0988
.2032	.6285	.1137
.1966	.7890	.1343
.2183	.9223	.1676

TABLE 14 con't

.2271	.9959	.1844
.2249	1.240	.2181
.2625	1.377	.2656
pH 12		
.0633	.1093	.0069
.1593	.1775	.0275
.1793	.2157	.0398
.2424	.2272	.0529
.2488	.2870	.0666
.2925	.2947	.0794
.3012	.3421	.0934
.3253	.3862	.1116
.3211	.4406	.1246
.3253	.5239	.1456
.3242	.7848	.2028
.3286	1.024	.2517

APPENDIX IV

SOLUTION ANALYSIS

The solutions were analyzed using the two isotope liquid scintillation techniques, similar to that used by Partridge[62]. The scintillation solution contained 100 gm naphthalene, and 6 gm P.P.O. in 1 gal. dioxane. All solutions were counted three times for five minutes using a Beckman model L55 1517A scintillation counter.

To determine the variation in counting efficiency with quenching, exactly ½ ml of the standard activity solutions was added to 10 mls of scintillation solution. To insure a wide range of quench ratios varying amounts of water (0 - 3.0 cc) was added to the vials. The vials were counted and the average efficiency calculated as the ratio of counts per minute to decompositions per minute. The quench ratio was obtained using the automatic "quench ratio" device of the scintillation counter. The gain setting on the counter was set low to insure that tritium was recorded only in window A while carbon-14 was recorded in both window A and window B. This simplifies calculations for specific activity and minimizes errors in carbon-14 calculations due to errors in the calibration curve for tritium. The efficiency and corresponding quench ratios obtained for the tritium and carbon-14 can be found in Table 15 and 16.

The counting efficiency of each isotope in the respective windows is plotted as a function of the quench

ratio (Fig. 38). The equations defining the curves were determined by assuming that an equation of the form

$$E = A + BQ + CQ^2 + DQ^3 \qquad (25)$$

would fit the data. E is the efficiency, Q is the quench ratio, and A,B,C,D are constants. The constants were determined by the least squares analysis. The resulting equations were:

$$EH_A^{\,3} = -38.28 + 38.15Q + 66.59Q^2 - 39.68Q^3 \qquad (26)$$

$$EC_A^{\,14} = 63.48 + 34.66Q - 9.67Q^2 - 4.53Q^3 \qquad (27)$$

$$EC_B^{\,14} = -43.94 + 87.62Q - 40.77Q^2 - 41.90Q^3 \qquad (28)$$

where $EH_A^{\,3}$ is efficiency for tritium in window A

$EC_A^{\,14}$ is efficiency for carbon-14 in window

$EC_B^{\,14}$ is efficiency for carbon-14 in window B

The 2σ limits for the curves were 1.66, 1.73 and 1.22 for $EH_A^{\,3}$, $EC_A^{\,14}$ and $EC_B^{\,14}$ respectively.

The specific activity of an unknown solution can be determined by solving the following simultaneous equations:

$$CTSB = EC_B^{\,14} \times C^{14} \qquad (29)$$

$$CTSA = EC_A^{\,14} \times C^{14} + EH_A^{\,3} \times H^3 \qquad (30)$$

FIGURE 38

EFFICIENCY VS QUENCH RATIO FOR

TRITIUM AND CARBON-14

⊙ Efficiency for Tritium in Window A

× Efficiency for Carbon-14 in Window A

⊡ Efficiency for Carbon-14 in Window B

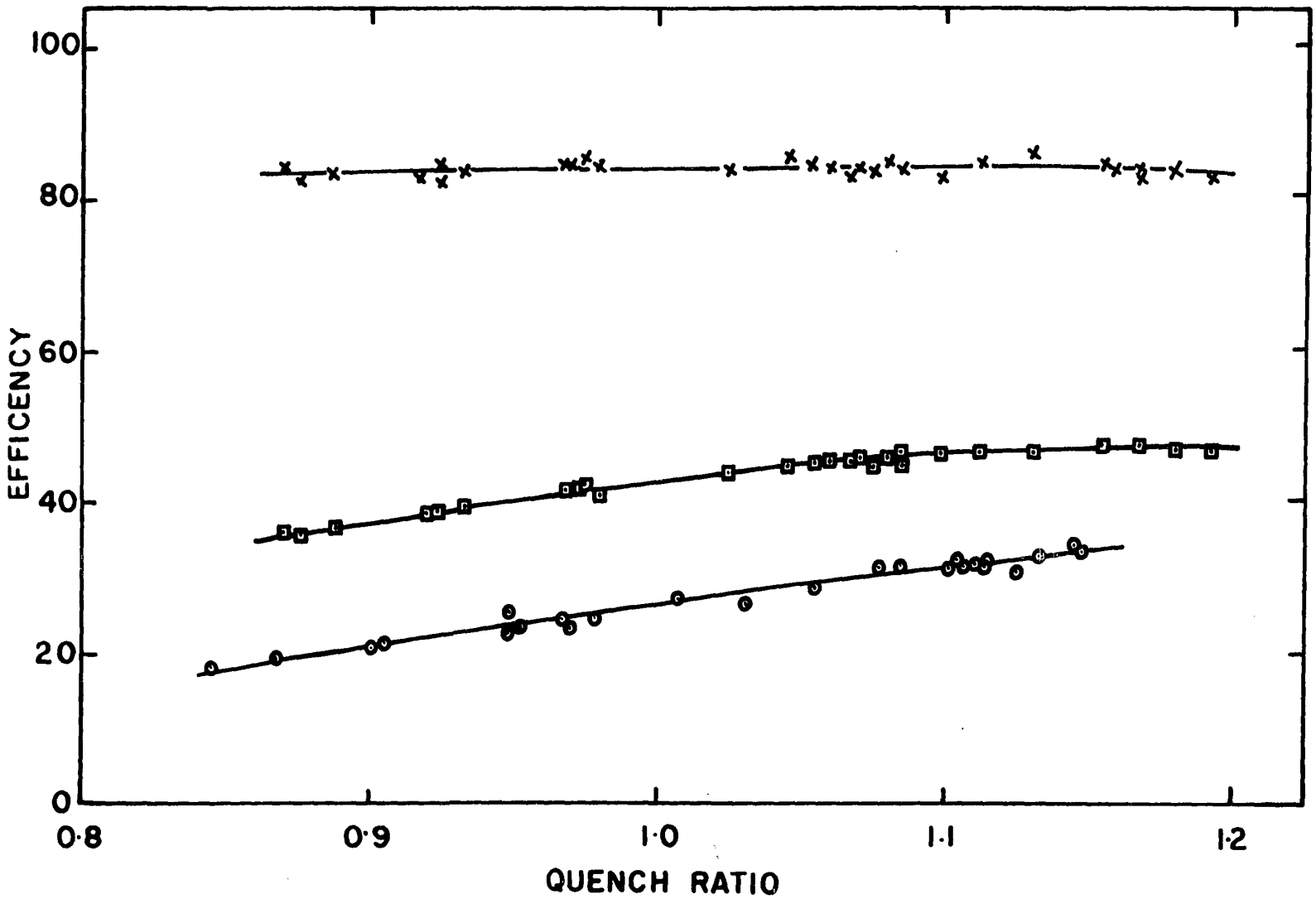
100
80
60
40
20
0
EFFICENCY
0·8
0·9
1·0
1·1
1·2
QUENCH RATIO

where EH_A^3, EC_A^{14} and EC_B^{14} are as above, H^3 and C^{14} are specific activity of tritium and carbon-14 and CTSA and CTSB are counts recorded in window A and B respectively. From equation (29) and (30) we obtain:

$$C^{14} = CTSB/EC_B^{14} \tag{31}$$

$$H^3 = (CTSA - EC_A^{14} \times C^{14})/EH_A^3 \tag{32}$$

Triplicate samples of all solutions were taken. Each sample was counted three times. The specific activity of each sample was determined and the average of the three samples was taken as the specific activity of the test solutions.

Since there is a linear relationship between concentration and specific activity, the concentration of amine and starch is found by solving the following equations.

$$\text{FINAL AMINE} = \frac{H^3 \text{ (final)}}{H^3 \text{(initial)}} \times \text{INITIAL AMINE CONCENTRATION} \tag{33}$$

$$\text{FINAL STARCH} = \frac{C^{14} \text{ (final)}}{C^{14} \text{(initial)}} \times \text{INITIAL STARCH CONCENTRATION} \tag{34}$$

The difference between initial and final concentration of reagents can be found and adsorption density calculated.

TABLE 15

EFFICIENCY AND QUENCH RATIO FOR TRITIUM STANDARDS

(WINDOW A)

EFFICIENCY	QUENCH RATIO	EFFICIENCY	QUENCH RATIO
30.98	1.126	28.83	1.056
18.67	0.847	31.54	1.079
22.85	0.948	24.63	0.979
23.88	0.970	25.88	0.949
21.17	0.901	31.16	1.101
21.71	0.906	31.31	1.085
24.77	0.969	34.07	1.114
26.65	1.031	33.08	1.132
27.29	1.008	33.05	1.130
23.65	0.952	31.39	1.099
19.78	0.869	32.42	1.115
35.08	1.225	31.41	1.114
33.70	1.148	31.62	1.110
32.55	1.105	30.54	1.087
33.14	1.122		

TABLE 16

EFFICIENCY AND QUENCH RATIO OF CARBON-14 STANDARDS

STARCH			BENZOIC ACID		
EFFICIENCY WINDOW		QUENCH RATIO	EFFICIENCY WINDOW		QUENCH RATIO
A	B		A	B	
83.31	43.73	1.026	83.24	46.92	1.159
82.64	46.74	1.098	83.12	46.84	1.181
82.80	45.54	1.068	83.08	47.25	1.169
82.27	39.22	0.949	84.14	47.53	1.155
83.28	36.79	0.887	82.87	46.88	1.169
84.00	46.40	1.086	84.18	46.15	1.112
85.41	44.85	1.045	83.56	44.30	1.076
83.91	46.11	1.064	84.36	45.96	1.108
85.13	42.18	0.978	85.99	46.14	1.131
83.27	39.09	0.933	83.90	45.48	1.108
84.60	41.71	0.969	84.12	45.08	1.055
84.46	36.23	0.870	84.39	40.84	0.980
82.45	35.87	0.876	83.66	48.49	1.233
82.95	38.21	0.917	83.11	38.18	0.932
84.55	38.93	0.924	82.25	46.69	1.192

APPENDIX V

TABLES OF FLOTATION AND ADSORPTION RESULTS ON QUARTZ

TABLE 17

INITIAL CONCENTRATION - AMINE - 10 μ mole/l

STARCH - zero

COUNTING VIAL	pH		%	EQUILIBRIUM CONCENTRATION		ADSORPTION DENSITY	
	INITIAL	FINAL	FLOAT	AMINE μmole/l	STARCH mg/l	AMINE μmole/m^2	STARCH mg/m^2
322-324	2.0	2.1	39.0	12.67	--	-0.148	--
325-327	2.0	2.1	24.0	12.70	--	-0.150	--
328-330	4.1	4.0	14.5	9.044	--	0.053	--
331-333	4.1	4.0	19.9	8.941	--	0.059	--
334-336	6.0	6.3	20.8	7.977	--	0.112	--
337-339	6.0	6.1	15.3	8.197	--	0.100	--
340-342	7.5	6.6	56.5	7.508	--	0.138	--
343-345	7.5	6.7	60.0	7.782	--	0.123	--
346-348	10.1	9.8	79.2	1.894	--	0.449	--
349-351	10.1	9.7	76.0	1.971	--	0.445	--
352-354	12.0	10.9	16.3	2.755	--	0.401	--
355-358	12.0	10.9	33.6	2.593	--	0.410	--

TABLE 18

INITIAL CONCENTRATION - AMINE - 10 μmole/l

STARCH - 100 mg/l

COUNTING VIAL	pH		% FLOAT	EQUILIBRIUM CONCENTRATION		ADSORPTION DENSITY	
	INITIAL	FINAL		AMINE μmole/l	STARCH mg/l	AMINE μmole/m^2	STARCH mg/m^2
451-453	2.1	2.3	25.3	6.772	106.8	0.182	-0.378
454-456	2.1	2.2	26.8	2.556	109.1	0.412	-0.502
457-459	4.0	4.2	14.4	9.132	99.4	0.048	0.028
460-462	4.0	4.2	14.8	5.038	95.9	0.275	0.225
463-465	6.0	5.9	67.9	8.998	92.3	0.056	0.425
466-468	6.0	6.0	51.6	8.511	90.8	0.083	0.506
469-471	8.2	6.9	66.7	7.131	91.6	0.159	0.460
472-474	8.2	7.1	73.0	6.709	93.8	0.182	0.343
475-477	10.1	10.0	80.8	3.273	94.0	0.372	0.329
478-480	10.1	9.9	78.4	3.634	94.8	0.352	0.285
481-483	12.0	11.8	10.6	2.236	95.0	0.430	0.273
484-486	12.0	11.9	6.6	2.390	90.1	0.421	0.544

TABLE 19

INITIAL CONCENTRATION - AMINE - 10 μmole/l

STARCH - 400 mg/l

COUNTING VIAL	pH		% FLOAT	EQUILIBRIUM CONCENTRATION		ADSORPTION DENSITY	
	INITIAL	FINAL		AMINE μmole/l	STARCH mg/l	AMINE μmole/m^2	STARCH mg/m^2
596-598	2.0	2.3	26.5	8.972	--	0.057	--
599-601	2.0	2.3	35.0	7.783	--	0.067	--
602-604	4.0	4.1	15.9	10.445	395.2	-0.025	0.267
605-607	4.0	4.2	20.3	10.267	393.9	-0.015	0.340
608-610	5.9	5.9	50.5	7.589	388.4	0.134	0.644
611-613	5.9	6.0	46.4	9.247	397.0	0.042	0.165
614-616	8.2	7.4	58.3	7.455	392.8	0.141	0.398
617-619	8.2	7.4	54.5	6.985	402.7	0.167	-0.150
620-622	10.1	9.8	48.1	5.136	397.8	0.269	0.120
623-625	10.1	9.9	--	4.467	402.1	0.306	-0.114
626-628	12.0	11.9	18.6	3.651	359.4	0.352	2.248
629-631	12.0	11.9	17.6	4.039	358.9	0.330	2.277

TABLE 20

INITIAL CONCENTRATION - AMINE - 10 μmole/l

STARCH - 1000 mg/l

COUNTING VIAL	pH		% FLOAT	EQUILIBRIUM CONCENTRATION		ADSORPTION DENSITY	
	INITIAL	FINAL		AMINE μmole/l	STARCH mg/l	AMINE μmole/m^2	STARCH mg/m^2
535-537	2.0	2.3	26.4	10.619	--	-0.034	--
538-540	2.0	2.2	12.0	10.370	--	-0.021	--
541-543	4.0	4.2	12.0	10.433	960.8	-0.024	2.172
544-546	4.0	4.2	8.8	10.228	963.1	-0.013	2.044
547-549	6.0	6.2	47.6	9.936	972.1	0.004	1.544
550-552	6.0	6.3	40.5	10.039	963.9	-0.002	1.998
553-555	8.3	7.3	37.8	7.827	961.9	0.120	2.107
556-558	8.3	7.2	40.9	7.569	925.9	0.135	4.101
559-561	10.3	9.8	27.6	7.416	909.0	0.254	5.039
562-564	10.3	9.8	27.8	6.252	887.4	0.208	6.231
565-567	12.0	11.8	6.1	5.082	860.4	0.272	7.731
568-571	12.0	11.8	10.4	5.249	873.5	0.263	7.004

TABLE 21

INITIAL CONCENTRATION - AMINE - 100 μ mole/l

STARCH - zero

COUNTING VIAL	pH		% FLOAT	EQUILIBRIUM CONCENTRATION		ADSORPTION DENSITY	
	INITIAL	FINAL		AMINE μmole/l	STARCH mg/l	AMINE μmole/m^2	STARCH mg/m^2
205-207	2.0	2.1	59.4	--	--	--	--
208-210	2.0	2.0	63.6	--	--	--	--
211-213	4.1	4.3	93.5	94.27	--	0.317	--
214-216	4.1	4.2	88.2	93.40	--	0.366	--
217-219	5.8	6.3	93.0	89.95	--	0.557	--
220-222	5.8	6.1	94.7	91.12	--	0.492	--
223-225	8.0	7.6	96.1	87.36	--	0.670	--
226-228	8.0	7.4	97.5	85.54	--	0.801	--
229-231	10.0	9.5	93.5	23.87	--	4.214	--
232-234	10.0	9.4	94.9	21.85	--	4.327	--
235-237	12.0	11.8	93.0	15.01	--	4.797	--
238-240	12.0	11.9	93.5	13.35	--	4.797	--

TABLE 22

INITIAL CONCENTRATION - AMINE - 100 μmole/l

STARCH - 100 mg/l

COUNTING VIAL	pH		%	EQUILIBRIUM CONCENTRATION		ADSORPTION DENSITY	
	INITIAL	FINAL	FLOAT	AMINE μmole/l	STARCH mg/l	AMINE μmole/m^2	STARCH mg/m^2
400-402	2.0	1.9	36.6	--	--	--	--
403-405	2.0	2.0	37.9	--	--	--	--
406-408	4.0	3.7	49.5	96.08	107.3	0.217	-0.41
409-411	4.0	3.7	49.2	94.92	105.6	0.281	-0.31
412-414	6.1	6.6	81.9	93.45	108.4	0.363	-0.47
415-417	6.1	6.7	81.2	92.95	105.6	0.391	-0.31
418-420	8.3	8.1	77.9	89.15	107.9	0.601	-0.44
421-423	8.3	8.2	76.7	86.39	104.5	0.753	-0.25
424-426	10.0	9.8	95.3	22.85	102.8	4.271	-0.16
427-429	10.0	9.9	96.7	26.12	103.9	4.090	-0.22
430-432	12.0	12.2	95.9	29.70	110.2	3.892	-0.57
433-435	12.0	12.1	96.8	25.92	105.2	4.101	-0.29

TABLE 23

INITIAL CONCENTRATION - AMINE - 100 μmole/l

STARCH - 400 mg/l

COUNTING VIAL	pH		%	EQUILIBRIUM CONCENTRATION		ADSORPTION DENSITY	
	INITIAL	FINAL	FLOAT	AMINE μmole/l	STARCH mg/l	AMINE μmole/m^2	STARCH mg/m^2
283-285	2.0	2.1	55.8	111,61	421.0	-0.643	-1.163
286-288	2.0	1.9	42.3	100.23	435.5	-0.013	-1.965
289-291	4.2	4.4	63.7	81.89	378.6	1.003	1.184
292-294	4.2	4.3	58.6	81.33	381.5	1.034	1.025
295-297	6.3	6.4	62.6	80.08	380.9	1.103	1.057
298-300	6.3	6.4	71.1	77.87	379.8	1.225	1.120
301-303	7.7	7.1	67.9	76.32	381.4	1.311	1.032
304-306	7.7	7.1	78.0	76.30	387.9	1.312	0.667
307-309	10.1	9.7	96.8	26.71	370.1	4.057	1.653
310-312	10.1	9.8	96.4	24.08	379.1	4.203	1.157
313-315	12.0	12.0	93.0	27.42	344.0	4.018	3.101
316-319	12.0	11.9	91.4	33.50	339.4	3.681	3.354

TABLE 24

INITIAL CONCENTRATION - AMINE - 100 μ mole/l

STARCH - 1000 mg/l

COUNTING VIAL	pH		%	EQUILIBRIUM CONCENTRATION		ADSORPTION DENSITY	
	INITIAL	FINAL	FLOAT	AMINE μ mole/l	STARCH mg/l	AMINE μ mole/m^2	STARCH mg/m^2
244-246	2.0	2.2	42.1	103.93	1084.5	-0.218	-4.679
247-249	2.0	2.2	44.2	98.10	1006.8	0.105	-0.377
250-252	3.8	3.9	47.9	91.56	896.5	0.467	5.730
253-255	3.8	4.0	45.9	92.91	909.4	0.393	5.015
256-258	6.0	6.1	63.4	87.21	903.2	0.708	5.361
259-261	6.0	6.1	46.6	86.67	884.8	0.738	6.378
262-264	7.8	7.1	61.2	79.97	875.5	1.109	6.891
265-267	7.8	7.1	50.0	79.82	873.9	1.117	6.980
268-270	10.1	9.8	100.0	42.83	888.2	3.165	6.191
271-273	10.1	9.7	100.0	45.08	886.5	3.040	6.286
274-276	12.0	11.9	98.3	41.46	798.8	3.241	11.139
277-279	12.0	11.9	86.8	42.54	807.6	3.181	10.653

TABLE 25

INITIAL CONCENTRATION - AMINE - 1000 μmole/l

STARCH - zero

COUNTING VIAL	pH		% FLOAT	EQUILIBRIUM CONCENTRATION		ADSORPTION DENSITY	
	INITIAL	FINAL		AMINE μmole/l	STARCH mg/l	AMINE μmole/m^2	STARCH mg/m^2
574-576	2.1	2.3	72.0	1104.4	--	-5.780	--
577-579	2.1	2.3	73.2	1114.9	--	-6.360	--
580-582	4.1	4.2	94.1	923.1	--	4.256	--
583-585	4.1	4.2	93.8	921.6	--	4.338	--
586-588	6.3	6.3	94.7	950.5	--	2.741	--
589-591	6.3	6.3	97.3	937.5	--	3.460	--
592-594	8.0	6.8	97.2	908.2	--	5.084	--
595-597	8.0	6.8	98.9	912.3	--	4.855	--
598-600	10.3	10.1	93.0	556.1	--	24.575	--
601-603	10.3	10.1	91.8	550.6	--	24.877	--
604-606	12.2	12.0	74.1	840.1	--	9.856	--
607-609	12.2	12.0	88.8	836.6	--	9.046	--

TABLE 26

INITIAL CONCENTRATION - AMINE - 1000 μmole/l

STARCH - 100 mg/l

COUNTING VIAL	pH		%	EQUILIBRIUM CONCENTRATION		ADSORPTION DENSITY	
	INITIAL	FINAL	FLOAT	AMINE μmole/l	STARCH mg/l	AMINE μmole/m^2	STARCH mg/m^2
697-699	2.0	2.3	52.3	1096.5	117.8	-5.341	-0.988
700-702	2.0	2.3	50.3	1138.9	120.9	-7.690	-1.159
703-705	4.3	4.7	78.3	1056.2	102.5	-3.112	-0.138
706-708	4.3	4.7	87.8	1105.4	107.8	-5.834	-0.434
709-711	5.7	5.5	95.3	1062.1	104.7	-3.437	-0.261
712-714	5.7	5.6	92.9	699.6	71.3	16.63	1.590
715-717	8.6	8.7	98.4	815.3	106.6	10.23	-0.366
718-720	8.6	8.7	94.9	748.0	102.2	13.95	-0.397
721-723	10.0	9.7	93.2	675.4	104.7	17.97	-0.259
724-726	10.0	9.8	92.6	664.7	107.0	18.56	-0.390
727-729	12.0	11.8	95.8	797.8	93.4	11.20	0.365
730-733	12.0	11.9	8418	840.9	97.9	8.809	0.116

TABLE 27

INITIAL CONCENTRATION - AMINE - 1000 μmole/l

STARCH - 400 mg/l

COUNTING VIAL	pH		% FLOAT	EQUILIBRIUM CONCENTRATION		ADSORPTION DENSITY	
	INITIAL	FINAL		AMINE μmole/l	STARCH mg/l	AMINE μmole/m^2	STARCH mg/m^2
652-654	2.0	2.1	*	--	--	--	--
655-657	2.0	2.1	*	--	--	--	--
658-660	4.0	4.0	*	990.5	398.0	0.527	0.110
661-663	4.0	4.0	*	1009.8	406.1	-0.544	-0.337
664-666	6.0	6.1	99.5	993.6	403.9	0.353	-0.218
667-669	6.0	6.2	99.5	986.8	400.9	0.728	-0.052
670-672	8.4	8.3	99.5	625.0	379.8	20.76	1.118
673-675	8.4	8.4	99.5	617.3	384.1	21.19	0.883
675-678	10.0	9.6	98,5	626.8	395.9	20.66	0.225
679-681	10.0	9.6	97.9	610.6	394.0	21.56	0.333
682-684	12.1	11.8	93.6	788.6	374.0	11.71	1.441
685-687	12.1	11.8	94.0	790.4	362.4	11.60	2.084

* cell broken

TABLE 28

INITIAL CONCENTRATION - AMINE - 1000 μ mole/l

STARCH - 1000 mg/l

COUNTING VIAL	pH		% FLOAT	EQUILIBRIUM CONCENTRATION		ADSORPTION DENSITY	
	INITIAL	FINAL		AMINE μmole/l	STARCH mg/l	AMINE μ mole/m^2	STARCH mg/m^2
613-615	2.0	2.6	82.2	--	--	--	--
616-618	2.0	2:6	84.8	--	--	--	--
619-621	4.0	4.1	99.4	978.9	990.5	1.173	0.525
622-624	4.0	4.1	95.1	941.8	995.2	3.223	0.267
625-627	5.9	6.4	98.9	921.1	950.7	4.368	2.732
628-630	5.9	6.5	94.5	929.9	967.1	3.883	1.823
631-633	8.1	7.2	99.4	870.0	949.5	7.196	2.796
634-636	8.1	7.3	98.9	843.6	930.7	8.659	3.834
637-639	10.0	9.4	98.4	702.6	933.3	16.466	3.695
640-642	10.0	9.5	98.9	699.9	972.0	16.614	1.594
643-645	12.0	11.8	93.6	838.3	935.0	8.951	3.596
646-648	12.0	11.8	93.7	832.1	867.3	9.396	7.345

TABLE 29

INITIAL CONCENTRATION- AMINE - 10,000 μmole/l

STARCH - zero

COUNTING VIAL	pH		% FLOAT	EQUILIBRIUM CONCENTRATION		ADSORPTION DENSITY	
	INITIAL	FINAL		AMINE μmole/l	STARCH mg/l	AMINE μmole/m^2	STARCH mg/m^2
799-801	2.0	2.1	40.6	--	--	--	--
802-804	2.0	2.1	36.7	--	--	--	--
805-807	4.0	3.9	67.8	9677.3	--	17.87	--
808-810	4.0	3.9	60.7	9841.6	--	8.77	--
811-813	6.0	5.5	97.4	9221.6	--	43.09	--
814-816	6.0	5.5	98.0	9197.8	--	44.41	--
817-819	8.0	8.0	87.4	8779.2	--	67.58	--
820-822	8.0	7.9	87.9	8923.5	--	59.59	--
823-825	10.0	9.8	52.4	8717.0	--	71.03	--
826-828	10.0	9.9	58.7	8477.2	--	84.30	--
- -	12.0	11.5	59.4	--	--	--	--
- -	12.0	11.5	63.5	--	--	--	--

TABLE 30

INITIAL CONCENTRATION - AMINE - 10,000 μmole/l

STARCH - 100 mg/l

COUNTING VIAL	pH		% FLOAT	EQUILIBRIUM CONCENTRATION		ADSORPTION DENSITY	
	INITIAL	FINAL		AMINE μmole/l	STARCH mg/l	AMINE $\mu mole/m^2$	STARCH mg/m^2
910-912	2.0	2.2	68.0	--	--	--	--
913-915	2.0	2.1	45.8	--	--	--	--
916-918	3.9	4.0	46.0	9995.5	193.2	0.246	-0.179
919-921	3.9	4.0	47.4	9970.5	98.8	1.632	0.064
922-924	5.9	5.6	44.9	9552.8	95.3	24.48	0.261
925-927	5.9	5.6	53.8	9484.2	94.5	28.55	0.303
928-930	8.3	8.1	88.4	8941.1	102.8	58.62	-0.154
931-933	8.3	8.1	86.7	9031.0	103.1	53.64	-0.170
934-936	10.0	9.9	66.3	8464.5	100.9	85.00	-0.050
937-939	10.0	9.8	71.9	8114.5	99.9	104.38	0.003
- -	11.8	11.6	69.2	--	--	--	--
- -	11.8	11.6	65.8	--	--	--	--

TABLE 31

INITIAL CONCENTRATION - AMINE - 10,000 μmole/l

STARCH - 400 mg/l

COUNTING VIAL	pH		% FLOAT	EQUILIBRIUM CONCENTRATION		ADSORPTION DENSITY	
	INITIAL	FINAL		AMINE μmole/l	STARCH mg/l	AMINE μmole/m^2	STARCH mg/m^2
874-876	2.0	2.2	55.1	--	--	--	--
877-879	2.0	2.3	46.6	--	--	--	--
880- 882	4.1	4.3	52.1	9860.1	425.4	7.747	-1.406
883-885	4.1	4.2	61.3	9811.6	423.1	10.43	-1.277
886-888	6.1	6.0	74.0	9496.6	406.6	27.87	-0.367
889-891	6.1	6.0	70.0	9678.3	417.4	17.81	-0.964
892-894	8.2	8.4	90.6	9135.1	427.1	47.88	-1.498
895-897	8.2	8.4	91.3	8876.6	412.0	62.19	-0.664
898-900	10.0	10.1	82.4	8432.1	409.7	86.79	-0.538
901-903	10.0	10.2	80.5	8486.4	412.2	83.79	-0.674
- -	12.0	11.9	75.3	--	--	--	--
- -	12.0	12.0	81.1	--	--	--	--

TABLE 32

INITIAL CONCENTRATION - AMINE - 10,000 μmole/l

STARCH - 1000 mg/l

COUNTING VIAL	pH		% FLOAT	EQUILIBRIUM CONCENTRATION		ADSORPTION DENSITY	
	INITIAL	FINAL		AMINE μmole/l	STARCH mg/l	AMINE μmole/m^2	STARCH mg/m^2
838-840	2.2	2.2	53.0	--	--	--	--
841-843	2.2	2.2	56.3	--	--	--	--
844-846	4.2	3.9	52.3	19455.	1071.0	-25.19	-3.928
847-849	4.2	3.9	55.4	10618.	1083.9	-34.21	-4.647
850-852	6.1	6.0	77.9	10090.	1033.9	-5.00	-1.871
853-855	6.1	6.0	69.7	9877.7	1001.3	6.768	-0.071
856-858	8.3	8.0	88.9	9608.1	1032.1	21.70	-1.780
859-861	8.3	8.0	85.7	9402.2	1014.9	33.10	-0.826
862-864	10.2	9.8	74.1	8144.6	963.7	102.7	2.007
865-867	10.2	9.9	73.5	8851.6	1007.6	63.61	-0.423
- -	12.0	11.8	72.9	--	--	--	--
- -	12.0	11.7	84.8	--	--	--	--

TABLE 33

RESULTS - AMINE - zero

STARCH - 100, 400, 1000 mg/l

COUNTING VIAL	pH		% FLOAT	EQUILIBRIUM CONCENTRATION mg/l	ADSORPTION DENSITY mg/gm
	INITIAL	FINAL			
			INITIAL STARCH - 100 mg/l		
736-738	2.1	2.4	16.0	115.0	-0.831
739-741	4.0	4.3	7.4	101.6	-0.086
742-744	6.0	6.1	8.0	101.2	-0.066
745-747	8.3	7.0	9.2	103.6	-0.2--
748-750	10.0	9.6	6,3	101.4	-0.079
751-754	12.0	11.8	12.3	95.1	0.270
			INITIAL STARCH - 400 mg/l		
757-759	2.0	2.3	10.1	443.6	-2.412
760-762	3.9	4.0	10.5	392.3	0.425
763-765	6.0	6.2	12.3	402.8	-1.156
766-768	7.8	7.0	8.7	411.1	-0.616

TABLE 33 con't

769-771	10.1	9.7	11.0	396.7	0.183
772-774	12.0	11.9	11.2	364.6	1.962
			INITIAL STARCH - 1000 mg/l		
778-780	2.1	2.5	1.0	1182.5	-10.10
781-783	4.0	4.2	2.1	1010.5	-0.579
784-786	6.0	6.1	3.6	1016.8	-0.931
787-789	7.9	6.9	2.6	992.4	0.423
790-792	9.7	8.7	3.7	991.0	0.499
793-795	12.0	11.9	5.2	920.3	4.412

TABLE 34

NATURAL FLOATABILITY OF QUARTZ

AMINE - zero

STARCH - zero

pH		%
INITIAL	FINAL	FLOAT
2.0	2.1	2.7
3.9	3.95	2.7
5.9	6.40	2.2
8.0	7.40	2.1
9.95	9.80	3:4
12.0	11.90	4.1

BIBLIOGRAPHY

1 Schneider, V.B.; Iron Ore, Reprint 22 for the Candian Minerals Yearbook 1968, Dept of Energy, Mines and Resources, Ottawa, 1969

2 Buck, W.K.; Mining - Annual Review 1970, pg. 245

3 Cofield, G.E. and MacKnight; Mining Review 52 Vol.10 March 1963

4 Pryor, E.J.; Mineral Processing, Elsevier, New York 1965

5 McKim, A.M. and Ambler, J.; Ore Dressing-Scully Mine Paper 94 71st A.G.M., C.I.M. Montreal 1969

6 Major Marothy, G.; Flotation experiments with Earthly Iron Ores - Bull C.I.M. 60,1060,(1967)

7 Iwasaki, I; Iron Ore Concentration U.S. Patent 3371778, (1968)

8 Shultz, N.S. and Cooke, S.R.B.; Froth Flotation of Iron Ores-Adsorption of Starch Products and Dodecylamine Ind.Eng.Chem.45(12), 2767,(1953)

9 Chang, C.S., Cooke, S.R.B. and Huch, R.Q.; Starch and Starch Products as Depressants in Amine Flotation of Iron Ores. Trans. A.I.M.E. 196, 1282, (1953)

10 De Witt, C.C.; Anionic Flotation of Quartz Trans A.I.M.E., 202, 1955

11 Helmholtz, H.L.F. Von; Studien ueber elektrische Gremzschichten Ann. Physik 7 N° 4, 337, (1879)

12 Gouy, M.; Sur la constitution de la Charge Electrique à la Surface d'un Electrolyte.
J. Phys. Chem. 9 N'6, 475, (1910)

13 Chapman, P.L.; A Contribution to the Theory of Electrocapillarity
Phil. Mag. 25 N° 6, 475, (1913)

14 Stern, O.; The Theory of the Electrical Double Layer
Z. Electrochemie 30, 508, (1924)

15 Grahame, D.C.; The Electrical Double Layer and the Theory of Electrocapillarity
Chem. Revs. 41, 441, (1947)

16 Smith, G.W., and Salman T.; Zero-Point-of-Charge of Hematite and Zirconia
Cdn. Met. Quart. 5 N° 2, 93, (1966)

17 Joy, A.S. and Robinson A.J.; Flotation - Recent Progress in Surface Science 2 Academic Press N.Y. 172, (1964)

18 Langmuir, I.; The Adsorption of Gases on Planar Surfaces of Glass, Mica and Platinum
J. Amer. Chem. Soc. 40, 1361, (1918)

19 Moore, W.J.; Physical Chemistry, Longman's, London 1957 page 514

20 Gaudin, A.M.; Flotation, Ed'n 2 McGraw Hill N.Y. (1957), Page 82

21 Freundlich, I.; Colloid and Capillary Chemistry Matheun and Co. London (1926)

22 Brunauer, S., Emmett, P.H. and Teller, E.; Adsorption of gases in Multimolecular Films. J. Amer. Chem. Soc. 60, 309, (1938)

23 Cook, M.A., The Theory of Adsorption of Gases on Solids
J. Amer. Chem Soc. 70, 2925, (1948)

24 Harkins, W.P. and Jura, G., A Vapour Adsorption Method for Determination of Areas of Solids.
J. Amer. Chem Soc. 70, 1727, (1948)

25 Anderson, R.B., and Hall W.K., Modifications of the Brunauer, Emmett and Teller Equation
J. Amer. Chem Soc. 70, 1727, (1948)

26 Keenan, A.G., Concerning Anderson's Modification of the B.E.T. Method.
J. Amer. Chem Soc. 70, 3947, (1948)

27 Hansen, R.S., Fu, Y. and Bartell, F.E., Thermodynamics of Adsorption from Solution
J. Phy. and Coll. Chem. 53, 769, (1949)

28 Ewing, W.W. and Liu, F.W.J., Adsorption of Dyes from Aqueous Solution on Pigments
J. Coll. Chem. 8, 204, (1953)

29 Hoer, C.W., McCorkle, D. and Ralston, A.W., Studies on High Molecular Weight Aliphatic Amines and their Salts,
J. Amer. Chem Soc. 65, 328, (1943)

30 Brown, D.J. Unpublished Results, Dept. Met. M.I.T. quoted by de Bruyn, P.L., trans. A.I.M.E. 202, 292, (1955)

31 Kellogg, H.H. and Vasquès-Rosas, Amine Flotation of Sphalerite-Galena Ores. Trans A.I.M.E. 169, 476, (1946)

32 Williams, J.M., The Chemical Evidence for the Structure of Starch, in Starch and its Derivatives, J.A. Radley Ed. Chapman and Hall, London (1968) page 125

33 Reference 32, page 120

34 Gaudin, A.M. and Morrow, J.G., Adsorption of Dodecylamine on Hematite and its Flotation Effect. Mining Engineering Dec. 1954 page 1196

35 Klassen, V.I., An Introduction to the Theory of Flotation Butterworth, London 1963, page 266

36 Somasundaran, P., Fuerstenau, D.W., and Healy, T.W., Surfactant Adsorption at Solid-Liquid Interface-Dependence of Mechanism on Chain Length J. Phys. Chem. 68(12), 3562-6, (1964)

37 Gaudin, A.M. and Bloecher, F.W., Adsorption of Dodecylamine on Quartz. Trans A.I.M.E. 187, 499-05, (1950)

38 Sutherland, K.L. and Wark, I.W.; Principles of Flotation Aust. Inst. of Min. and Met. Melbourne 1955, page 41

39 Danelov, E.U., "Flotation of Feldspar by Laurylamine", Concentration of Valuable Minerals (papers), Mekhanobr Inst. 1, (1952)

40 Taggart, A.,and Arbiter, N., The Chemistry of Collection of Non- Metallic Minerals by Amine-type Collectors Min. Tech. 8, Tech Bull 1685, (1944)

41 Lidstrom,L., Surface and Bond Forming Properties of Quartz and Silicate Minerals and their Application to Mineral Processing Techniques. Acta Polyteck Scand. Chem Met. Ser. N^{O} 5,(1968)

42 Gaudin, A.M. and Fuerstenau, D.W., Quartz Flotation with Cationic Collectors, Trans A.I.M.E. 202, 958,(1955)

43 Sandvik, K.L. and Slobbaken, A., Adsorption of Long Chained Amines on Quartz, Trans A.I.M.E. 241, 418,(1968)

44 De Bruyn, P.L., Flotation of Quartz by Cationic Collectors J. Phys. Chem. 202, 191 (1955)

45 Smith, R.W. and Lai, R.W.M., Relationship Between Contact Angle and Flotation Behaviours. Trans A.I.M.E. 235, 413,(1966)

46 Rykov, K.E. and Rykova, Yu.S., Collector Properties of Ionic and Molecular Forms of Amines in Quartz Flotation. Isu. Vyssh. Veheb Zoved, Tsvet Met. 11(4), 3, (1968)

47 Bogdanov, O.S. and Mikharlova, N.S., Reaction of Cationic Collectors with Quartz and Ferruginous Minerals Tr. Nauch. Tekh. Sess., Inst. Mekhanobre 5(2), (1965)

48 Somasundaran, P., The Relationship between Adsorption at Different Interfaces and Flotation Behaviour. Trans. A.I.M.E. 241, 105,(1968)

49 Digre, M. and Sandvik, K.L., Adsorption of Amine on Quartz thru Bubble Interaction. Trans I.M.M. 77, C61,(1968)

50 Wada, M., Surface Energy and Adsorption in Fine Particle Flotation, presented at the IV Internationale Aufbereitungskolloquim Forschungsintitut Fur Aufbereitung, Freiburg (Sachs) (May 1966)

51 Bunge, F.H., Iron Ore Flotation, presented at national meeting of A.I.C.L.E. Chicago (Dec. 1962)

52 Reference 7

53 Balajee, S.R. and Iwasaki, I., Interaction of British Gum and Dodecylamine Chloride on Quartz and Hematite Surfaces. Trans. A.I.M.E. 244, 407 (1969)

54 Iwasaki, I., Interaction of Starch and Calcium in Soap Flotation of Activated Silica from Iron Ores Trans. A.I.M.E., 232, 383, (1965)

55. Iwasaki, I. and Lai, R.W., Starch and Starch Products as Depressants in Soap Flotation of Activated Silica from Iron Ores. Trans. A.I.M.E. 232, 364, (1965)

56 Shultz, N.S. and Cook, S.R.B., Froth Flotation of Iron Ores - Adsorption of Starch Products and Laurylamine Acetate. Ind. and Eng. Chem. 45, 2767, (1953)

57 Takashi, K. and Takeo, K., Complex Formation of Starch with Organic Substances. Agr. Bio. Chem. 31(2), 257, (1967)

58 Nasegawa, K. and Hirano, T., Adsorption of Iron and Aluminium on Oxidized Starch. Kogyo Kagaku Zasshi, 71(12), 2086, (1968)

59 Bear, S.R., Complex Formation between Starch and Organic Molecules. J. Amer. Chem. Soc. 66, 2122, (1944)

60 Somasundaran, P., Adsorption of Starch and Oleate and Interaction between them on Calcite in Aqueous Solution J. Coll. Interface Sci. 31(4), 557, (1969)

61 Lipparini, L. and Garutti, M.A., Amine Derivatives of Starch and Dextrin. Quad. Merceol 6(1), 65, (1967)

62 Partridge, A.C., Flotation and Adsorption Characteristics of the Hematite-Dodecylamine-Starch Systems M.Sc. Thesis, McGill University (1970)

63 Smith, G.W., The Adsorption of Dehydroabietylamine Acetate on Mineral Oxides, Ph.D. Thesis McGill (1967)

64 Oko, M.U., Adsorption of Fatty Acid Soaps on Hematite M.Eng. Thesis McGill (1965)

65 Harwood, J.H. and Ralston, A.W., The Synthesis of Lauric Acid and Dodecylamine containing carbon-14 J. Org. Chem. 12, 740, (1947)

66 Morrow, J.G. Adsorption of Dodecylammonium Acetate on Hematite and Sphalerite. Ph.D. Thesis M.I.T. 1952

67 Finch, J., Private Communication, 1971

68 Cooke, S.R.B., Shultz, N.F. and Lindroos, E.W., Effect of Certain Starches on Quartz and Hematite Suspensions Trans. A.I.M.E. 193, 697, (1952)

69 Frommer, D.W., Preparation of Non Magnetic Taconites for Flotation by Selective Flocculation. 8th I.M.P.C. Leningrade 1968 pre-print D-9 Institute MekhanObra, Leningrade (1968)

70 Shinoda et al. Colloidal Surfactants. Academic Press, New York (1963) page 159

71 Takagi, T. and Isemura, T., Interaction of Surface Active Agents with Amylose. Bull. Chem. Soc. Japan 33, 437, (1960)

72 Reference 35, page 261

73 Salman, T. and Robertson, R.F., Adsorption of Hexyl Mercaptans on Sphalerite. Ph.D. Thesis McGill 1965

74 Dictionary of Organic Compounds Vol. 2. Eyre and Spottiswoode Ltd, London

75 Paterson, J. G., The Adsorption of Sodium Oleate on Metal Hydroxides. Ph.D. Thesis McGill University 1968

76 Giles et al. J. Applied Chem. 12, 266,(1962)

77 Czerniawski, M., The Double Layer Structure of Colloidal Surfactants V The Heat of Micellization of Cetylpyridinium Bromide. Roczniki Chem 39(9), 1275, (1965)

78 Greenland, O.J. and Quirk, J.P., Determination of Surface Areas by Adsorption of Cetyl Pyridinium Bromide from Aqueous Solution. J. Phys. Chem. 67, 2886, (1963)